Quantitative Modeling of the Potato Cyst Nematode *Globodera pallida* in Idaho

A Dissertation

Presented in Partial Fulfillment of the Requirements for the

Degree of Doctor of Philosophy

with a

Major in Plant Science

in the

College of Graduate Studies

University of Idaho

by

Jn Bertrand Contina

Major Professor: Louise-Marie Dandurand, Ph.D.

Committee Members: Alexander Karasev, Ph.D.; Joseph Kuhl, Ph.D.;

Christine Parent, Ph.D.

Department Administrator: Edwin Lewis, Ph.D.

May 2019

Authorization to Submit Dissertation

This dissertation of Jn Bertrand Contina, submitted for the degree of Doctor of Philosophy with a Major in Plant Science and titled "Quantitative modeling of the potato cyst nematode *Globodera pallida* in Idaho" has been reviewed in final form. Permission, as indicated by the signatures and dates below, is now granted to submit final copies to the College of Graduate Studies for approval.

Major Professor: _____ Date: _____
Louise-Marie Dandurand, Ph.D.

Committee Members: _____ Date: _____
Alexander Karasev, Ph.D.

_____ Date: _____
Joseph Kuhl, Ph.D.

_____ Date: _____
Christine Parent, Ph.D.

Department Administrator: _____ Date: _____
Edwin Lewis, Ph.D.

Abstract

The potato cyst nematode *Globodera pallida* is a globally regulated potato pest. It was detected for the first time in the U.S. in the state of Idaho in 2006, and as of February 2019, the infestation is limited to 1,326 ha. *Globodera pallida* is a specialized obligate sedentary endoparasite that can survive in the soil for up to 30 years in the absence of its potato host. In highly infested fields, the nematode can reduce tuber yields up to 80% and is spread mainly through soil, tubers or farm equipment. The objectives of this study were to: (i) describe the regional spatial arrangement of fields infested with *G. pallida* in southeastern Idaho; (ii) describe the spatiotemporal distribution of *G. pallida* in infested fields and the dispersal patterns of the nematode; (iii) determine the effect of the Idaho population of *G. pallida* on potato yield based on greenhouse assays; and (iv) simulate potato yield losses in Idaho field conditions by integrating the coefficients of potato yield into the SUBSTOR-DSSAT crop simulation model. For Idaho, the regional distribution patterns of fields infested with *G. pallida* was spatially-aggregated, and the spread of this nematode grew in diameter from the original center of infestation toward the southwest as an ellipsoidal-shaped cluster. In this area, the infestation of the nematode is spatially-clustered particularly around the edges of the fields, and the dispersal patterns of *G. pallida* followed the direction of cultivation. The prevalence of cysts declined in a non-linear process as the distance separation from the primary infestation focus increased. A power-law model was used to fit the nematode dispersal capabilities. Under greenhouse conditions, fresh tuber weight was reduced between 39% and 87% at *G. pallida* initial nematode density of 80 eggs/g soil. SUBSTOR-DSSAT model predicted a minimum yield between 12 and 58 ton/ha when initial nematode density was 80 eggs/g soil compared to 96 ton/ha in non-infested soil. The main goals of this study is to first provide information on the spatial pattern of the Idaho *G. pallida* infestation, and secondly, determine the impact of the Idaho population of *G. pallida* on potato yield to policymakers, stakeholders, potato growers and researchers to facilitate common understandings on the challenges and opportunities for controlling this pest in Idaho.

Acknowledgements

I would like to express my deepest appreciation to Dr. Louise-Marie Dandurand for imparting her knowledge and expertise during my research. I would like to thank my committee members Dr. Alexander Karasev, Dr. Joseph Kuhl and Dr. Christine Parent for their services on the graduate committee and for their constructive comments on the dissertation manuscript. I shall be forever grateful to the late Emeritus Professor Guy R. Knudsen for his guidance during the early years of my graduate research and for laying out the foundation of this modeling work. I gratefully acknowledge USDA National Institute of Food and Agriculture competitive grant no. 2015-69004-23634 for providing funding for this research. I would like to thank Dr. Tina Gresham of the USDA-APHIS for providing the field data for spatial analysis. I would like to thank the 2016 International Training Program on DSSAT (University of Georgia, Griffin, GA) for training in crop model simulation in DSSAT v.4.6; Dr. Steven Radil for training in spatial analysis; and Amanda Gray and Zahra Amiri for plant maintenance in greenhouse.

Dedication

I would like to thank my family and friends for their support during my academic formation.

Table of Contents

List of Tables

List of Figures

Chapter 1: *Globodera pallida*: A Global Menace for Potato Production Worldwide

Abstract

Plant-parasitic nematodes constitute a considerable menace for agricultural production worldwide. Approximately 4,100 species of plant-parasitic nematodes cause between $80 and $118 billion per year in crop losses worldwide. The world population is fast-approaching 9 billion people, which imposes serious challenge to food security. In order to increase food production, a comprehensive understanding of plant disease epidemiology and spatial patterns are warranted to better manage and control disease epidemics. The potato cyst nematode, *Globodera pallida,* is a globally regulated potato pest. It was detected for the first time in the U.S. in the state of Idaho in 2006, and the current infestation is limited to 1,326 ha. *Globodera pallida* is a specialized obligate sedentary endoparasite that can survive in soil for up to 30 years in the absence of its host. In highly infested fields, *G. pallida* can reduce tuber yields up to 80%. It is spread mainly through soil, tubers or farm equipment. This review focuses on, *G. pallida* ecology and parasitism, its impact for potato growers, phytosanitary measures for controlling and limiting its spread, and advances in understanding plant disease epidemiology as well as quantitative nematology. The framework of this review should facilitate a greater understanding of the threat and challenges of *G. pallida* for the potato industry, as well as possible opportunities for controlling this economically important pest.

Introduction

Plant-parasitic nematodes are economically important pests and a major threat for food security worldwide. Approximately 4,100 species of plant-parasitic nematodes have been identified (Decraemer and Hunt, 2006), and they cause between $80 and $118 billion per year in crop losses (Koenning et al., 1999; Sasser and Freckman, 1987). Nematodes were estimated to cause annual crop losses of $10 billion in the U.S. (Gianessi and Carpenter, 1999). The world population is fast-approaching 9 billion people, which imposes serious challenges to a secure and increased food production. Despite the increased need for a secure food supply, the scale and frequency of major plant disease outbreaks will continue to rise. In order to secure food production, a comprehensive understanding of plant disease epidemiology and spatial patterns are warranted to better manage and control epidemics that could potentially endanger our food provision and energy resources. In this globalized and more integrated world, international trade represents an important invasion pathway for non-native plant pests. Pest invasion consists of several phases (Ferris et al., 2003): (i) entry of the organism; (ii) establishment through local reproduction; (iii) integration into the local environment; and (iv) spread. Because of these risks, international trade agreements and phytosanitary measures were established and re-enforced to minimize risks of accidental introduction of plant pests to non-native areas. The United States Department of Agriculture-Animal and Plant Health Inspection Service (USDA-APHIS) is the U.S. Federal Agency charged to protect agricultural health from pests and diseases, and to rapidly manage or eradicate outbreak in the U.S.

The potato cyst nematode *Globodera pallida* (Behrens, 1975; Stone, 1972) is a globally regulated potato pest. It was detected for the first time in the U.S. in the state of Idaho in 2006, and currently the infestation is limited to 1,326 ha (USDA-APHIS, 2019). *Globodera pallida* and *Globodera rostochiensis* (Wollenweber, 1923; Skarbilovich, 1959), both potato cyst nematodes (PCN), co-evolved with potato and other native *Solanum* species in the Andean Region of South America (Picard et al., 2004). Potato cyst nematodes were first observed on potato roots in Germany in 1881, before spreading worldwide (CABI, 2018; Picard et al., 2004; Wollenweber, 1923). According to recent survey data, *G. rostochiensis* has been detected in 68 countries and *G. pallida* in 48 (CABI, 2018). *Globodera pallida* is a

specialized obligate sedentary endoparasite that can survive in the soil for up to 30 years in the absence of its potato host (Turner, 1996). In highly infested fields, *G. pallida* can reduce tuber yields up to 80% and is spread mainly through soil, tubers or farm equipment (Talavera et al., 1998; Vasyutin and Yakovleva, 1998). In Europe, where resistant varieties are available, PCN have been estimated to reduce potato production by 9% annually (Turner and Rowe, 2006). European PCN populations are divided into eight groups or pathotypes [*G. rostochiensis* (Ro1, Ro2, Ro3, Ro4, and Ro5); *G. pallida* (Pa1, Pa2, and Pa3)] based on their virulence, and are extensively dispersed across the continent in high density levels in some fields (Kort et al. 1977). The first symptomatic presence of PCN in potato in the UK was reported by a farmer in Yorkshire in 1904 (Massee, 1913; Strachan and Taylor, 1926), since then, PCN populations built up to high density levels and became widespread into most major potato growing areas. In the UK, PCN are the second most economically important potato pest after late blight, costing £26 million per year in potato yield loss (Twining et al., 2009). In the UK, following the widespread planting of potato cultivars resistant to only *G. rostochiensis,* an increase in *G. pallida* infestations was observed (Minnis et al., 2002). Potato cyst nematodes are found in 64% of the potato fields in the UK, with *G. pallida* found in over 90% of infestations (Minnis et al., 2002).

Plant disease epidemiology is a rapidly growing research topic in plant pathology. The first models of crop disease epidemics were developed by Van Der Planck (1960), building the foundation for subsequent crop disease modeling. Kranz and Royle (1978) classified epidemiological models into three types: (i) descriptive models, which provide hypothesis and generalize experimental results; (ii) predictive models (also descriptive), which allow prediction of the occurrence and severity of epidemics; and (iii) conceptual models, which identify the causes and effects of specific events on epidemic development. Quantitative research on plant nematode disease epidemics are focused on: (i) modeling the relationship between initial (P_i) and final (P_f) egg densities; and (ii) evaluating the impacts of nematode infection on host growth (Brodie, 1996; Ferris, 1985; Jones et al., 1967; Jones and Kempton, 1978; LaMondia and Brodie, 1986; Seinhorst, 1965; Seinhorst and Ouden, 1971). Potato cyst nematodes produce only one infection cycle per crop cycle in temperate regions and cause the development of monocyclic disease. In a monocyclic epidemic, such as with *G. pallida*, the initial nematode inoculum represents a fundamental component of disease

intensity over time (Seinhorst, 1965). The early stages of monocyclic epidemics are characterized by a linear model, and a reduction in the initial inoculum or the rate of infection will result in a reduction of the disease level by the same proportion at any time throughout the epidemic (Madden et al., 2007). Pylypenko (1999) reported a linear relationship for *G. rostochiensis*; for a resistant potato cultivar, 55 eggs per gram soil were associated with a 3.3% yield loss, whereas a 37.7% yield loss was observed for susceptible variety; but populations of 121 eggs per gram soil were associated with losses of 16.9% and 63.3%, respectively.

The main objective of crop disease modeling is to capture and understand the determinants of epidemic development in order to develop comprehensive disease management and control programs. The pathogen reproduction rate, considered as one measure of disease risk, provides quantitative information on the disease development and provides a basis for developing disease control programs that will reduce crop losses and disease incidence (Madden and Nutter, 1995; Savary et al., 2006). The goals of disease management and control (Nutter, 2001; Zadoks, 1985) are to: (i) eliminate or reduce the initial pathogen inoculum; (ii) reduce the disease infection rate; and (iii) reduce the time of pathogen-host interactions to reduce disease intensity.

Ecology, parasitism and phytosanitary regulations

***Globodera pallida* ecology and distribution.** *Globodera pallida* is native to the central Andes (Peru and Bolivia) and is a parasite of the genus *Solanum*, its unique host-plant taxon, with which it shares a long co-evolutionary history (Evans and Stone, 1977). The major plant hosts of *Globodera* spp. are restricted to Solanaceae, in particular potato, tomato and aubergine, however tomato and aubergine are weak hosts (Mai, 1952; Roberts and Stone, 1981). *Globodera pallida* is mainly found between 2,000 m and 4,000 m above sea level, with the heaviest infestations between 2,900 m and 3,800 m above sea level (Evans and Stone, 1977). Plantard et al. (2008) located the origin of Western European *G. pallida* populations from a single restricted area in the extreme south of Peru, between the north shore of the Lake Titicaca and Cuzco. Potato culture is estimated to have begun 5,000 years ago in the Andean Cordillera, and the Inca growers struggled with the impact of PCN on

yield (Thurston, 1994). A 6 and 8-year rotation of potato crops were used by the Incas to avoid severe yield losses, and such rotation is believed to have allowed time for population levels to fall below the economic threshold (Thurston, 1994). Phylogeographical studies using mitochondrial and nuclear markers showed that a northward colonization of PCN in the Andes during geological times suggested multiple host-shifts from wild to cultivated potatoes (Picard et al., 2007). However, long-range dispersal (more than 320 km) was probably limited by major biogeographical barriers (Andean mountain range), and the limited active dispersal of juveniles from their cyst coincided with high level of population inbreeding, as demonstrated by Picard et al. (2004) using eight polymorphic microsatellites markers. Picard and Plantard (2006) showed that genetic differentiation occurred among infested fields with *G. pallida* at a distance more than 50 km of separation, where the process of isolation by distance (IBD) forced the development of population genetic diversity in *G. pallida*. High level of PCN population inbreeding have serious consequences for the control and deployment of resistant potato cultivars because of the production of homozygotes (most plant disease-resistance genes are known to be dominant while the corresponding pathogen-avirulence genes are recessive) (Picard et al., 2004).

***Globodera pallida* life cycle and feeding mechanisms**. Potato root exudates are required to stimulate *G. pallida* egg hatchings (Rawsthorne and Brodie, 1986), and the stimulatory effect can be detected up to 80 cm away from roots and persisted in soil for a long time after plant removal (Malinowska, 1996). After hatching, the infective second-stage juvenile (J2) locates the potato root, penetrates, and initiates the formation of a syncytium (fusion of cells), which provides the nutrients necessary for continued development and reproduction, and once feeding begins, the J2 swells and becomes sedentary (Koenning and Sipes, 1998). The second-stage juveniles are sexually undifferentiated, and sex is determined through epigenetic factors such as environmental conditions, and the amount and quality of food supply (Betka et al., 1991; Grundler et al., 1991; Mugniéry and Bossis, 1985; Mugniéry and Fayet, 1981, 1984). Further growth and development of the J2 leads to the third-stage juvenile (J3). Cyst nematodes are sexually dimorphic species, adult males are vermiform and motile, whereas adult females are swollen and sedentary (Raski, 1950). At the fourth-stage juvenile (J4), spermatogenesis takes place, and the male may produce several thousand sperms, exit the roots, and seek females (Shepherd and Clark, 1983). The J3 females continue

to swell in the roots, becoming globose-shaped, then rupture the root epidermis with her posterior end, exposing her vulva to the rhizosphere for insemination by the adult males (Raski, 1950). After insemination, females begin production of up to 600 eggs (Brodie et al. 1993), leading to subsequent transformation into a cyst which encapsulates the eggs. The persistence of *G. pallida* cysts for many years in the soil in the absence of potato crops remains a challenge for control and eradication strategies. Plant nematode resistance genes are usually derived from wild relatives of crop species (Tomczak et al., 2008), and resistance against cyst nematodes decreases nematode population density (Müller, 1998). Proliferation of the syncytial cytoplasm is weak or not observed, as showed when *G. rostochiensis* J2s invade potato roots with the *H1* resistance gene, and necrosis appears in cells located around the juvenile and then in cells surrounding the syncytium, isolating it from adjacent alive cells (Bleve-Zacheo et al., 1990; Rice et al., 1985).

Phytosanitary legislations and plant health regulations. Phytosanitary measures are used to minimize the transport and spread of harmful plant pathogens. The International Plant Protection Convention (IPPC) defines 'quarantine pest' as 'a pest of potential economic importance to the area endangered thereby and not yet present there, or present but not widely distributed and being officially controlled'. The invasion process of exotic nematode species consists of arrival, establishment, integration, and spread (Ferris et al. 2003). Plant-parasitic nematodes gain entry to new areas through imported agricultural commodities, while establishment and integration are achieved mainly through local nematode reproduction before spreading to nearby fields (Ferris et al. 2003). Intervention strategies to prevent the establishment of exotic nematodes include (Ferris et al. 2003): (i) exclusion through cultural methods of control (use of certified seed) and quarantines (prohibition of planting host crops in infested fields); (ii) eradication of the nematode from infested sites (fumigation); and (iii) containment to minimize the potential spread of the nematode (restrictions of soil and plant materials movement, and decontamination of field equipment). However, when plant-parasitic nematodes are long-established and integrated into the cropping system, a management program is required to keep the local population below the level of economic damage threshold or detection limit. Phytosanitary measures against plant-parasitic nematodes were first implemented in the U.S. in 1909 against cherry trees infested with *Meloidogyne* spp., and the first Plant Quarantine Act to protect the nation's agricultural

health was approved by U.S. Congress in 1912 (Hockland et al., 2006). The Golden Nematode Act was passed in 1948 to protect the U.S. potato industry against *G. rostochiensis* (Hockland et al., 2006). The enforcement of quarantine regulation in Idaho greatly contributed in restricting *G. pallida* infested fields to a small area of 1,326 ha (USDA-APHIS, 2019). As PCN can suppress potato yields by more than 80%, the benefits of excluding these nematodes from potato growing areas in the U.S. are estimated to be $300 million annually (Dwinell and Lehman, 2004; Hockland et al., 2006). These benefits are far greater than the $445,000 annual costs required for preventing the spread of *G. rostochiensis* in and outside New York and $8.4 million annually (from 2006 to 2012) for eradicating *G. pallida* in Idaho (Dwinell and Lehman, 2004; Hockland et al., 2006). Hodda and Cook (2009) estimated, in the absence of potato cyst nematodes regulation, the economic losses for Australian agriculture could exceed $370 million.

The situation of *Globodera pallida* in Idaho. This pest was found in southeastern Idaho in 2006 in two potato fields in Bingham County (Hafez et al., 2007; USDA-APHIS, 2019). USDA-APHIS and the Idaho State Department of Agriculture (ISDA) have listed *G. pallida* as a quarantine pest for Idaho under Title 7 CFR 301.86 Federal Regulation. USDA-APHIS and ISDA have implemented a containment and eradication program to prevent *G. pallida* spread to other potato fields. In fields infested with *G. pallida*, the program outlines: (i) restrictions on the movement of soil and plant materials; (ii) prohibition of planting potato and other solanaceous crops; and (iii) sanitation procedures for farm equipment. Soil fumigation with the nematicide Telone II (1,3-dichloropropene) are being conducted in infested fields as part of the *G. pallida* eradication program (USDA-APHIS, 2019). Growing the trap crop *Solanum sisymbriifolium* 'litchi tomato' is being investigated in large field trials (USDA-APHIS, 2019). The regulated area includes portions of northern Bingham and southern Bonneville Counties and is currently limited to 3,057 hectares, of which 1,326 ha are fields infested with *G. pallida* (USDA-APHIS, 2019). USDA-APHIS have issued a list of regulated articles: (i) *G. pallida*; (ii) *G. pallida* host crops (eggplant [*Solanum melongena*], pepper [*Capsicum* spp.], tomatillo [*Physalis philadelphica*], tomato [*Solanum esculentum*]); (iii) root crops; (iv) garden and dry beans (*Phaseolus* spp.) and peas (*Pisum* spp.); (v) all nursery stock; (vi) soil, compost, humus, muck, peat and manure; (vii) hay, straw and fodder; and (viii) any equipment or conveyance used in an infested or associated field that can carry

soil if move out of the field. USDA-APHIS provides steps for deregulating *G. pallida* infested fields: (i) no viable eggs detected (collected eggs are testing for viability); (ii) three rounds of greenhouse bioassay of field cysts to confirm absence of reproduction; and (iii) in-field bioassay where fields can be released from quarantine status after three more negative viability surveys after harvests of a susceptible crop. As of 2019, 22 fields (969 ha) have passed step 1 (no viable eggs found) and 18 fields (720 ha) have passed step 2 (no reproduction) (USDA-APHIS, 2019).

Idaho is the largest producer, packer and processor of potatoes in the U.S. with a production value of $1.19 billion in 2017 (USDA-NASS, 2018). In 2017, the U.S. value of potato production is estimated to $4.56 billion, and Japan, Canada, Mexico and South Korea are the top customers of U.S. potatoes (USDA-NASS, 2018). The presence of *G. pallida* in Idaho constitutes a considerable threat for the potato industry and resistance to this nematode in russet-type potato cultivars is currently unavailable for the U.S. (Whitworth et al., 2018). However, the extent of *G. pallida* in Idaho is limited to a small area with low nematode population levels and represents less than 1% of annual potato production areas. Contina et al. (2018) showed that the fields infested with *G. pallida* in Idaho are spatially aggregated as an ellipsoidal-shaped cluster around a radius of 12 km. *Globodera pallida* spread followed a contagion effect scenario, where infested fields contributed to the infestation of nearby fields, probably through soil contaminated agricultural equipment (Contina et al., 2018). The presence of *G. pallida* in Idaho is unlikely to be associated with new introductions from outside the state (Contina et al., 2018). USDA-APHIS quarantine and eradication programs are monitoring the presence of *G. pallida* in potato fields through intensive soil sampling and testing at regular time intervals. Research on the control of *G. pallida* in Idaho is focused on developing resistant potato varieties, trap crops as well as biofumigants and biocontrol agents (Contina et al., 2017; Dandurand and Knudsen, 2016; Dandurand et al., 2017; Whitworth et al., 2018).

Plant disease epidemiology and quantitative nematology

Plant disease epidemiology. Quantitative epidemiology provides the tools for measuring plant diseases and assessing their determining factors. Stevens (1960) was probably the first to draw the disease triangle to illustrate the host-pathogen-environment pathosystem. Measuring the variables associated with the host, the pathogen and the environment helps in assessing the degree of pathogen virulence, the susceptibility of the host and the environmental conduciveness for disease development (Agrios, 2005; Campbell and Madden, 1990; Madden et al., 2007). Common mathematical procedures for quantitative epidemiology include: (i) analysis of variance, which allows to make inferences from observations of random samples obtained in experiments (Gilligan, 1986; Madden et al., 2007); (ii) linear regression analysis, which fits experimental data with linear models (Madden et al., 2007); (iii) path analysis, which uses linear regression techniques to explain relationships between variables (Hampton, 1975; Lundquist, 2007; Pethybridge et al., 2011; Van Bruggen and Arneson, 1986); (iv) non-linear regression analysis, which fits experimental data with non-linear models (Madden et., 2007); (v) discriminant analysis, which analyzes and describes the extent to which different groups of populations overlap or differ (Broders et al., 2009; Jiménez-Díaz et al., 2011; Noe and Barker, 1985); (vi) cluster analysis, which investigates the structure of a given data and divides them into groups (Ghazvini and Tekauz, 2008; Pataky et al., 1988); (vii) principal component analysis, which reduces complex relationships in observed data into simpler forms (Cowger and Murphy, 2007; Jeger, 1980; Madden and Pennypacker, 1979; Okubara et al., 2014); (viii) Bayesian analysis, which uses statistical probability to predict plant diseases outbreak (Mila and Carriquiry, 2004; Mila and Ngugi, 2011; Yuen and Hughes, 2002); (ix) spatial analysis, which analyses and describes the spatial distribution of disease epidemics (Contina et al., 2018; Gavassoni et al., 2001; Holguin et al., 2015; Knudsen, 1989; Knudsen et al., 2006; Knudsen and Schotzko, 1999; Turechek and Madden, 1999); and (x) artificial neural network analysis (machine learning and data mining), which learns from the information provided by training itself using the data, extracting subtle patterns, deciphering complex relationships among variables and optimizing the variable weights (weights are analogous to coefficients

in regression modeling) for a better prediction (Ahmadi et al., 2017; De Wolf and Francl, 1997; De Wolf and Francl, 2000; Francl, 2004; Yang and Batchelor, 1997).

Quantitative nematology. Numerous PCN models and simulation platforms, based on many years of field trials, were directly developed to evaluate the impact of PCN on yields, determine the economic threshold, estimating soil sampling methods and nematode probability detection, and to assess the effectiveness of nematicides, trap crops and resistant cultivars on nematode population dynamics in the field (Been et al., 2005; Jones and Kempton, 1980; Moxnes and Hausken, 2007; Schomaker and Been, 1999; Ward et al., 1985). Ward et al. (1985) constructed a model to simulate the population dynamics of *G. pallida* and its effect on potato growth. They found that the dispersal of *G. pallida* is severely limited and that long-term control measures can be planned. Been et al. (2005) developed NemaDecide, a decision support system for the management of PCN, based on the results from 50 years of Dutch quantitative nematological research that had been structured into stochastic models and integrated in a software package. NemaDecide was used as a quantitative information system to enable growers to estimate risks of yield losses, to determine population development, to estimate the probability of detection of nematode foci by soil sampling, to calculate the cost/benefit of control measures and to provide adequate advice for growers to optimize financial returns. Moxnes and Hausken (2007) provided a mathematical model based on the theory of differential equations to explain the population dynamics of PCN. They simulated the effect of altering the season length, growing resistant potatoes, not growing potatoes, and the effect of nematicides on disease incidence and severity. Their model enabled the prediction of PCN proliferations and outlined the implications of intervention scenarios to regulate this pest in order to secure optimal potato growth.

Spatial analysis applied to plant-parasitic nematodes. Spatial analysis of plant pathogen infestations in fields provides useful information on the spatial pattern and spatio-temporal dynamics of disease progression and outlines the probabilities of pathogens entering new areas. Therefore, spatial analysis and modeling techniques can be used to assess and evaluate the threat of plant diseases for agricultural production. The term ‘spatial analysis’ can be traced back to the 1950s, widely used in the Geographical Information Systems (GIS), and represents a collection of techniques and models that use the spatial referencing associated with each data value and attributes to explain a phenomenon (Haining,

2003; Tobler, 1979). Spatial analysis is divided into three main components (Haining, 2003): (i) cartographic modeling, where a data set is represented as a map; (ii) mathematical modeling, where the outcomes of a model are dependent on the characteristic of spatial interaction between the geographical positioning of objects within the model; and (iii) statistical application, where statistical tools and packages are used to fit spatial data into a predictive model. Within spatial analysis, point pattern analysis is used to characterize the distribution pattern of a set of events delimited in the Euclidean space R^2 or R^3. Knowledge is generated by fitting models to patterns, while ascribing scientific interpretations to model parameters.

Point pattern analysis (PPA) is divided into: (i) first-order property of PPA, where under the presence of complete spatial randomness (CSR), each random location of an event is drawn independently from an unknown distribution and is associated with a probability density function (Silverman, 1986); and (ii) second-order property of PPA, where the occurrences of events are related in some way (Ripley, 1976, 1981). CSR analysis validates that events are distributed randomly over a study region, and common tests performed under CSR hypothesis are quadrat analysis and maximum absolute deviation (Ripley, 1977, 1981; Thomas, 1977). The kernel density estimation (KDE) is used as a non-parametric method to estimate the probability density function of a random variable (Silverman, 1986). The Ripley's K-function analysis is used as a second-order property of PPA to evaluate deviations of events from spatial homogeneity toward spatial clustering or dispersion (Ripley, 1976, 1981) and is widely used in plant ecology; it has been applied to study the distribution patterns of herbs (Kenkel, 1993), desert shrubs (Prentice and Werger, 1985; Skarpe, 1991) and tropical forest trees (Sterner et al. 1986).

Geostatistics is used as a tool of spatial interpolation analysis to process the effect of event aggregations or dispersions along with the uncertainties represented by spatial heterogeneity and to estimate a spatial prediction model known as kriging (Cressie, 1993). Kriging is a linear unbiased spatial interpolation method that provides minimum mean-squared error estimates at unsampled locations and is controlled by semivariogram models, which quantify spatial variability of the data and provide information on the spatial autocorrelation of the datasets (Oliver, 1990; Royle et al. 1981). Kriging generates spatial data using a number generator based on the specified semivariogram model and the pre-

existing set of the sample data (Englund, 1993). Other global interpolators like the nearest neighbor algorithm (NN) and the inverse distance weighting (IDW) are widely used in spatial interpolation analysis to approximate attributes to unsampled locations based on sampled ones within a study region. Unlike kriging, NN and IDW are referred to as deterministic interpolation methods because they are directly based on the surrounding measured values or on specified mathematical formulas that determine the smoothness of the resulting surface (Jenkins et al. 1985).

Spatial analysis applied to plant-parasitic nematodes has been used to develop accurate sampling methods in fields (Dinardo-Miranda and Fracasso, 2009; Francl, 1986), determine ecological patterns of nematode distribution (Porazinska et al. 2012), support the use of site-specific management in nematode infested fields (Avendaño et al. 2003), model spatial pattern distribution of nematode populations and estimate the likelihood of new infestation (Madden and Hughes, 1995; Noe and Campbell, 1985; Schomaker and Been, 1999; Shaukat and Khan, 1993). Schomaker and Been (1999) designed a model for infestation foci of potato cyst nematodes by using multiple sampling grids from eighty-two infested fields, and the data were analyzed and fitted for spatial distribution of cysts using exponential models. Gavassoni et al. (2001) used geostatistical analysis to quantify the effects of tillage on the spatial patterns of *Heterodera glycines* in infested fields. Evans et al. (2003) used spatial analysis to target 'hot spots' of potato cyst nematode infestations for additional treatment with fumigant, thereby reducing the cost of chemicals applied and minimizing possible environmental damage.

The objectives of this dissertation were to: (i) describe the regional spatial arrangement of fields infested with *G. pallida* in southeastern Idaho; (ii) describe the spatiotemporal distribution of *G. pallida* in infested fields and the dispersal patterns of the nematode; (iii) determine the effect of the Idaho population of *G. pallida* on potato yield; and (iv) simulate potato yield losses in Idaho field conditions by integrating the coefficients of potato yield into the SUBSTOR-DSSAT crop simulation model. The main goals of this study is to provide information on *G. pallida* distribution and its impact on potato yield to policymakers, stakeholders, potato growers, and researchers to facilitate common understandings on the challenges and opportunities for controlling this pest in Idaho.

Literature cited

Agrios, G. N. 2005. Plant pathology. 5th ed. Elsevier-Academic Press. San Diego, CA.

Ahmadi, P., Muharam, F. M., Ahmad, K., Mansor, S., and Seman, I. A. 2017. Early detection of Ganoderma basal stem rot of oil palms using artificial neural network spectral analysis. Plant Dis. 101:1009-1016.

Avendaño, F., Schabenberger, O., Pierce, F. J., and Melakeberhan, H. 2003. Geostatistical analysis of field spatial distribution patterns of soybean cyst nematode. Agron. J. 95:936-948.

Been, T. H., Schomaker, C. H., and Molendijk, L. P. G. 2005. NemaDecide: A decision support system for the management of potato cyst nematodes. Pages 143-155 in: Potato in progress: Science meets practice, A. J. Haverkort, and P. C. Struik, eds. Wageningen Academic Publishers, Netherlands.

Behrens, E. 1975. *Globodera Skarbilovic*, 1959, eine selbstaendige Gattung in der Unterfamilie Heteroderinae Skarbilovic, 1947 (Nematoda: Heteroderidae). Vortragstagung zu aktuellen Problemen der Phytonematologie am 29/5/1975 in Rostock. Manuskriptdruck der Vortraege. Rostock, 1975:12-26.

Betka, M., Grundler, F., and Wyss, U. 1991. Influence of changes in the nurse cell system (syncytium) on the development of the cyst nematode Heterodera schachtii: Single amino acids. Phytopathology 81:75-79.

Bleve-Zacheo, T., Melillo, M. T., and Zacheo, G. 1990. Ultrastructural response of potato roots resistant to cyst nematode Globodera rostochiensis pathotype Ro1. Rev Nématol 13:29-36.

Broders, K. D., Wallhead, M. W., Austin, G. D., Lipps, P. E., Paul, P. A., Mullen, R. W., and Dorrance, A. E. 2009. Association of soil chemical and physical properties with *Pythium* species diversity, community composition, and disease incidence. Phytopathology 99:957-967.

Brodie, B. B. 1996. Effect of initial nematode density on managing *Globodera rostochiensis* with resistant cultivars and nonhosts. J. Nematol. 28:510-519.

Brodie, B. B., Evans, K., and Franco, F. 1993. Nematode parasites of potatoes. Pages 87-132 in: Plant-parasitic Nematodes in Temperate Agriculture. K. Evans, D. L. Trudgill, J. M. Webster, eds. CAB International, Wallingford, UK.

CABI. 2018. *Globodera pallida* (white potato cyst nematode). Online publication. Centre for Agriculture and Biosciences International. https://www.cabi.org/ISC/datasheet/27033.

Campbell, C. L., and Madden, L. V. 1990. Introduction to plant disease epidemiology. John Wiley & Sons, New York.

Contina, J. B., Dandurand, L. M., and Knudsen, G. R. 2017. Use of GFP-tagged *Trichoderma harzianum* as a tool to study the biological control of the potato cyst nematode *Globodera pallida*. Appl. Soil Ecol. 115:31-37.

Contina, J. B., Dandurand, L. M., and Knudsen, G. R. 2018. A spatial analysis of the potato cyst nematode *Globodera pallida* in Idaho. Phytopathology 108:988-1001.

Cowger, C., and Murphy, J. P. 2007. Artificial inoculation of wheat for selecting resistance to *Stagonospora nodorum* blotch. Plant Dis. 91:539-545.

Cressie, N. 1993. Geostatistics: A tool for environmental modelers. Pages 415-421 in: Environmental modelling with GIS, M. F. Goodchild, B. O Parks, and L. T Steyaert, eds. Oxford University Press Inc., New York.

Dandurand, L. M., and Knudsen, G. R. 2016. Effect of the trap crop *Solanum sisymbriifolium* and two biocontrol fungi on reproduction of the potato cyst nematode *Globodera pallida*. Ann. Appl. Biol. 169:180-189.

Dandurand, L. M., Morra, M. J., Zasada, I. A., Phillips, W. S., Popova, I., and Harder, C. 2017. Control of *Globodera* spp. using *Brassica juncea* seed meal and seed meal extract. J. Nematol. 49:437-445.

Decraemer, W., and Hunt, D. J. 2006. Structure and classification. Pages 3-52 in: Plant Pathology, R. N. Perry, and M. Moens, eds. CABI Publishing, Wallingford, UK.

De Wolf, E. D., and Francl, L. J. 1997. Neural networks that distinguish infection periods of wheat tan spot in an outdoor environment. Phytopathology 87:83-87.

De Wolf, E. D., and Francl, L. J. 2000. Neural network classification of tan spot and Stagonospora blotch infection periods in a wheat field environment. Phytopathology 90:108-113.

Dinardo-Miranda, L. L., and Fracasso, J. V. 2009. Spatial distribution of plant-parasitic nematodes in sugarcane fields. Sci. Agric. 66:188-194.

Dwinell, L. D., and Lehman, P. S. 2004. Plant-parasitic nematodes which are exotic pests in agriculture and forestry. Pages 51-70 in: Biological Pollution: An Emerging Global Menace, K. O. Briton, ed. American Phytopathological Society Press, St Paul, Minnesota.

Englund, E. J. 1993. Spatial simulation: Environmental applications. Pages 432-437 in: Environmental modelling with GIS, M. F. Goodchild, B. O Parks, and L. T Steyaert, eds. Oxford University Press Inc., New York.

Evans, K., and Stone, A. R. 1977. A review of the distribution and biology of the potato cyst nematodes *Globodera rostochiensis* and *G. pallida*. Pans. 23:178-189.

Evans, K., Webster, R., Barker, A., Halford, P., and Russel, M. 2003. Mapping infestations of potato cyst nematodes and the potential for spatially varying application of nematicides. Prec. Agric. 4:149-162.

Francl, L. J. 2004. Squeezing the turnip with artificial neural nets. Phytopathology 94:1007-1012.

Ferris, H. 1985. Population assessment and management strategies for plant-parasitic nematodes. Agric. Ecosyst. Env. 12:285-299.

Ferris, H., Jetter, K. M., Zasada, I., Chitambar, J. J., Venette, R. C., Klonsky, K. M., and Becker, J. O. 2003. Risk assessment of plant-parasitic nematodes. Pages 99-119 in: Exotic pests and diseases: Biology and economics for biosecurity, D. A. Summer, ed. Iowa State University Press.

Francl, L. J. 1986. Spatial analysis of *Heterodera glycines* populations in field plots. J. Nematol. 18:183-189.

Gavassoni, W. L., Tylka, G. L., and Munkvold, G. P. 2001. Relationships between tillage and spatial patterns of *Heterodera glycines*. Phytopathology 91:534-545.

Ghazvini, H., and Tekauz, A. 2008. Host-pathogen interactions among barley genotypes and *Bipolaris sorokiniana* isolates. Plant Dis. 92:225-233.

Gianessi, L. P., and Carpenter, J. E. 1999. Introduction. Pages 1-2 in: Agricultural biotechnology: Insect control benefits. Report of the National Center for food and Agricultural Policy, Washington, DC.

Gilligan, C. A. 1986. Use and misuse of the analysis of variance in plant pathology. Pages 225-261 in: Advances in Plant Pathology. D. S. Ingram, and P. H. William, eds. Academic Press, London, New York.

Gilligan, C. A. 1990. Comparison of disease progress curves. New Phytol. 115:223-242.

Hafez, S. L., Sundararaj, P., Handoo, Z. A., Skantar, L., Carta, K., and Chitwood, D. J. 2007. First report of the Pale Cyst Nematode, *Globodera pallida*, in the United States. Plant Dis. 91:325.

Haining, R. 2003. Spatial data analysis: Theory and practice. Cambridge University Press. Cambridge, UK.

Hampton, R. O. 1975. The nature of bean yield reduction by bean yellow and bean common mosaic virus. Phytopathology 65:1342-1346.

Hockland, S., Inserra, R. N., Millar, L., and Lehman, P. S. 2006. International plant health: Putting legislation into practice. Pages 328-343 in: Plant Nematology. R. N. Perry and M. Moens, eds. CAB International, Oxfordshire, UK.

Hodda, M., and Cook, D. C. 2009. Economic impact from unrestricted spread of potato cyst nematodes in Australia. Phytopathology 99:1387-1393.

Holguin, C. M., Gerard, P., Mueller, J. D., Khalilian, A., and Agudelo, P. 2015. Spatial distribution of reniform nematode in cotton as influenced by soil texture and crop rotations. Phytopathology 105:674-683.

Jeger, M. J. 1980. Multivariate models of components of partial resistance. Prot. Ecol. 2:265-269.

Jenkins, W., Mather, B., and Munson, D. 1985. Nearest neighbor and generalized inverse distance interpolation for Fourier domain image reconstruction. Proc. IEEE. 73:1069-1072.

Jiménez-Díaz, R. M., Olivares-García, C., Landa, B. B., Jiménez-Gasco, M. M., and Navas-Cortés, J. A. 2011. Region-wide analysis of genetic diversity in *Verticillium dahlia* populations infecting olive in southern Spain and agricultural factors influencing the distribution and prevalence of vegetative compatibility groups and pathotypes. Phytopathology 101:304-315.

Jones, F. G. W., Parrott, D. M., and Ross, G. J. S. 1967. The population genetics of the potato cyst nematode, *Heterodera rostochiensis*: Mathematical models to simulate the

effects of growing eelworm-resistant potatoes bred from *Solanum tuberosum* ssp. *andigena*. Ann. Appl. Biol. 60:151-171.

Jones, F. G. W., and Perry, J. N. 1978. Modelling populations of cyst-nematodes (Nematoda: Heteroderidae). J. Appl. Ecol. 15:349-371.

Jones, F. G. W., and Kempton, R. A. 1978. Population dynamics, population models and integrated control. Page 333 in: Plant Nematology. J. F. Southey, ed. M.A.F.F. A.S. Publication G.D./1 H.M. Stationary Office, London.

Kenkel, N. C. 1993. Modeling Markovian dependence in populations of *Aralia nudicaulis*. Ecology 74:1700-1706.

Koenning, S. R., Overstreet, C., Noling, J. W., Donald, P. A., Becker, J. O., and Fortnum, B. A. 1999. Survey of crop losses in response to phytoparasitic nematodes in the United States for 1994. J. Nematol. 31:587-618.

Koenning, S. R., and Sipes, B. S. 1998. Biology of cyst nematodes. Page 159 in: the cyst Nematodes. S. B. Sharma, ed. Chapman and Hall, London, UK.

Knudsen, G. R. 1989. Model to predict aerial dispersal of bacteria during environmental release. Appl. Environ. Microbiol. 55:2641-2647.

Knudsen, G. R., and Schotzko, D. J. 1999. Spatial simulation of epizootics caused by *Beauveria bassiana* in Russian wheat aphid populations. Biological control 16:318-326.

Knudsen, G. R., Stack, J. P., Schuhmann, S. O., Orr, K., and LaPaglia, C. 2006. Individual-based approach to modeling hyphal growth of a biocontrol fungus in soil. Phytopathology 96:1108-1115.

Kort, J., Ross, H., Rumpenhost, H. J., and Stone, A. R. 1977. An interaction scheme for identifying and classifying pathotypes of potato cyst nematodes *Globodera rostochiensis* and *G. pallida*. Nematologica 23:333-339.

Kranz, J., and Royle, D. J. 1978. Perspectives in mathematical modelling of plant disease epidemics. Pages 111-120 in: Plant Disease Epidemiology. P. R. Scott, and A. Bainbridge, eds. Blackwell Scientific Publications, Oxford, London, Edinburgh, Melbourne.

LaMondia, J. A., and Brodie, B. B. 1986. Effects of initial nematode density on population dynamics of *Globodera rostochiensis* on resistant and susceptible potatoes. J. Nematol. 18:159-165.

Lundquist, J. E. 2007. The relative influence of diseases and other small-scale disturbances on fuel loading in the Black Hills. Plant Dis. 91:147-152.

Madden, L. V., and Hughes, G. 1995. Plant disease incidence: Distributions, heterogeneity, and temporal analysis. Ann. Rev. Phytopathology 33:529-64.

Madden, L. V., Hughes, G., and van den Bosch, F. 2007. The study of plant disease epidemics. The American Phytopathological Society, APS Press St. Paul, Minnesota.

Madden, L. V., and Nutter, F.W. 1995. Modeling crop losses at field scale. Can. J. Plant Pathol. 17:174-185.

Madden, L. V., and Pennypacker, S. P. 1979. Principal component analysis of tomato early blight epidemics. Phytopathology 95:364-369.

Mai, W. F. 1952. Susceptibility of *Lycopersicon* species to the golden nematode. Phytopathology 42:461.

Malinowska, E. 1996. The range of stimulatory action of the nematode resistant cultivar Tarpan on hatching of juveniles from the cysts of golden potato nematode (Ro1 pathotype) under field conditions. Biuletyn Instytut Ziemniaka 46:104.

Massee, G. 1913. Nematodes or eelworms. Kew Bulletin 9:343-351.

Mila, A. L., and Carriquiry, A. L. 2004. Bayesian analysis in plant pathology. Phytopathology 94:1027-1030.

Mila, A. L., and Ngugi, H. K. 2011. A Bayesian approach to meta-analysis of plant pathology studies. Phytopathology 101:42-51.

Minnis, S. T., Haydock, P. P. J., Ibrahim, S. K., and Grove, I. G. 2002. Potato cyst nematodes in England and Wales: Occurrence and distribution. Ann. Appl. Biol. 102:187-195.

Moxnes, J. F., and Hausken, K. 2007. The population dynamics of potato cyst nematodes. Ecol. Model. 207:339-348.

Mugniéry, D., and Bossis, M. 1985. Influence de l'hôte, de la compétition et de l'état physiologique des juvéniles sur la pénétration, le développement et le sexe de *Heterodera carotae* Jones. Nematologica 35:335-343.

Mugniéry, D., and Fayet, G. 1981. Détermination du sexe chez *Globodera pallida* Stone. Rev. Nématol. 4:41-45.

Mugniéry, D., and Fayet, G. 1984. Détermination du sexe de *Globodera rostochiensis* Woll et influence des niveaux d'infestation sur la pénétration, le développement et le sexe de ce nématode. Rev. Nématol. 7:233-238.

Müller, J. 1998. New pathotypes of the beet cyst nematode (*Heterodera schachtii*) differentiated on alien genes for resistance in beet (*Beta vulgaris*). Fund. Appl. Nematol. 21:519-526.

Noe, J. P., and Barker, K. R. 1985. Relation of within-field spatial variation of plant-parasitic nematode population densities and edaphic factors. Phytopathology 75:247-252.

Noe, J. P., and Campbell, C. L. 1985. Spatial pattern analysis of plant-parasitic nematodes. J. Nematol. 17:86-93.

Nutter, F. W. 2001. Disease assessment terms and concepts. Pages 312-323 in: Encyclopedia of Plant Pathology. O. C. Maloy, and T. D. Murray, eds. John Wiley and Sons, Inc., New York.

Okubara, P. A., Schroeder, K. L., Abatzoglou, J. T., and Paulitz, T. C. 2014. Agroecological factors correlated to soil DNA concentrations of *Rhizoctonia* in dryland wheat production zones of Washington state, USA. Phytopathology 104:683-691.

Oliver, M. A. 1990. Kriging: A method of interpolation for Geographical Information Systems. Int. J. Geogr. Inf. Sci. 4:313-332.

Pataky, J. K, Headrick, J. M., and Suparyono. 1988. Classification of sweet corn hybrid reactions to common rust, northern leaf blight, Stewart's wilt, and Goss's wilt and associated yield reductions. Phytopathology 78:172-178.

Pethybridge, S. J., Gent, D. H., and Hay, F. S. 2011. Epidemics of ray blight on pyrethrum are linked to seed contamination and overwintering inoculum of *Phoma ligulicola* var. *inoxydabilis*. Phytopathology 101:1112-1121.

Picard, D., and Plantard, O. 2006. What constitutes a population for the plant parasitic nematode *Globodera pallida* in its native area (Peru)? Int. J. Parasitol. 36:115-122.

Picard, D., Plantard, O., Scurrah, M., and Mugniéry, D. 2004. Inbreeding and population structure of the potato cyst nematode (*Globodera pallida*) in its native area (Peru). Mol. Ecol. 13:2899-2908.

Picard, D., Sempere, T., and Plantard, O. 2007. A northward colonization of the Andes by the potato cyst nematode during geological times suggests multiple host-shifts from wild to cultivated potatoes. Mol. Phylogen. Evol. 42:308-316.

Plantard, O., Picard, D., Valette, S., Scurrah, M., Grenier, E., and Mugniéry, D. 2008. Origin and genetic diversity of Western European populations of the potato cyst nematode (*Globodera pallida*) inferred from mitochondrial sequences and microsatellite loci. Mol. Ecol. 17:2208-2218.

Porazinska, D. L., Giblin-Davis, R. M., Powers, T. O., and Thomas, W. K. 2012. Nematode spatial and ecological patterns from tropical and temperate rainforests. PLoS One 7:1-11.

Prentice, I. C. and Werger, M. J. A. 1985. Clump spacing in a desert dwarf shrub community. Vegetatio 63:133-139.

Pylypenko, L. A. 1999. The interrelations in a system parasite-host plant at the globoderosis. PhD Diss. National Agrarian University, Kyiv, Ukraine.

Rawsthorne, D., and Brodie, B. 1986. Relationship between root growth of potato, root diffusate production and hatching of *Globodera rostochiensis*. J. Nematol. 18:379-384.

Rawsthorne, D., and Brodie, B. 1986. Relationship between root growth of potato, root diffusate production and hatching of *Globodera rostochiensis*. J. Nematol. 18:379-384.

Rice, S. L., Leadbeater, B. S. C., and Stone, A. R. 1985. Changes in cell structure in roots of resistant potatoes parasitized by potato cyst nematode. Potatoes with resistance gene *H1* derived from *Solanum tuberosum* ssp. *andigena*. Physiol. Plant Pathol. 27:219-234.

Ripley, B. D. 1976. The second-order analysis of stationary processes. J. Appl. Prob. 13:255-266.

Ripley, B. D. 1977. Modelling spatial patterns. J. Roy. Statist. Soc. B. 38:172-212.

Ripley, B. D. 1981. Spatial statistics. Wiley, New York.

Robert, P. A., and Stone, A. R. 1981. Host ranges of *Globodera* species within *Solanum* subgenus *Leptostemonum*. Nematologica 27:172-189.

Royle, A. G., Clausen, F. L., and Frederiksen, P. 1981. Practical universal Kriging and automatic contouring. Geoprocessing 1:377-394.

Shaukat, S. S., and Khan, A. 1993. Spatial pattern analysis of three nematode populations associated with chilli. Fundam. Appl. Nematol. 16:473-478.

Schomaker, C. H., and Been, T. H. 1999. A model for infestation foci of potato cyst nematodes *Globodera rostochiensis* and *G. pallida*. Phytopathology 89:583-590.

Savary, S., Teng, P. S., Willocquet, L., and Nutter, F. W. 2006. Quantification and modeling of crop losses: A review of purposes. Ann. Rev. Phytopathol. 44:89-112.

Sasser, J. N., and Freckman, D. W. 1987. A world perspective on nematology: The role of the society. Pages 7-14 in: Vistas on Nematology. J. A. Veech, and D. W. Dickson, eds. Society of Nematologists, Hyattsville, MD.

Seinhorst, J. W. 1965. The relation between nematode density and damage to plants. Nematologica 11:137-154.

Seinhorst, J. W., and Den Ouden, H. 1971. The relation between density of *Heterodera rostochiensis* and growth and yield of two potato varieties. Nematologica 17:347-369.

Shepherd, A. M., and Clark, S. A. 1983. Spermatogenesis and sperm structure in some *Meloidogyne* species (Heteroderidae, Meloidogynidae) and a comparison with those in some cyst nematodes (Heteroderidae, Heteroderidae). Rev. Nematol. 6:17-22.

Silverman, B. W. 1986. Density estimation for statistics and data analysis. Chapman and Hall, New York.

Skarbilovich, T. S. 1959. On the structure of the nematodes of the order Tylenchida Thorne, 1949. Acta Parasitol. Polonica 15:117-132.

Skarpe, C. 1991. Spatial patterns and dynamics of woody vegetation in an arid savanna. J. Veg. Sci. 2:565-572.

Sterner, R. W., Ribic, C. A., and Schatz, G. E. 1986. Testing for life historical changes in spatial patterns of four tropical tree species. J. Ecol. 74:621-633.

Stevens, R. B. 1960. Pages 357-429 in: Plant Pathology: An Advanced Treatise. J. G. Horsfall, and A. E. Dimond, eds. Academic Press, New York.

Stone, A. R. 1972. The round cyst species of *Heterodera* as a group. Ann. Appl. Biol. 71:280-283.

Strachan, J., and Taylor, T. H. 1926. Potato eelworm. J. Min. Agric. 32:941-947.

Talavera, M., Andreu, M., Valor, H., and Tobar, A. 1998. Nematodos fitoparásiticos en áreas productoras de patata de Motril y Salobreña. Invest. Agric. Prod. Prot. Veg. 13:87-95.

Thomas, R. W. 1977. An introduction to quadrat analysis. CATMOG 12. Geo Abstracts Ltd, Norwich, UK.

Thurston, H. D. 1994. Andean potato culture: 5,000 of experience with sustainable agriculture. Pages 6 –13 in: G. W. Zehnder, M. L. Powelson, R. K. Jansson, K. V. Raman, eds. The American Phytopathological Society, St. Paul, MN.

Tobler, W. 1979. Cellular Geography. Pages 379-386 in: S., Gale, and G., Olsson, eds. Philosophy in Geography. Reidel, Dordrecht, Netherlands.

Tomczak, A., Koropacka, K., Smant, G., Goverse, A., and Bakker, E. 2008. Resistant plant responses. Pages 83-113 in: Cell biology of plant nematode parasitism. R. H. Berg, C. G. Taylor, eds. Springer, Berlin, Germany.

Turechek, W. W., and Madden, L. V. 1999. Spatial pattern analysis of strawberry leaf blight in perennial production systems. Phytopathology 89:421-433.

Turner, S. J. 1996. Population decline of potato cyst nematodes (*Globodera rostochiensis* and *G. pallida*) in field soils in Northern Ireland. Ann. Appl. Biol. 129:315-322.

Turner, S. J., and Rowe, J. A. 2006. Cyst nematodes. Pages 91-120 in: Plant Nematology, R. N. Perry and M. Moens, eds. CABI, Wallingford, UK.

Twining, S., Clarke, J., Cook, S., Ellis, S., Gladders, P., Ritchie, F., and Wynn, S. 2009. Pesticide availability for potatoes following revision of Directive 91/414/EEC: Impact assessments and identification of research priorities. Project Report 2009. Potato Council, Oxford, UK.

USDA-APHIS. 2019. Pale cyst nematode eradication program, 4th Quarter Report (October 1-December 30). Online publication. United States Department of Agriculture's Animal and Plant Health Inspection Service. https://www.aphis.usda.gov/aphis /ourfocus/planthealth/plant-pest-and-disease-programs/pests-and diseases/ sa_nematode/sa_potato/ct_pcn_programupdates.

USDA-NASS. 2018. Crop values 2017 summary. Online publication. United States Department of Agriculture's National Agricultural Statistics Service. http://usda.mannlib.cornell.edu/usda/current/CropValuSu/CropValuSu-02-23-2018.pdf.

Van Bruggen, A. H. C., and Arneson, P. A. 1986. Path coefficient analysis of effects of *Rhizoctonia solani* on growth and development of dry beans. Phytopathology 76:874-878.

Van der Plank, J. E. 1960. Analysis of epidemics. Pages 229-289 in: Plant Pathology: An Advanced Treatise. J. G. Horsfall, and E. B. Cowling, eds. Academics Press, New York.

Vasyutin, A. S., and Yakovleva, V. A. 1998. *Globodera* in potatoes in Russia. Kartofel' I Ovoshchi 6:29-32.

Ward, S. A., Rabbinge, R., and Den Ouden, H. 1985. Construction and preliminary evaluation of a simulation model of the population dynamics of the potato cyst nematode *Globodera pallida*. Neth. J. Plant Pathol. 91:27-44.

Whitworth, J. L., Novy, R. G., Zasada, I. A., Wang, X., Dandurand, L. M., and Kuhl, J. C. 2018. Resistance of potato breeding clones and cultivars to three species of potato cyst nematode. Plant Dis. 102:2120-2128.

Wollenweber, H. W. 1923. Krankheiten und BeschSdigungen der Kartoffel. Arb. Forsch. Inst. Kartof. 7:1-56.

Yang, X. B., and Batchelor, W. D. 1997. Modeling plant disease dynamics using neural networks. AI Appl. 11:47-55.

Yuen, J. E., and Hughes, G. 2002. Bayesian analysis of plant disease prediction. Plant Pathol. 51:407-412.

Zadoks, J. C. 1985. On the conceptual basis of crop loss assessment: The threshold theory. Ann. Rev. Phytopathol. 23:455-473.

Chapter 2: A Spatial Analysis of the Potato Cyst Nematode *Globodera pallida* in Idaho

"A Spatial Analysis of the Potato Cyst Nematode *Globodera pallida* in Idaho". Phytopathology, vol. 108, no. 8, 2018, pp. 988-1001.

Abstract

The potato cyst nematode *Globodera pallida* is a globally regulated and quarantine potato pest. It was detected for the first time in the U.S. in the state of Idaho in 2006. A spatial analysis was performed to: (i) understand the spatial arrangement of fields infested with *G. pallida* in southern Idaho using spatial point pattern analysis; and (ii) evaluate the potential threat of *G. pallida* for entry to new areas using spatial interpolation techniques. Data point locations, cyst numbers and egg viability values for each infested field were collected by USDA-APHIS during 2006-2014. Results showed the presence of spatially clustered fields infested with *G. pallida* ($P = 0.003$). We determined that the spread of *G. pallida* grew in diameter from the original center of infestation toward the southwest as an ellipsoidal-shaped cluster. Based on the aggregated spatial pattern of distribution, we determined that *G. pallida* spread followed a contagion effect scenario, where nearby infested fields contributed to the infestation of new fields, probably through soil contaminated agricultural equipment or tubers. We determined that the presence of *G. pallida* in southern Idaho is unlikely to be associated with new introductions from outside the state of Idaho. The aggregation pattern of fields infested with *G. pallida*, with an average of 4,263 cysts/ha and egg viability of 25%, facilitates quarantine activities and confines the propagation of this pest to a small area, which, in 2017 was estimated to be 1,233 hectares. The tools and methods provided in this study facilitate comprehensive approaches to improve *G. pallida* control and eradication programs as well as to raise public awareness of the problems surrounding this economically important potato pest.

Introduction

The potato cyst nematode *Globodera pallida* (Behrens, 1975; Stone, 1972) is a globally regulated pest of potato (*Solanum tuberosum*) and is of great economic importance in many countries throughout the world (Hodda and Cook, 2009; Turner and Rowe, 2006). *Globodera pallida* and *G. rostochiensis*, both considered potato cyst nematodes, co-evolved in South America with potato and other *Solanum* species at altitudes up to 2,000 meters (Jones and Parrot, 1968). Potatoes were introduced into Europe around 1570 (Evans et al. 1975), however potato cyst nematodes arrived in Europe on tubers taken from the Andes around 1850 and the nematodes were first observed on potatoes in Germany in 1881, before spreading throughout the world (Baldwin and Mundo-Ocampo, 1991; Jatala, 1994; Jones, 1970).

Globodera pallida is a highly specialized obligate endoparasitic nematode that requires a living potato plant as a host to complete its life cycle. *Globodera pallida* can survive in the soil for up to 30 years without a suitable host (Turner, 1996). The cyst, which is the body of the dead female, contains 300-500 eggs. Cysts are usually spread by contaminated soils, tubers or farm equipment (Evans and Stone, 1977). Computer modelling showed that sufficient *G. pallida* eggs are likely to survive in the soil after nematicide applications, allowing a resurgence of large *G. pallida* populations in subsequent host crop cycle (Trudgill et al. 2003). When left uncontrolled, *G. pallida* can reduce tuber yields up to 80% (Talavera et al. 1998; Vasyutin and Yakovleva, 1998). In Ukraine, where *G. rostochiensis* was first identified in 1963, Pylypenko (1999) reported that 55 eggs per gram soil were associated with a loss of 3.3% of total yield in resistant potato cultivars and 37.7% in susceptible ones; and populations of 121 eggs per gram soil were associated with losses of 16.9% and 63.3%, respectively.

The first symptomatic presence of potato cyst nematodes in the UK was reported by a farmer in Yorkshire in 1904 (Massee, 1913; Strachan and Taylor, 1926). Since then, their populations built up to high levels and became widespread in the major potato growing areas of the UK. In the presence of repeated cropping of susceptible potato cultivars, potato cyst nematode populations and the probability of their detection progressively increase. In 2000,

about 64% of potato fields in the UK were reported to be infested with potato cyst nematodes (Minnis et al. 2000, 2002).

In Europe, overall losses due to potato cyst nematodes are estimated to be about 9% of potato production (Turner and Rowe, 2006). However, total losses of potato production can occur when no control or containment strategies are employed. Without action to prevent the spread and entry of potato cyst nematodes to new areas, Hodda and Cook (2009) estimated economic losses to Australian agriculture over a 20-year period could exceed $370 million.

Globodera pallida is a quarantine pest in the state of Idaho where it was found in 2006, during a routine inspection conducted jointly by the Idaho State Department of Agriculture (ISDA) and the U.S. Department of Agriculture's Animal and Plant Health Inspection Service (USDA-APHIS). Subsequent extensive sampling traced the nematode to two fields in northern Bingham County, Idaho (Hafez et al. 2007). The presence of *G. pallida* in Idaho constitutes a significant threat to the Idaho potato industry. Currently, Idaho is the nation's largest producer, packer and processor of potatoes. Idaho has been the number one potato-producing state for the past 50 years, producing about 29% of the U.S. potato crop, 40% of U.S. processed potato products and one-third of the nation's fresh potato shipments (Anonymous, 2014, 2017a).

Globodera pallida in Idaho is limited to a small area with low population levels and represents less than 1% of annual potato production areas, whereas in the UK more than 60% of potato fields are infested. Resistance to *G. pallida* in russet-type potato cultivars is currently unavailable for production in the U.S. Pacific Northwest. USDA-APHIS and ISDA have implemented a containment and eradication program designed to prevent *G. pallida* spread to other potato fields. The program outlines restrictions on the movement of plants and soil, requires sanitation procedures for equipment, and enforces limitations on planting potato in infested fields (Anonymous, 2017b). The use of *Solanum sisymbriifolium*, 'litchi tomato' as trap crop and chemical applications with the nematicide Telone II (1,3-dichloropropene) are being conducted in infested fields as part of the *G. pallida* eradication program. Current regulated areas in Idaho are limited to 3,777 hectares, of which 1,233 hectares are infested fields (Anonymous, 2017b).

The invasion process of exotic nematode species consists of arrival, establishment, integration, and spread (Ferris et al. 2003). Plant-parasitic nematodes gain entry to new areas through imported agricultural commodities, while establishment and integration are achieved mainly through local nematode reproduction before spreading to nearby fields (Ferris et al. 2003). Intervention strategies to prevent the establishment of exotic nematodes include (Ferris et al. 2003): (i) exclusion through cultural methods of control (use of certified seed) and quarantines (prohibition of planting host crops in infested fields); (ii) eradication of the nematode from infested sites (fumigation); and (iii) containment to minimize the potential spread of the nematode (restrictions of soil and plant materials movement, and decontamination of field equipment). However, when plant-parasitic nematodes are long-established and integrated into the cropping system, a management program is required to keep the local population below the level of economic damage threshold or detection limit.

From an epidemiological perspective, spatial analysis of plant pathogen infestations in fields provides useful information on the spatial pattern and spatio-temporal dynamics of disease progression and outlines the probabilities of pathogens entering new areas. Therefore, spatial analysis and modeling techniques can be used to assess and evaluate the threat of plant diseases for agricultural production. The term ‘spatial analysis’ can be traced back to the 1950s, widely used in the Geographical Information Systems (GIS), and represents a collection of techniques and models that use the spatial referencing associated with each data value and attributes to explain a phenomenon (Haining, 2003; Tobler, 1979).

Spatial analysis is divided into three main components (Haining, 2003): (i) cartographic modeling, where a data set is represented as a map; (ii) mathematical modeling, where the outcomes of a model are dependent on the characteristic of spatial interaction between the geographical positioning of objects within the model; and (iii) statistical application, where statistical tools and packages are used to fit spatial data into a predictive model. Within spatial analysis, point pattern analysis is used to characterize the distribution pattern of a set of events delimited in the Euclidean space R^2 or R^3. Knowledge is generated by fitting models to patterns, while ascribing scientific interpretations to model parameters. Point pattern analysis (PPA) is divided into: (i) first-order property of PPA, where under the presence of complete spatial randomness (CSR), each random location of an event is drawn independently from an unknown distribution and is associated with a probability density

function (Silverman, 1986); and (ii) second-order property of PPA, where the occurrences of events are related in some way (Ripley, 1976, 1981).

CSR analysis validates that events are distributed randomly over a study region, and common tests performed under CSR hypothesis are quadrat analysis and maximum absolute deviation (Ripley, 1977, 1981; Thomas, 1977). The kernel density estimation (KDE) is used as a non-parametric method to estimate the probability density function of a random variable (Silverman, 1986). The Ripley's K-function analysis is used as a second-order property of PPA to evaluate deviations of events from spatial homogeneity toward spatial clustering or dispersion (Ripley, 1976, 1981) and is widely used in plant ecology; it has been applied to study the distribution patterns of herbs (Kenkel, 1993), desert shrubs (Prentice and Werger, 1985; Skarpe, 1991) and tropical forest trees (Sterner et al. 1986).

Geostatistics is used as a tool of spatial interpolation analysis to process the effect of event aggregations or dispersions along with the uncertainties represented by spatial heterogeneity and to estimate a spatial prediction model known as kriging (Cressie, 1993). Kriging is a linear unbiased spatial interpolation method that provides minimum mean-squared error estimates at unsampled locations and is controlled by semivariogram models, which quantify spatial variability of the data and provide information on the spatial autocorrelation of the datasets (Oliver, 1990; Royle et al. 1981). Kriging generates spatial data using a number generator based on the specified semivariogram model and the pre-existing set of the sample data (Englund, 1993). Other global interpolators like the nearest neighbor algorithm (NN) and the inverse distance weighting (IDW) are widely used in spatial interpolation analysis to approximate attributes to unsampled locations based on sampled ones within a study region. Unlike kriging, NN and IDW are referred to as deterministic interpolation methods because they are directly based on the surrounding measured values or on specified mathematical formulas that determine the smoothness of the resulting surface (Jenkins et al. 1985).

Spatial analysis applied to plant-parasitic nematodes has been used to develop accurate sampling methods in fields (Dinardo-Miranda and Fracasso, 2009; Francl, 1986), determine ecological patterns of nematode distribution (Porazinska et al. 2012), support the use of site-specific management in nematode infested fields (Avendaño et al. 2003), model spatial pattern distribution of nematode populations and estimate the likelihood of new

infestation (Madden and Hughes, 1995; Noe and Campbell, 1985; Schomaker and Been, 1999; Shaukat and Khan, 1993). Schomaker and Been (1999) designed a model for infestation foci of potato cyst nematodes by using multiple sampling grids from eighty-two infested fields, and the data were analyzed and fitted for spatial distribution of cysts using exponential models. Gavassoni et al. (2001) used geostatistical analysis to quantify the effects of tillage on the spatial patterns of *Heterodera glycines* in infested fields. Evans et al. (2003) used spatial analysis to target 'hot spots' of potato cyst nematode infestations for additional treatment with fumigant, thereby reducing the cost of chemicals applied and minimizing possible environmental damage.

Unlike the examples cited in the previous paragraph, our study focuses on using spatial analysis to define the spatial pattern of fields infested with *G. pallida* in southern Idaho at a regional level (macroscale) and it is not intended to describe *G. pallida* distribution at individual field (microscale). In this study, we proceeded in exploring the data by doing a cluster analysis followed by a point pattern analysis and spatial interpolation of fields infested with *G. pallida* using the attribute variables of number of cysts and the values of egg viability. There is a need to integrate spatial analysis into risk model assessment of plant diseases to widen the scope of control strategies and to identify potential hidden variables of interest. Such integration would allow remotely sensed biological data to be constantly monitored and to assess the success of control interventions in preventing or limiting the spread of exotic or native plant pathogens.

The objectives of this study were to describe the spatial distribution pattern of fields infested with *G. pallida* in southern Idaho and to evaluate the potential risk of *G. pallida* spread to new areas. *Globodera pallida* is known to be present in 1,233 hectares in Idaho, which represent less than 1% of annual potato production areas. Therefore, a comprehensive spatial analysis will embolden policymakers and stakeholders to implement stringent phytosanitary measures to eradicate *G. pallida* from Idaho potato fields and will provide a framework of analysis for other exotic plant-parasitic nematodes.

Materials and Methods

Data collection. Data point locations of fields infested with *G. pallida* in southern Idaho with the associated number of cysts and the values of egg viability were collected by USDA-APHIS from 2006 to 2014 (Fig. 2.1) (Table 2.1). Sampling system used by USDA-APHIS consisted in collecting 22.42 kg of soil samples per hectare. Soil samples were processed for cyst extractions using the Fenwick flotation method (Fenwick, 1940). *Globodera pallida* egg viability was assessed using Meldola Blue as the staining agent (Ogiga and Estey, 1974). The identity of *G. pallida* was confirmed by morphological and molecular methods (Skantar et al. 2007). The data collected is represented as a set of marked point pattern illustrated in algebraic terms as following:

$$y = \{(x_1, m_1), \dots, (x_n, m_n)\}$$

where x_i are the locations of fields infested with *G. pallida* (longitude and latitude) and m_i are the number of cysts collected or the values of egg viability. A conceptual framework was built to describe the spatial analysis processes used in this study (Fig. 2.2).

Data exploration. A distance matrix (n x n) was built using a pairwise distance measurement of fields infested with *G. pallida*. Agglomerative hierarchical cluster analysis was performed using Ward's minimum variance method defined as the squared Euclidean distance between points (Ward, 1963), as illustrated in algebraic terms:

$$d_{ij} = d(\{X_i\}, \{X_j\}) = \|X_i - X_j\|^2$$

where d_{ij} is the pairwise distances between clusters and X_i, X_j are the distance points arranged in a matrix.

The variable number of cysts and variable egg viability were standardized before performing a cluster analysis using the average linkage method, where the distance between two clusters is defined as the average dissimilarities between the points in one cluster and the points in the other cluster (Kaufman and Rousseeuw, 1990). The agglomerative coefficient, a quality index, was performed to measure the amount of clustering structure found (Rousseeuw, 1986).

A non-parametric Mantel test, originally designed for analyzing disease clustering in epidemiological studies (Mantel, 1967), was performed to evaluate the relationship between *G. pallida* infested field distance matrix and the number of cysts and the values of egg

viability. The variable cyst numbers were transformed into a logarithmic expression before running a Mantel test. The analysis was executed by running 1,000 replicates in a Monte-Carlo simulation. The Mantel test null hypothesis is the absence of relationship between values in two dissimilarity matrices and it is not intended to test the independence between two random variables or data tables (Mantel and Valand, 1970; Legendre et al. 2015).

Point pattern analysis (PPA). The kernel density estimation (KDE) was used as a first-order property of PPA under the assumption that each random location x_i is drawn independently from an unknown distribution with probability density function $f(x_i)$. Silverman (1986) described KDE as the average of a series of small 'bumps' (probability distributions in two dimensions) centered on each observed point, as illustrated in algebraic terms:

$$\hat{f}(x) = \hat{f}(x,y) = \frac{1}{nh_x h_y}\Sigma k\left(\frac{x-x_i}{h_x}, \frac{y-y_i}{h_y}\right)$$

where x, y is the coordinate point location, and h_x, h_y are referred as the bandwidths (which represent the radii of the bumps in each direction). A fixed bandwidth of 2,000 meters was computed for KDE analysis used in this study.

The quadrat analysis, also known as the chi-squared test of complete spatial randomness (Thomas, 1977), was used to examine the frequency of points occurring in various parts of a study area. A set of quadrats of cells is superimposed on a study area, and number of points in each cell is determined. By analyzing the distribution of cell frequencies, the point pattern arrangement can be described using the variance and mean of point counts and the variance to mean ratio (VMR), as illustrated in algebraic terms:

$$VAR = \frac{\Sigma f_i x_i^2 - [\frac{(\Sigma f_i x_i)^2}{m}]}{m-1}, \qquad Mean = \frac{n}{m}, \qquad VMR = \frac{VAR}{Mean}$$

where VAR is the variance of the cell frequencies, $Mean$ is the mean cell frequency, f_i is the frequency of cells, x_i is the number per cell, n is the number of points, m is the number of cells, and VMR is the variance to mean ratio. For a uniform (dispersed) intensity, the variance is equal to 0 and so is VMR. For a random intensity, the variance is equal to the mean and so VMR is equal to 1. For a clustered intensity, the variance is greater than the mean and so VMR is greater than 1.

In addition to being used as descriptive index, the VAR can be applied to test a distribution for randomness using chi-squared statistical test, where the null hypothesis is the presence of complete spatial randomness.

The K-function was used as a second-order analysis of point PPA (Ripley, 1976, 1981). This process described situations in which the occurrences of events are related in some way. The K-function is a function of distance, defined by:

$$K(d) = \lambda^{-1}E(N_d)$$

where N_d is the number of events x_i within a distance d of a randomly chosen event from all recorded events $\{x_1, \dots, x_n\}$, and λ is the intensity of the process measured in events per unit area.

CSR or Poisson process occurred when the distributions of x_i are independent and the marginal densities are uniform. Under CSR, the K-function is defined by:

$$K_{CSR}(d) = \lambda\pi d^2$$

where d is the radius of a circle. When $K(d) > K_{CSR}(d)$, excess of nearby points occurred, and the process is termed as a spatial clustering of points. When $K(d) < K_{CSR}(d)$, this relation suggests the presence of spatial dispersion of points. The maximum absolute deviation (MAD) was used to evaluate the null hypothesis of CSR (Ripley, 1977, 1981). MAD is consisted of the absolute value of the largest discrepancy between the two functions and was calculated using a Monte Carlo test based on 99 simulations:

$$MAD = max_d|K(d) - K_{CSR}(d)|$$

Spatial interpolation. This method was used to estimate the values of the number of *G. pallida* cysts and egg viability at any point location within a study region. Spatial dependence allowed nearby locations to influence each other and to possess similar attributes. Given the value of the number of cysts or egg viability, such as $\{z_1, \dots, z_n\}$ at locations $\{x_1, \dots, x_n\}$, the objective is to estimate the value z at some new point x. Three basic global interpolators were used to create estimated surfaces across the study region: (i) nearest neighbor algorithm; (ii) inverse distance weighting; and (iii) ordinary kriging.

The nearest neighbor interpolation estimated the value z at x using the value z_i at the closest observation point to x. Voronoi tessellation (Thiessen polygons) was used to divide the study region into zones, defined by boundaries located at equidistance between pairs of

points, where the number of cysts or the value of egg viability for each corresponding set of points were estimated.

The inverse distance weighting (IDW) used similar techniques as the nearest neighbor approach, however a weighted mean of nearby observations is taken, rather than relying on a single nearest neighbor. The IDW can be expressed algebraically as follows:

$$\hat{z}(x) = \frac{\Sigma_i w_i z_i}{\Sigma_i w_i}, \quad w_i = |x - x_i|^{-\alpha}$$

where $\alpha \geq 0$, as an inverse square relationship.

The ordinary kriging was used as a probabilistic interpolator to estimate the value of a random variable, z, at one or more unsampled points. The kriging estimate of variable z at point x_0, $\hat{z}(x_0)$, is a linear weighted sum of n observations surrounding the estimate (Armstrong and Boufassa, 1988; Stein, 1999):

$$\hat{z}(x_0) = \sum_{i=1}^{n} \lambda_i z(x_i)$$

where λ_i are the weights and $z(x_i)$ is the known value of variable z at sampling site x_i.

An ordinary kriging was performed to interpolate the values of egg viability. For the interpolation of the number of cysts, due to the strong positive skewness of the cyst values, the data was transformed into a logarithmic expression. Consequently, an ordinary lognormal kriging was performed to interpolate the number of cysts from sampled areas to unsampled ones.

Kriging, as a probabilistic interpolator, relies on an experimental variogram to measure the spatial correlation of the random function $\hat{z}(x_0)$ (Stein, 1999; Wackernagel, 2003). The variogram is defined by calculating the semivariance as a function of distance:

$$\gamma(d) = \frac{1}{2}\Sigma\{[\hat{z}(x_1) - \hat{z}(x_2)]^2\}$$

Data analysis. R version 3.4.1 was used as a modeling language environment for data exploration and spatial analysis in this study (R Core Team, 2017). For data exploration, the following packages were used: (i) ‘cluster’ and ‘heatmap3’ were used to perform the agglomerative hierarchical cluster analysis; and (ii) ‘ade4’ and ‘ecodist’ were used to calculate the Mantel correlation test for dissimilarity matrices. For spatial point pattern analysis, the following packages were used: (i) ‘GISTools’, ‘maptools’ and ‘sp’ were used to map the study area and to calculate the kernel density estimation; and (ii) ‘spatstat’ was used

to estimate the Ripley's K-function, the quadrat analysis for the chi-square test and the maximum absolute deviation test. For spatial interpolation, the following packages were used: (i) 'deldir' was used to calculate the Voronoi tessellation for the nearest neighbor estimation; (ii) 'gstat' was used to calculate the inverse distance weighting; and (iii) 'automap' package was used to estimate the ordinary kriging and the ordinary lognormal kriging. The 'automap' package automatically fits a variogram to the data and provides initial estimates for the sill (variance), range (distance at which the variogram reaches the sill), nugget (error measurement) and kappa (a smoothing parameter). A kriging prediction and a standard error maps were also generated in this procedure.

Results

The distance matrix, based on the distances between fields infested with *G. pallida* in pairwise comparisons, revealed that most of the infested fields are separated from each other at distances ranging from 1 to 5 kilometers (Table 2.2). However, three infested fields (ID10, ID11 and ID18) had greater distance separation from neighboring fields, ranging from 5 to 24 kilometers (Table 2.2). Additionally, the heat map highlighted hue shifting colors for these three fields from nearby ones (Fig. 2.3A). The agglomerative hierarchical cluster analysis applied on the distance matrix identified three main clusters of fields infested with *G. pallida* using Ward's minimum variance algorithm (Fig. 2.3B). Similarly, standardized data values of cyst number and egg viability identified, based on their combined weight, three main clusters of fields infested with *G. pallida* using the average linkage method (Fig. 2.4). The agglomerative coefficient was 0.87, representing a high-quality index for the amount of clustering structure found.

The Mantel correlation test showed no significant relationship between the field distance matrix and the number of cysts collected ($P = 0.93$ and $R^2 = -0.15$) (Table 2.3). Similarly, the Mantel correlation test between the field distance matrix and the values of egg viability showed no significant relationship ($P = 0.28$ and $R^2 = 0.08$) (Table 2.3).

The KDE showed the densities of *G. pallida*-infested fields point locations in the study area. The KDE visual illustration of the color density map revealed areas with strong yellow and red colors corresponding to point locations of high density of fields infested with

G. pallida (Fig. 2.5A). A 3-D representation of KDE displayed a smooth peak of high-density incidence with a fixed bandwidth of 2,000 meters (Fig. 2.5B).

The chi-squared test of CSR using quadrat counts revealed significant spatial clustering of fields infested with *G. pallida* ($P = 0.003$). This result showed that the infested fields, rather than being distributed randomly across the study area, followed a pattern of distribution toward aggregation as confirmed by the low *p*-value from the chi-squared test.

The Ripley's K-function analysis illustrated evidence of spatial clustering as the observed K-function values, generated by 99 simulations in a Monte Carlo test procedure, were much higher at greater distances than the expected values under CSR (Fig. 2.5C). This result demonstrated that the number of fields infested with *G. pallida* found within a given distance (distance matrix) of each individual field was greater than that for a random distribution. The observed K-function values appeared to merge with the expected values at a distance range from 0 to 500 meters and pointing to a random distribution of infested fields. However, at distances of greater than 500 meters, the overall observed values were higher than the expected ones and above the confidence interval (envelope), therefore pointing toward aggregation. The maximum absolute deviation test confirmed the visual interpretation of the K-function plot of significant departure from CSR toward spatial clustering ($P = 0.01$) of fields infested with *G. pallida*.

The nearest neighbor interpolation model illustrated the number of *G. pallida* cysts per hectare and the values of viable eggs intercalated for each of the 18 Voronoi polygons, representing each of the 18 fields infested with *G. pallida*. Five major polygons in the subset 50 to 250 cysts/ha occupied over 60% of the interpolated areas, followed by other five polygons estimated under 50 cysts/ha (Fig. 2.6A). Only one small-sized polygon was estimated over 15,000 cysts/ha. The values of egg viability in the subsets 0.25 to 0.35 and over 0.35 occupied over 65% of the interpolated areas (Fig. 2.6B).

The IDW model consisted of 10,000 grids upon which the number of cysts and the values of egg viability were extrapolated using an alpha of 3, as the inverse square relationship. The subset 1,000 to 8,000 cysts/ha occupied over 85% of the interpolated areas and only a small area is estimated over 15,000 cysts/ha (Fig. 2.7A). The values of egg viability in the subset 0.15 to 0.25 occupied over 60% of the interpolated areas (Fig. 2.7B). 3-

D representations of IDW for the number of cysts and the values of egg viability illustrated important variabilities in their distributions across the interpolated areas (Fig. 2.7C, D).

The ordinary lognormal kriging model showed high cyst values around a centered focal area in the kriging prediction map (Fig. 2.8). The kriging standard error map illustrated the degree of confidence associated with the kriging prediction map and showed that the error measurement is lower toward the centered focal area (Fig. 2.8). The Ste (Matern, M. Stein's parameterization) model was used to fit the experimental variogram with the following initial parameters: sill (2.3), range (3,427), nugget (1.3) and kappa (0.05). The Ste model adapted to the experimental variogram of cyst values illustrated a weak spatial correlation, as represented by a continuous flat line.

The ordinary kriging prediction model for values of egg viability showed most areas were estimated between 0.25 to 0.35 and the error measurement associated with the prediction map followed similar patterns than the cyst values model (Fig. 2.9). The Ste model was used to fit the experimental variogram for values of egg viability with the following initial parameters: sill (0.02), range (2,831), nugget (0.01) and kappa (10) (Fig. 2.9). The Ste model for values of egg viability showed a relatively strong spatial correlation, as illustrated by a curved line that marked the boundary between correlated and non-correlated values.

Discussion

This study provides a holistic analysis of the extent and distribution of fields infested with *G. pallida* in southern Idaho using spatial analysis techniques. The agglomerative hierarchical cluster analysis classified the distance matrix of fields into three clusters based on the distance separation between all possible pairwise fields. From this analysis, we determined that about 80% of the fields are in a radius of less than 10 kilometers. Cluster analysis of standardized values of cysts and egg viability indicated three major groups of clusters based on their dissimilarities. Ferris et al. (1971) used cluster analysis to classify population structure of plant-parasitic nematodes and found that different community structures differed from soil types. Several cluster algorithms have been used to study the similarity in range and distribution of marine nematode species (Field et al. 1982; Hodda, 1986).

The kernel density estimation determined the location of the highest concentration of fields infested with *G. pallida*. The focal point of locations coincided with the first reports of *G. pallida* detections during 2006. Based in our analysis, we determined that the spread of *G. pallida* grew in diameter from the original center of infestation toward the southwest as an ellipsoidal-shaped cluster. Spatial statistical tests confirmed the presence of spatial clustering of fields infested with *G. pallida*, as illustrated in the Ripley's K-function analysis. This result demonstrated that the number of infested fields found within a given distance of each individual field was greater than that for a random distribution. From this clustering arrangement, we determined that *G. pallida* spread followed a contagion effect scenario prior to containment measures, where nearby infested fields contributed to the infestation of new fields, probably through plant materials or agricultural equipment contaminated with infested soil. Similarly, Banks et al. (2012) concluded that the original site of *G. pallida* and *G. rostochiensis* introductions may act as a point source for subsequent spread occurring at a relatively constant rate over time. Similar aggregated patterns of potato cyst nematodes and other plant-parasitic nematodes have been reported for individual fields (Avendaño et al. 2003; Noe and Campbell, 1985; Schomaker and Been, 1999; Shaukat and Khan, 1993). It is unlikely that the recent *G. pallida* presence in southern Idaho is associated with new *G. pallida* entry from outside Idaho. Our assessment is based on previous studies indicating that *G. pallida* populations differ between themselves generally only in areas throughout Europe and South America where *G. pallida* has been long-established (based on molecular phylogenetic analysis), suggesting multiple waves of *G. pallida* entry (Grenier et al. 2010; Picard et al. 2004, 2007; Plantard et al. 2008).

Using deterministic spatial interpolation techniques, we enumerated the number of *G. pallida* cysts and the values of egg viability in associated areas close to initial infestation foci. The models used for spatial interpolation predicted the contagion effect of *G. pallida* to nearby fields. The inverse distance weighting model (IDW) differed from the nearest neighbor approach (NN) due to the nature of the model calculation. In the case of IDW, a weighted measurement of multiple number of cysts is taken from different nearby fields instead of relying on a single field measurement for prediction, as is done with NN modeling. As the distribution of the number of cysts varied greatly between fields, we determined for this study that IDW was the best model to describe the contagion effect. For egg viability, we

determined that NN and IDW models yielded relatively similar prediction maps in the subset ranging from under 0.05 to 0.15, however they failed to provide similar results as the values of egg viability increase. Therefore, we determined that IDW was the best deterministic model adapted for the interpolation of the values of egg viability. The variability in the number of cysts per hectare observed in this study could be explained by the relative success of quarantine measures imposed on infested fields, where potato plantings are prohibited, and entrance is limited to authorized personnel only, leading to a disruption of the initial *G. pallida* spread momentum.

The use of ordinary kriging for building a stochastic interpolation model unveiled some inherent limitations when applied to a restrained and skewed dataset. A kriging interpolation model is built on an experimental variogram to make predictions from known to unknown locations using estimated variations in the known data values. Mantel correlation test previously indicated no significant relationship between field distance matrix and the cyst numbers collected. The experimental variogram built for the variable cyst numbers showed weak spatial correlation indicating the absence of spatial dependency. As a result, kriging prediction map was associated with large error measurement values indicating high level of uncertainties in interpolated areas for cyst numbers. Because of the absence of spatial correlation, the use of inverse distance weighting as a deterministic interpolation model for cyst numbers is recommended.

The experimental variogram adapted for the values of egg viability showed a relatively strong spatial correlation indicating the presence of spatial dependency. The relative normal distribution of the egg viability dataset explained this result, and the Ste ordinary kriging interpolation model seemed to reduce the level of uncertainty associated with the kriging prediction map. Although the Mantel correlation test for egg viability showed no significant spatial correlation, the Ste ordinary kriging was found to be a better model for spatial correlation using advanced spatial analysis techniques. We determined that both IDW and ordinary kriging provided comparatively similar prediction maps for the interpolation of the values of egg viability.

Various interpolation models have been applied for studying the spatial distribution of plant-parasitic nematodes in individual fields with gridded sampling methods (microscale) (Caswell and Chellemi, 1986; Evans et al. 2003; Farias et al. 2002; Webster and Boag, 1992).

However, to our knowledge, this study represents the first use of stochastic interpolation models for plant-parasitic nematodes at a regional level (macroscale). We determined that stochastic interpolation models for plant-parasitic nematodes applied to a macroscale level are subjected to strong variations when the datasets are restrained and skewed, as was the case in this study.

Based on the spatial aggregation of fields infested with *G. pallida*, with an average of 4,263 cysts/ha and egg viability of 0.25, we determined that active programs of quarantine and eradication can limit the spread of *G. pallida* in southern Idaho. An eradication program requires strict containment protocols and the prohibition of growing potato in infested sites. Intensive soil sampling and testing are required as part of the program to monitor and evaluate the progress of *G. pallida* eradication at regular time intervals. The use of *G. pallida* resistant potato varieties, trap crops, crop rotations, biofumigants and biocontrol agents is a crucial first step to rapidly reduce *G. pallida* population densities to undetected levels and to return previously infested fields to potato production. Studies found that the use of *Solanum sisymbriifolium* (trap crop), *Trichoderma harzianum* and *Plectosphaerella cucumerina* (fungal biocontrol agents) showed significant reduction of *G. pallida* reproduction rate in greenhouse experiments (Contina et al. 2017; Dandurand and Knudsen, 2016).

Globodera rostochiensis was found in the Sharon region of Israel in 1954 and in 1965 where potatoes are grown in the winter. After detection, eradication was carried out by soil fumigation with ethylene dibromide and soil testing was performed at regular intervals. In 1987, the European and Mediterranean Plant Protection Organization (EPPO) reported that Israel was declared free from this pest, after a negative *G. rostochiensis* presence in subsequent soil testing (Anonymous, 1987). *Globodera rostochiensis* eradication from Western Australia (first found in 1986) has proven to be another successful program. *Globodera rostochiensis* has not been detected since 1989 in Western Australia where the intensity of soil sampling used provides 96-100% *G. rostochiensis* detection probability (Anonymous, 2010). In 2010, after 24 years of *G. rostochiensis* eradication, Western Australia was declared free of this pest. *Globodera pallida* was detected in Finland in four fields in 2002 and two fields in 2004. After nine years of eradication program, all soil samples tested in 2011 gave negative results for the presence of *G. pallida* (Anonymous, 2012).

This study provides a scientifically based decision method that promotes eradication measures instead of management for *G. pallida* in Idaho. To our knowledge, this is the first use of spatial analysis for understanding *G. pallida* distribution at a macroscale level in Idaho. The use of spatial analysis in risk assessment models provides important information on the distribution, potential spread, and control strategies for exotic plant-parasitic nematodes. The tools and methods provided in this study should facilitate comprehensive approaches to improve *G. pallida* control and eradication programs as well as to raise public awareness of the problematic of this economically important potato pest.

Literature Cited

Anonymous. 1987. Non-occurrence of *Globodera rostochiensis* in Israel. Online publication. European and Mediterranean Plant Protection Organization (EPPO) reporting service no. 18. https://gd.eppo.int/reporting/article-5754.

Anonymous. 2010. Eradication of potato cyst nematode (PCN) from Western Australia. Online publication. International Plant Protection Convention (IPPC). https://www.ippc.int/en/countries/australia/pestreports/2010/09/eradication-of-potato-cyst-nematode-pcn-from-western-australia/.

Anonymous. 2012. Situation of *Globodera pallida* in Finland in 2011. Online publication. European and Mediterranean Plant Protection Organization (EPPO) reporting service no. 04. https://gd.eppo.int/reporting/article-1900.

Anonymous. 2014. Potatoes 2013 Summary. Online publication. USDA-NASS. https://www.census.gov/history/pdf/idahopotatoes2014.pdf.

Anonymous. 2017a. Potato stocks. Online publication. USDA. http://usda.mannlib.cornell.edu/usda/current/PotaStoc/PotaStoc-06-16-2017.pdf.

Anonymous. 2017b. Pale cyst nematode (PCN) eradication program, Idaho Falls, Idaho. Second Quarter Report (April-June). Online publication. USDA-APHIS. https://www.aphis.usda.gov/plant_health/plant_pest_info/potato/downloads/pcndocs/surveyupdates/2017/pcn-2nd-quarter-2017.pdf.

Armstrong, M., and Boufassa, A. 1988. Comparing the robustness of ordinary kriging and lognormal kriging: Outlier resistance. Math. Geol. 20:447-457.

Avendaño, F., Schabenberger, O., Pierce, F. J., and Melakeberhan, H. 2003. Geostatistical analysis of field spatial distribution patterns of soybean cyst nematode. Agron. J. 95:936-948.

Baldwin, J. G., and Mundo-Ocampo, M. 1991. Heteroderinae cyst and non-cyst forming nematodes. Pages 275-362 in: Manual of Agricultural Nematology, W. R., Nickle, ed. Decker Inc., New York.

Banks, N. C., Hodda, M., Singh, S. K., and Matveeva, E. M. 2012. Dispersal of potato cyst nematodes measured using historical and spatial statistical analyses. Phytopathology 102:620-626.

Behrens, E. 1975. *Globodera Skarbilovic*, 1959, eine selbstaendige Gattung in der Unterfamilie Heteroderinae Skarbilovic, 1947 (Nematoda: Heteroderidae). Vortragstagung zu aktuellen Problemen der Phytonematologie am 29/5/1975 in Rostock. Manuskriptdruck der Vortraege. Rostock, 1975:12-26.

Caswell, E. P., and Chellemi, D. A. 1986. A geostatistical analysis of spatial pattern of *Rotylenchulus reniformis* in Hawaiian pineapple field. J. Nematol. 18:603.

Contina, J. B., Dandurand, L. M., and Knudsen, G. R. 2017. Use of GFP-tagged *Trichoderma harzianum* as a tool to study the biological control of the potato cyst nematode *Globodera pallida*. Appl. Soil Ecol. 115:31-37.

Cressie, N. 1993. Geostatistics: A tool for environmental modelers. Pages 415-421 in: Environmental modelling with GIS, M. F. Goodchild, B. O Parks, and L. T Steyaert, eds. Oxford University Press Inc., New York.

Dandurand, L. M., and Knudsen, G. R. 2016. Effect of the trap crop *Solanum sisymbriifolium* and two biocontrol fungi on reproduction of the potato cyst nematode *Globodera pallida*. Ann. Appl. Biol. 169:180-189.

Dinardo-Miranda, L. L., and Fracasso, J. V. 2009. Spatial distribution of plant-parasitic nematodes in sugarcane fields. Sci. Agric. 66:188-194.

Englund, E. J. 1993. Spatial simulation: Environmental applications. Pages 432-437 in: Environmental modelling with GIS, M. F. Goodchild, B. O Parks, and L. T Steyaert, eds. Oxford University Press Inc., New York.

Evans, K., Franco, J., and Scurrah, M. M. 1975. Distribution of species of potato cyst-nematodes in South America. Nematologica 21:365-69.

Evans, K., and Stone, A. R. 1977. A review of the distribution and biology of the potato cyst nematodes *Globodera rostochiensis* and *G. pallida*. Int. J. Pest Manag. 23:178-189.

Evans, K., Webster, R., Barker, A., Halford, P., and Russel, M. 2003. Mapping infestations of potato cyst nematodes and the potential for spatially varying application of nematicides. Prec. Agric. 4:149-162.

Farias, P. R. S., Sánchez-Vila, X., Barbosa, J. C., Vieira, S. R., Ferraz, L. C. C. B., and Solís-Delfin. 2002. Using geostatistical analysis to evaluate the presence of *Rotylenchulus reniformis* in cotton crops in Brazil: Economic implications. J. Nematol. 34:232-238.

Fenwick, D. W. 1940. Methods for the recovery and counting of cysts of *Heterodera schachtii* from soil. J. Helminthol. 18:155-172.

Ferris, V. R., Ferris, J. M., Bernard, R. L., and Probst, A. H. 1971. Community structure of plant-parasitic nematodes related to soil types in Illinois and Indiana soybean fields. J. Nematol. 3:399-408.

Ferris, H., Jetter, K. M., Zasada, I., Chitambar, J. J., Venette, R. C., Klonsky, K. M., and Becker, J. O. 2003. Risk assessment of plant-parasitic nematodes. Pages 99-119 in: Exotic pests and diseases: Biology and economics for biosecurity, D. A. Summer, ed. Iowa State University Press.

Field, J. G., Clarke, K. R., and Warwick, R. M. 1982. A practical strategy for analyzing multispecies distribution patterns. Mar. Ecol. Prog. Ser. 8:37-52.

Francl, L. J. 1986. Spatial analysis of *Heterodera glycines* populations in field plots. J. Nematol. 18:183-189.

Gavassoni, W. L., Tylka, G. L., and Munkvold, G. P. 2001. Relationships between tillage and spatial patterns of *Heterodera glycines*. Phytopathology 91:534-545.

Grenier, E., Fournet, S., Petit, E., and Anthoine, G. 2010. A cyst nematode 'species factory' called the Andes. Nematology 12:163-169.

Hafez, S. L., Sundararaj, P., Handoo, Z. A., Skantar, L., Carta, K., and Chitwood, D. J. 2007. First report of the Pale Cyst Nematode, *Globodera pallida*, in the United States. Plant Dis. 91:325.

Haining, R. 2003. Spatial data analysis: Theory and practice. Cambridge University Press. Cambridge, UK.

Hodda, M. 1986. Cluster analysis of marine nematodes. Nematologica 32:419-438.

Hodda, M., and Cook, D. C. 2009. Economic impact from unrestricted spread of potato cyst nematodes in Australia. Phytopathology 99:1387-1393.

Jatala, P. 1994. Biology and management of nematode parasites of potato in developing countries. Page 215 in: Advances in potato pest biology and management, M. L. Powelson, G. W. Zehnder, and R. K. Jansson, eds. Amer. Phytopathological Soc., St. Paul, Minnesota.

Jenkins, W., Mather, B., and Munson, D. 1985. Nearest neighbor and generalized inverse distance interpolation for Fourier domain image reconstruction. Proc. IEEE. 73:1069-1072.

Jones, F. G. W. 1970. The control of the potato cyst nematode. J. R. Soc. Arts 118:179-199.

Jones, F. G. W., and Parrott, D. M. 1968. Potato production using resistant varieties on land infested with potato cyst-eelworm, *Heterodera rostochiensis* Woll. Outlook Agric. 5:215-222.

Kaufman, L., and Rousseeuw, P. J. 1990. Finding groups in data: An introduction to cluster analysis. Wiley, New York.

Kenkel, N. C. 1993. Modeling Markovian dependence in populations of *Aralia nudicaulis*. Ecology 74:1700-1706.

Legendre, P., Fortin, M. J., and Borcard, D. 2015. Should the Mantel test be used in spatial analysis? Meth. Ecol. Evol. 6:1239-1247.

Madden, L. V., and Hughes, G. 1995. Plant disease incidence: Distributions, heterogeneity, and temporal analysis. Ann. Rev. Phytopathology 33:529-64.

Mantel, N. 1967. The detection of disease clustering and a generalized regression approach. Cancer Res. 27:209-220.

Mantel, N., and Valand, R. S. 1970. A technique of non-parametric multivariate analysis. Biometrics 26:547-558.

Massee, G. 1913. Nematodes or eelworms. Kew Bulletin 9:343-351.

Minnis, S. T., Haydock, P. P. J., Ibrahim, S. K., Grove, I. G., Evans, K., and Russell, M. D. 2000. The occurrence and distribution of potato cyst nematodes in England and Wales. Asp. Appl. Biol. 59:1-9.

Minnis, S. T., Haydock, P. P. J., Ibrahim, S. K., Grove, I. G., Evans, K., and Russell, M. D. 2002. Potato cyst nematodes in England and Wales: Occurrence and distribution. Ann. Appl. Biol. 140:187-195.

Noe, J. P., and Campbell, C. L. 1985. Spatial pattern analysis of plant-parasitic nematodes. J. Nematol. 17:86-93.

Ogiga, I. R., and Estey, R. H. 1974. The use of Meldola Blue and Nile Blue A for distinguishing dead from living nematodes. Nematologica 20:271-276.

Oliver, M. A. 1990. Kriging: A method of interpolation for Geographical Information Systems. Int. J. Geogr. Inf. Sci. 4:313-332.

Picard, D., Plantard, O., Scurrah, M., and Mugniéry, D. 2004. Inbreeding and population structure of the potato cyst nematode (*Globodera pallida*) in its native area (Peru). Mol. Ecol. 13:2899-2908.

Picard, D., Sempere, T., and Plantard, O. 2007. A northward colonization of the Andes by the potato cyst nematode during geological times suggests multiple host-shifts from wild to cultivated potatoes. Mol. Phylogenet. Evol. 42:308-316.

Plantard, O., Picard, D., Valette, S., Scurrah, M., Grenier, E., and Mugniéry, D. 2008. Origin and genetic diversity of Western European populations of the potato cyst nematode (*Globodera pallida*) inferred from mitochondrial sequences and microsatellite loci. Mol. Ecol. 17:2208-2218.

Porazinska, D. L., Giblin-Davis, R. M., Powers, T. O., and Thomas, W. K. 2012. Nematode spatial and ecological patterns from tropical and temperate rainforests. PLoS One 7:1-11.

Prentice, I. C. and Werger, M. J. A. 1985. Clump spacing in a desert dwarf shrub community. Vegetatio 63:133-139.

Pylypenko, L. A. 1999. The interrelations in a system parasite-host plant at the globoderosis. PhD thesis. National Agrarian University, Kyiv, Ukraine.

R Core Team. 2017. R: A language and environment for statistical computing. R Foundation for statistical computing, Vienna, Austria. http://www.R-project.org/.

Ripley, B. D. 1976. The second-order analysis of stationary processes. J. Appl. Prob. 13:255-266.

Ripley, B. D. 1977. Modelling spatial patterns. J. Roy. Statist. Soc. B. 38:172-212.

Ripley, B. D. 1981. Spatial statistics. Wiley, New York.

Rousseeuw, P. J. 1986. A visual display for hierarchical classification. Pages 743-748 in: Data Analysis and Informatics IV. E. Diday, Y. Escoufier, L. Lebart, J. Pagés, Y. Schektman, and R. Tomassone, eds. Elsevier Science Pub. Co., New York.

Royle, A. G., Clausen, F. L., and Frederiksen, P. 1981. Practical universal Kriging and automatic contouring. Geoprocessing 1:377-394.

Schomaker, C. H., and Been, T. H. 1999. A model for infestation foci of potato cyst nematodes *Globodera rostochiensis* and *G. pallida*. Phytopathology 89:583-590.

Shaukat, S. S., and Khan, A. 1993. Spatial pattern analysis of three nematode populations associated with chilli. Fundam. Appl. Nematol. 16:473-478.

Silverman, B. W. 1986. Density estimation for statistics and data analysis. Chapman and Hall, New York.

Skantar, A. M., Handoo, Z. A., Carta, L. K., and Chitwood, D. J. 2007. Morphological and molecular identification of *Globodera pallida* associated with potato in Idaho. J. Nematol. 39:133-144.

Skarpe, C. 1991. Spatial patterns and dynamics of woody vegetation in an arid savanna. J. Veg. Sci. 2:565-572.

Stein, M. L. 1999. Interpolation of spatial data: Some theory for kriging. Springer Verlag, New York.

Sterner, R. W., Ribic, C. A., and Schatz, G. E. 1986. Testing for life historical changes in spatial patterns of four tropical tree species. J. Ecol. 74:621-633.

Stone, A. R. 1972. The round cyst species of *Heterodera* as a group. Ann. Appl. Biol. 71:280-283.

Strachan, J., and Taylor, T. H. 1926. Potato eelworm. J. Min. Agric. 32:941-947.

Talavera, M., Andreu, M., Valor, H., and Tobar, A. 1998. Nematodos fitoparásiticos en áreas productoras de patata de Motril y Salobreña. Invest. Agric. Prod. Prot. Veg. 13:87-95.

Thomas, R. W. 1977. An introduction to quadrat analysis. CATMOG 12. Geo Abstracts Ltd, Norwich, UK.

Tobler, W. 1979. Cellular Geography. Pages 379-386 in: S., Gale, and G., Olsson, eds. Philosophy in Geography. Reidel, Dordrecht, Netherlands.

Trudgill, D. L., Elliott, M. J., Evans, K., and Phillips, M. S. 2003. The white potato cyst nematode (*Globodera pallida*): A critical analysis of the threat in Britain. Ann. Appl. Biol. 143:73-80.

Turner, S. J. 1996. Population decline of potato cyst nematodes (*Globodera rostochiensis* and *G. pallida*) in field soils in Northern Ireland. Ann. Appl. Biol. 129:315-322.

Turner, S. J., and Rowe, J. A. 2006. Cyst nematodes. Pages 91-120 in: Plant Nematology, R. N. Perry and M. Moens, eds. CABI, Wallingford, UK.

Vasyutin, A. S., and Yakovleva, V. A. 1998. *Globodera* in potatoes in Russia. Kartofel' I Ovoshchi 6:29-32.

Wackernagel, H. 2003. Multivariate geostatistics. Springer Verlag, Berlin.

Ward, J. H. 1963. Hierarchical grouping to optimize an objective function. J. Am. Stat. Assoc. 22:151-183.

Webster, R., and Boag, B. 1992. Geostatistical analysis of cyst nematodes in soil. J. Soil Sci. 43:583-595.

Table 2.1. The list of fields infested with *Globodera pallida* in southern Idaho with the year of detection, the number of cysts per hectare, the values of egg viability and the geographic point locations.

Field	Year of *G. pallida* detection	Number of *G. pallida* cysts/ha	Viability of *G. pallida* eggs[a]	Easting[b]	Northing[b]
ID01	2006	7,416	0.13	204912.6	191793.2
ID02	2006	10	0.39	205322.2	193219.5
ID03	2006	10,934	0.18	205538.4	191635.4
ID04	2006	4,374	0.33	207136.9	191635.7
ID05	2006	996	0.25	205936.9	193287.6
ID06	2006	1,611	0.36	206337.6	194080.4
ID07	2006	44,523	0.20	204433.5	193151.7
ID08	2007	961	0.09	205527.8	192467.5
ID09	2008	141	0.31	204497.3	193872.1
ID10	2011	5	0.25	208926.5	196381.2
ID11	2011	210	0.45	212759.2	198874.2
ID12	2012	5	0.15	204908.0	192348.2
ID13	2012	5	0.21	207769.3	191528.3
ID14	2012	7	0.05	200081.2	195904.2
ID15	2012	111	0.00	202527.8	190691.4
ID16	2013	89	0.50	206141.0	189258.5
ID17	2013	5,234	0.30	208758.5	192456.3
ID18	2014	104	0.28	199417.4	179078.1

[a]The values of *G. pallida* egg viability represent the proportions of eggs that are viable from extracted cysts (*i.e.* a value of 0.13 means that 13% of eggs contained inside a cyst are viable and likely to be hatched).
[b]Easting (the *x*-coordinate) and northing (the *y*-coordinate) are geographic Cartesian coordinates for a point and are measured in meters.

Table 2.2. A distance matrix of the fields infested with *Globodera pallida* in southern Idaho. The distances between fields are measured in pairwise comparisons and are expressed in kilometers.

	ID01	ID02	ID03	ID04	ID05	ID06	ID07	ID08	ID09	ID10	ID11	ID12	ID13	ID14	ID15	ID16	ID17	ID18
ID01	0	1	1	2	2	3	1	1	2	6	11	1	3	6	3	3	4	14
ID02	1	0	2	2	1	1	1	1	1	5	9	1	3	6	4	4	4	15
ID03	1	2	0	2	2	3	2	1	2	6	10	1	2	7	3	2	3	14
ID04	2	2	2	0	2	3	3	2	3	5	9	2	1	8	5	3	2	15
ID05	2	1	2	2	0	1	2	1	2	4	9	1	3	6	4	4	3	16
ID06	3	1	3	3	1	0	2	2	2	3	8	2	3	7	5	5	3	17
ID07	1	1	2	3	2	2	0	1	1	6	10	1	4	5	3	4	4	15
ID08	1	1	1	2	1	2	1	0	2	5	10	1	2	6	3	3	3	15
ID09	2	1	2	3	2	2	1	2	0	5	10	2	4	5	4	5	4	16
ID10	6	5	6	5	4	3	6	5	5	0	5	6	5	9	9	8	4	20
ID11	11	9	10	9	9	8	10	10	10	5	0	10	9	13	13	12	8	24
ID12	1	1	1	2	1	2	1	1	2	6	10	0	3	6	3	3	4	14
ID13	3	3	2	1	3	3	4	2	4	5	9	3	0	9	5	3	1	15
ID14	6	6	7	8	6	7	5	6	5	9	13	6	9	0	6	9	9	17
ID15	3	4	3	5	4	5	3	3	4	9	13	3	5	6	0	4	6	12
ID16	3	4	2	3	4	5	4	3	5	8	12	3	3	9	4	0	4	12
ID17	4	4	3	2	3	3	4	3	4	4	8	4	1	9	6	4	0	16
ID18	14	15	14	15	16	17	15	15	16	20	24	14	15	17	12	12	16	0

Table 2.3. Results of the Mantel correlation test for the values of *Globodera pallida* cyst and egg viability with simulated *p*-value and variance using 1,000 replicates run on a Monte-Carlo simulation.

Parameters	Distance matrix vs number of cysts	Distance matrix vs egg viability
Mantel correlation[a]	-0.15	0.08
Simulated *p*-value[b]	0.93	0.28
Variance	0.01	0.02

[a]Mantel correlation statistic is equivalent to r-squared (-1 perfect negative correlation, 0 absence of correlation, 1 perfect positive correlation).

[b]Simulated *p*-values are not significant ($P > 0.05$).

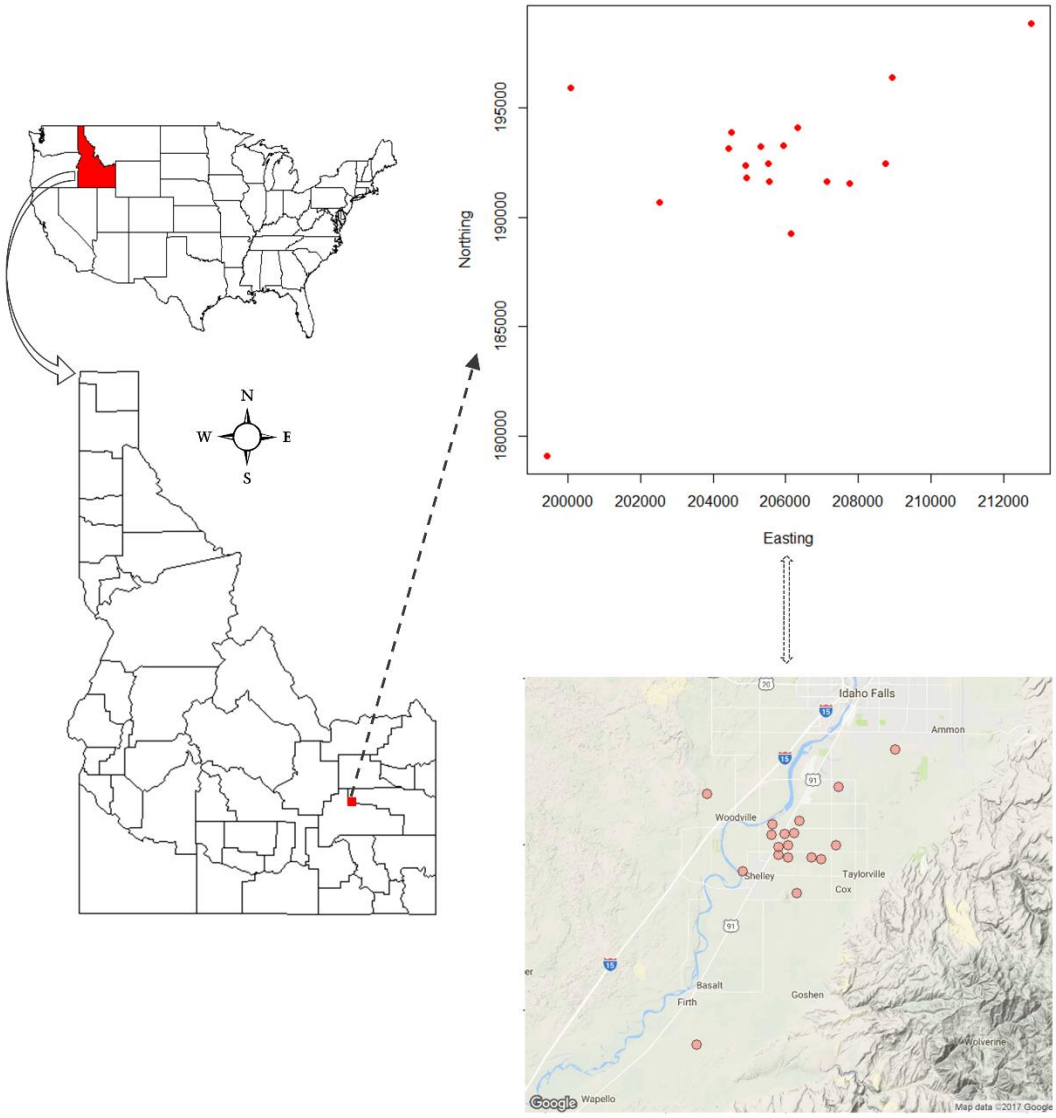

Fig. 2.1. Map of the state of Idaho (left) and location of the fields infested with *Globodera pallida* in southern Idaho (right). *Globodera pallida* was first found in 2006 in the Shelley, ID area located in the Bingham County. The data used for spatial analysis in this study came from 18 infested potato fields where *G. pallida* cysts were collected, and egg viability was evaluated by USDA-APHIS.

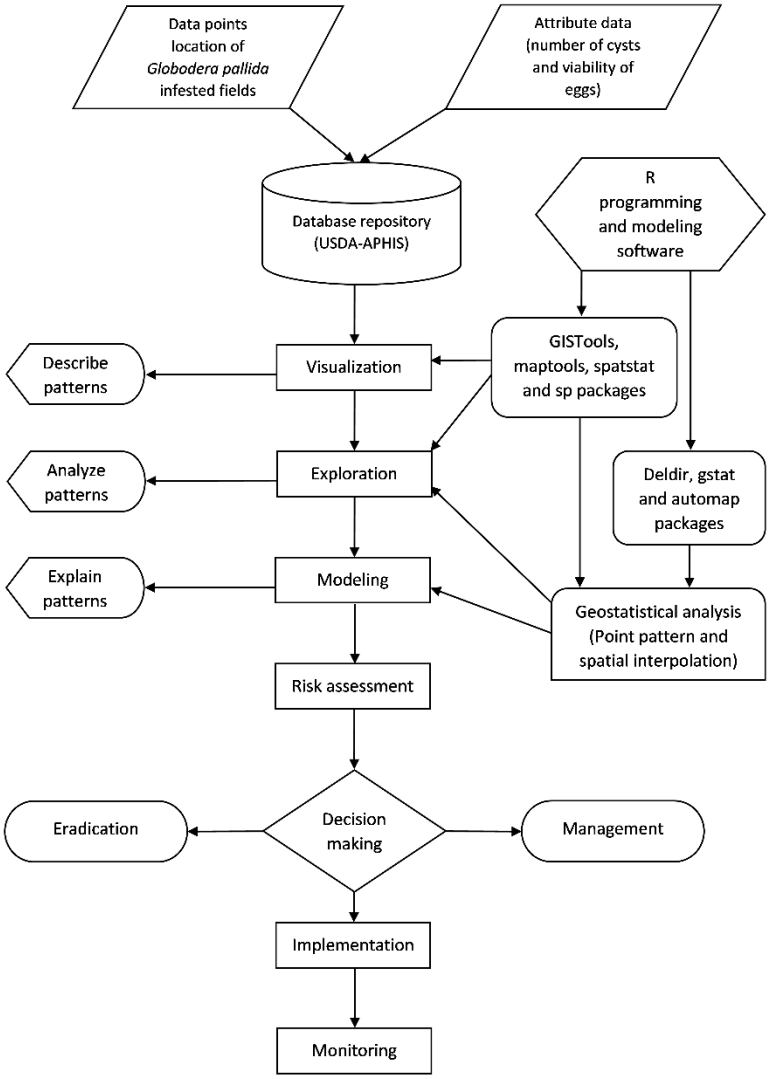

Fig. 2.2. Conceptual framework for spatial analysis of *Globodera pallida* in southern Idaho. The diagram provides a succinct summary of the methodology applied in this study. It consists of data retrieval, data analysis and processing using R programming software and elaboration of a decision-making statement based on the results. Spatial analytical methods used included: (i) nearest neighbor algorithm and inverse distance weighting, as deterministic interpolators; (ii) ordinary kriging method as probabilistic interpolator.

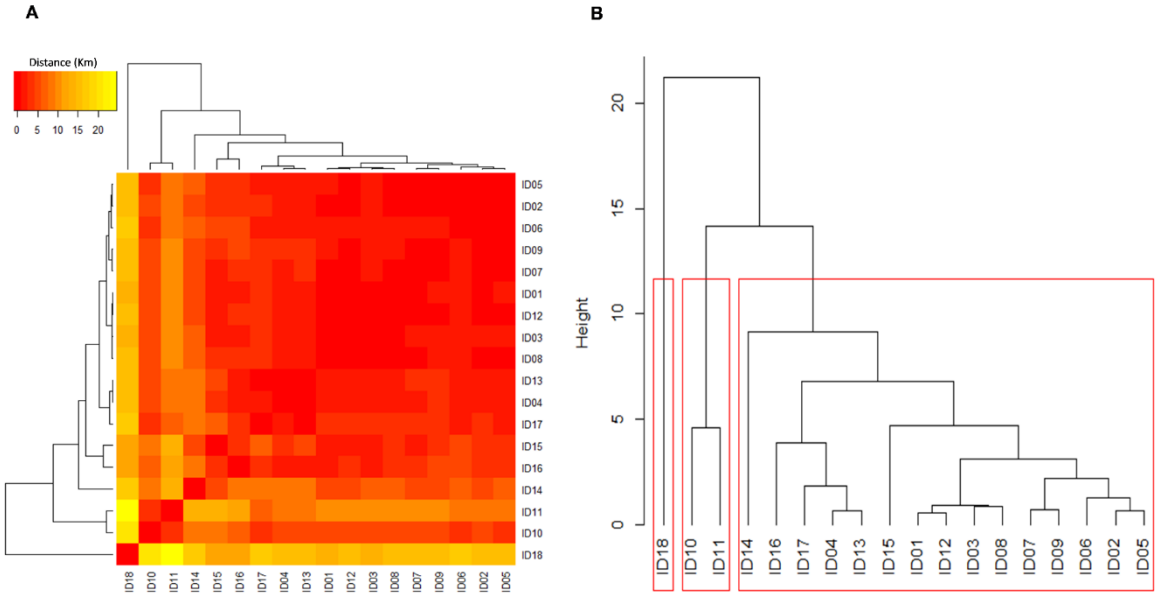

Fig. 2.3. A. The heat map representation of *Globodera pallida* infested field distance matrix showed similarities in hue shifting colors when pair of fields are closed (red-orange) and dissimilarities when distance separations between pair of fields are significant (orange-yellow). **B.** The agglomerative hierarchical cluster analysis of *G. pallida* infested field distance matrix identified the presence of three main clusters (red rectangles) of infested fields using Ward's minimum variance method defined as the squared Euclidean distance between points.

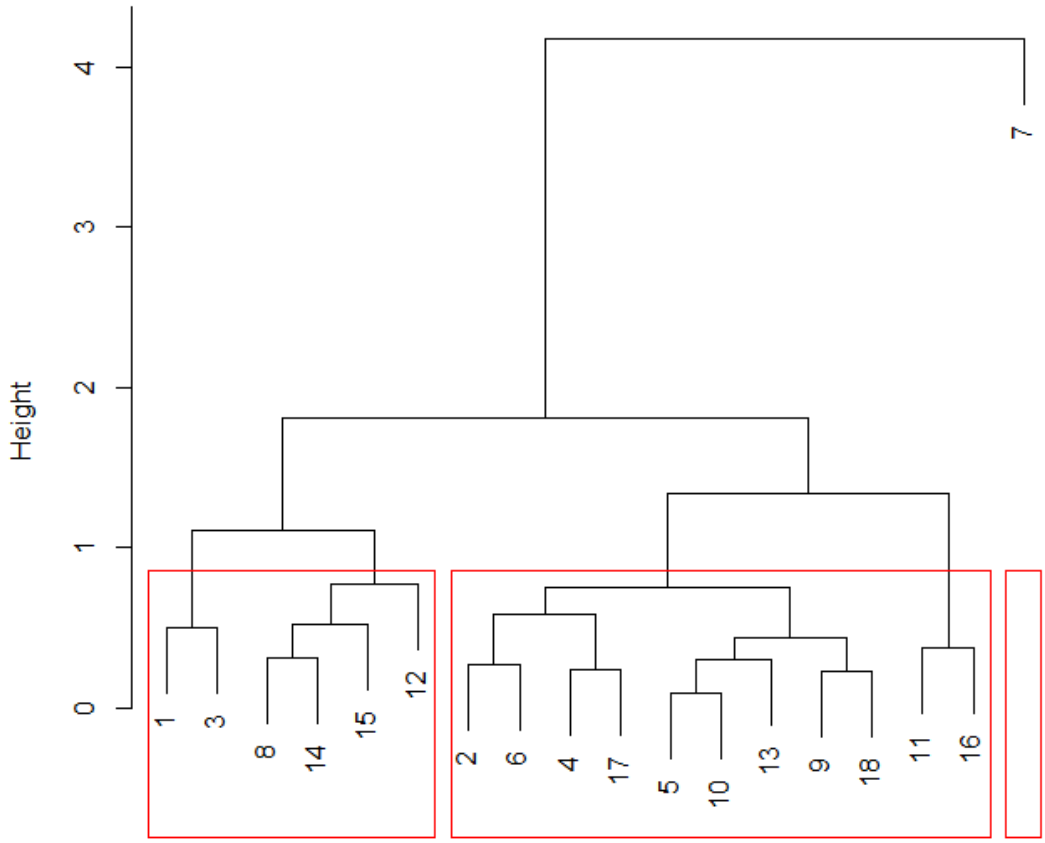

Fig. 2.4. The agglomerative hierarchical cluster analysis applied on the standardized data values of *Globodera pallida* cyst number and egg viability identified, based on their combined weight, three main clusters (red rectangles) of fields infested with *G. pallida* using the average linkage method. The agglomerative coefficient was 0.87 representing a high-quality index for the amount of clustering structure found.

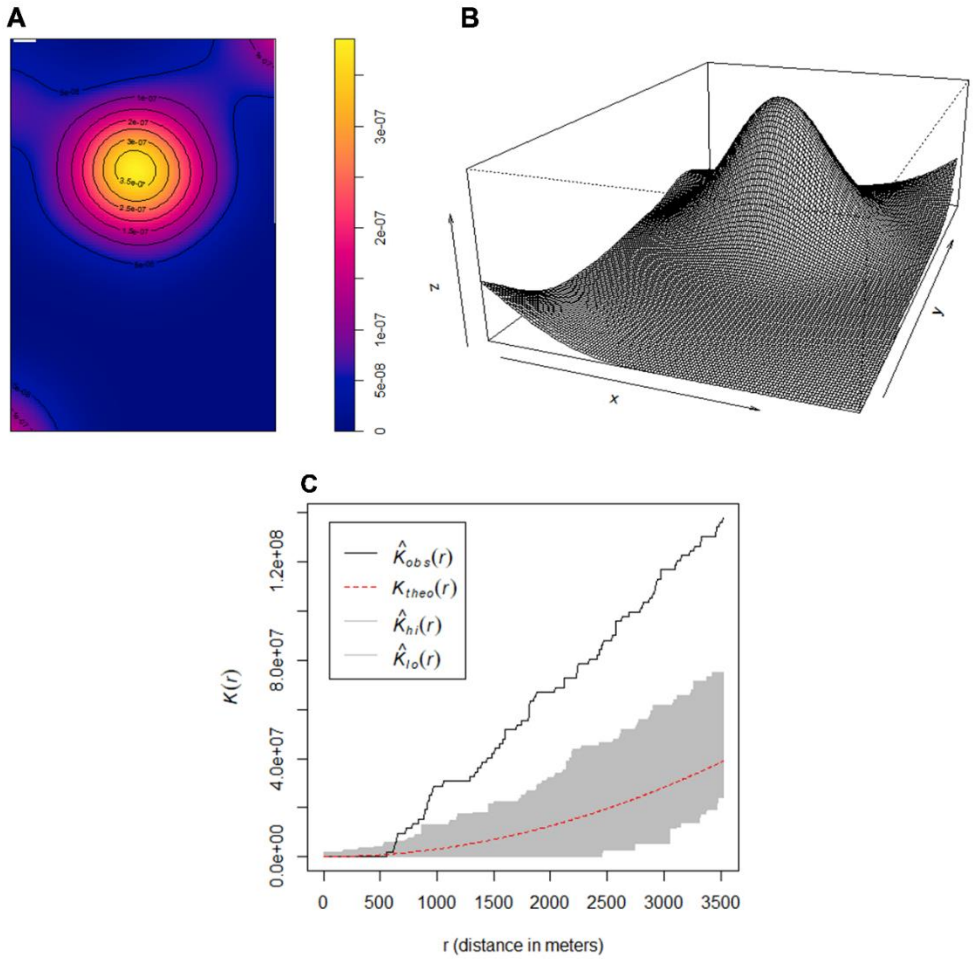

Fig. 2.5. A. The kernel density estimation (KDE) showed the location of the highest densities of fields infested with *Globodera pallida*. The color intensity is described as follows: yellow color or highest number corresponded to highest density and blue color or lowest number corresponded to lowest density. A bandwidth of 2,000 meters was used to cover the study area. **B.** A 3-D representation of the KDE analysis showing a smooth peak representing the highest densities of *G. pallida* infested fields in the landscape. **C.** Ripley's K-function plot showing evidence of spatial clustering of fields infested with *G. pallida*, confirmed by the maximum absolute deviation test of complete spatial randomness ($P = 0.01$) and by the quadrat test ($P = 0.003$). The observed K-function values (black line on plot) are much higher than the expected values under complete spatial randomness (red dashed line). The gray area represents the envelope or confidence interval of the expected values.

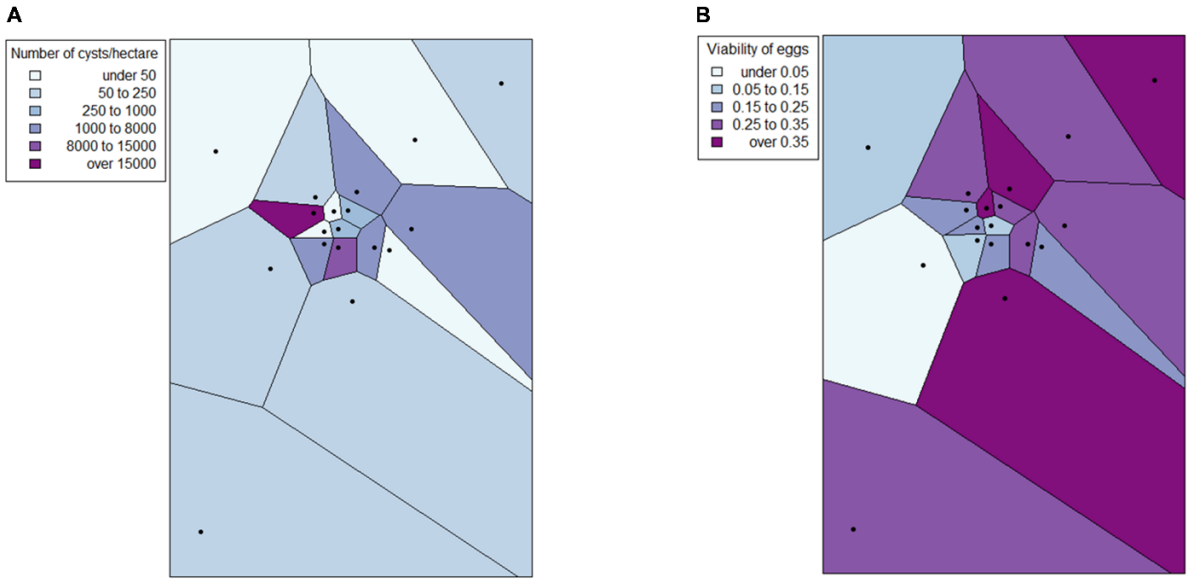

Fig. 2.6. A. The nearest neighbor interpolation model used 18 Voronoi tessellation (Thiessen polygons) and was designed to assign a polygon to each field infested with *Globodera pallida* (black dots [•]). Five major polygons in the subset 50 to 250 cysts/ha occupied over 60% of the interpolated areas, followed by other five polygons estimated under 50 cysts/ha. **B.** The values of *G. pallida* egg viability in the subsets 0.25 to 0.35 and over 0.35 occupied over 65% of the interpolated areas.

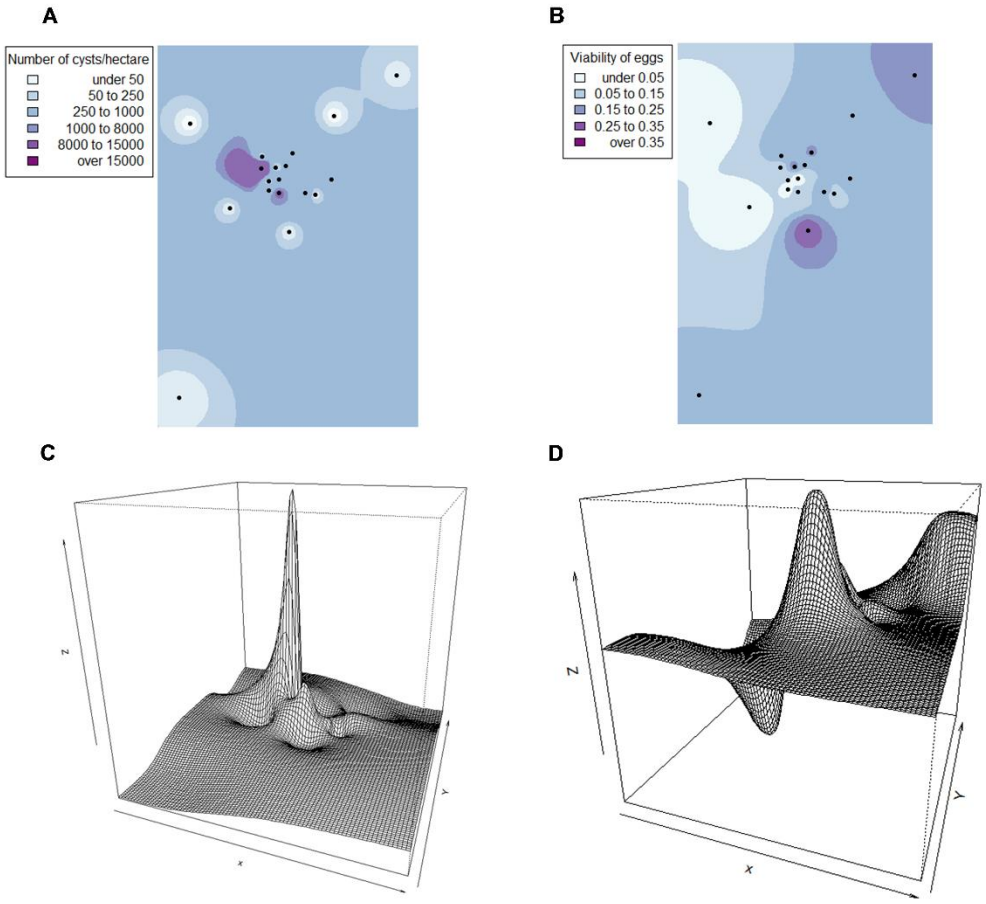

Fig. 2.7. A. The inverse distance weighting (IDW) surface consisted of 10,000 grids upon which the number of *Globodera pallida* cysts and the values of egg viability (black dots [•]) were extrapolated using an alpha of 3, as the inverse square relationship. The subset 1,000 to 8,000 cysts/ha occupied over 85% of the interpolated areas and only a small area is estimated over 15,000 cysts/ha. **B.** The values of *G. pallida* egg viability in the subset 0.15 to 0.25 occupied over 60% of the interpolated areas. **C.** 3-D representations of the inverse distance weighting for the number of *G. pallida* cysts. The model showed a relatively smooth surface with high and low peaks in the interpolated locations corresponding to areas of high number of *G. pallida* cysts per hectare. **D.** 3-D representations of the inverse distance weighting for the values of *G. pallida* egg viability. The model showed many smooth peaks in the interpolated locations corresponding to areas of low and high values of *G. pallida* egg viability.

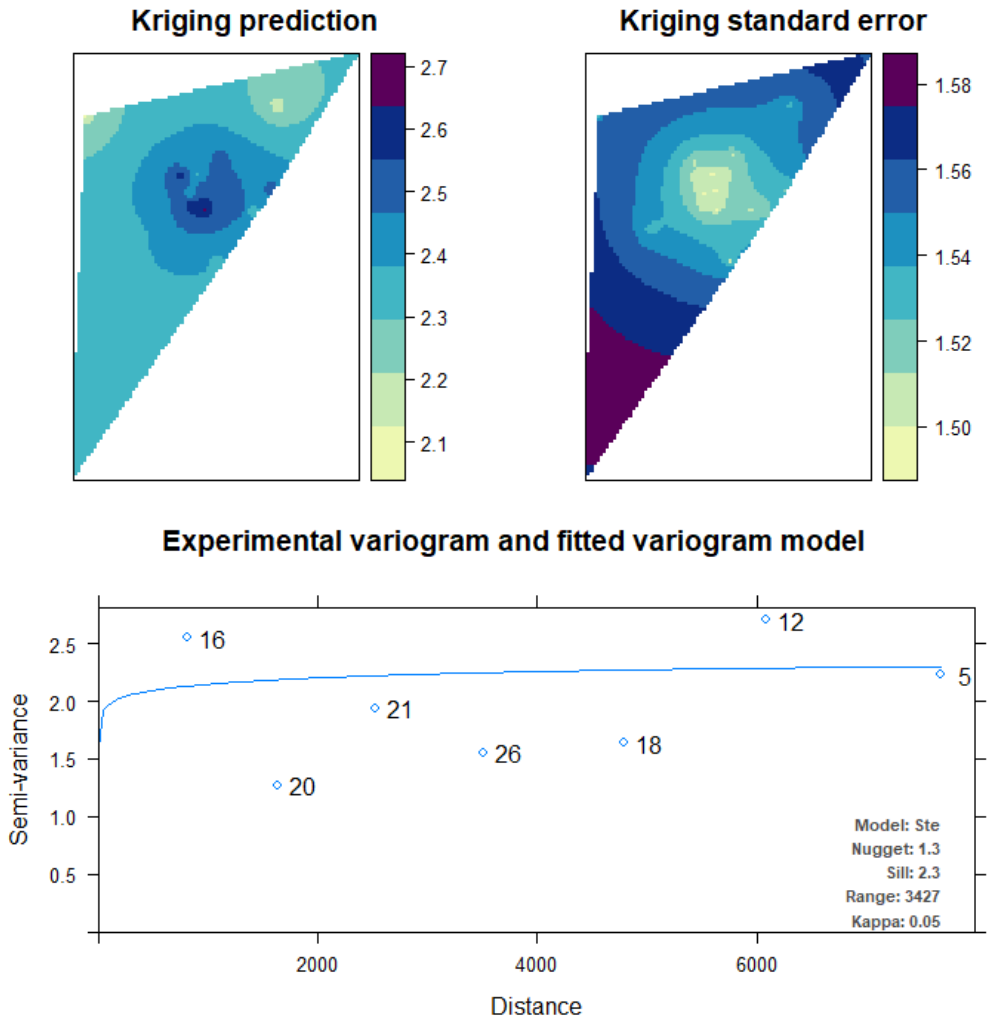

Fig. 2.8. The ordinary lognormal kriging model showed high *Globodera pallida* cyst values around a centered focal area in the kriging prediction map. The kriging standard error map illustrated the degree of confidence associated with the kriging prediction map and showed that the error measurement is lower toward the centered focal area. The Ste (Matern, M. Stein's parameterization) model was used to fit the experimental variogram for *G. pallida* cyst values with the following initial parameters: sill (2.3), range (3,427), nugget (1.3) and kappa (0.05). The Ste model adapted to the experimental variogram of *G. pallida* cyst values illustrated a weak spatial correlation, as represented by a continuous flat line.

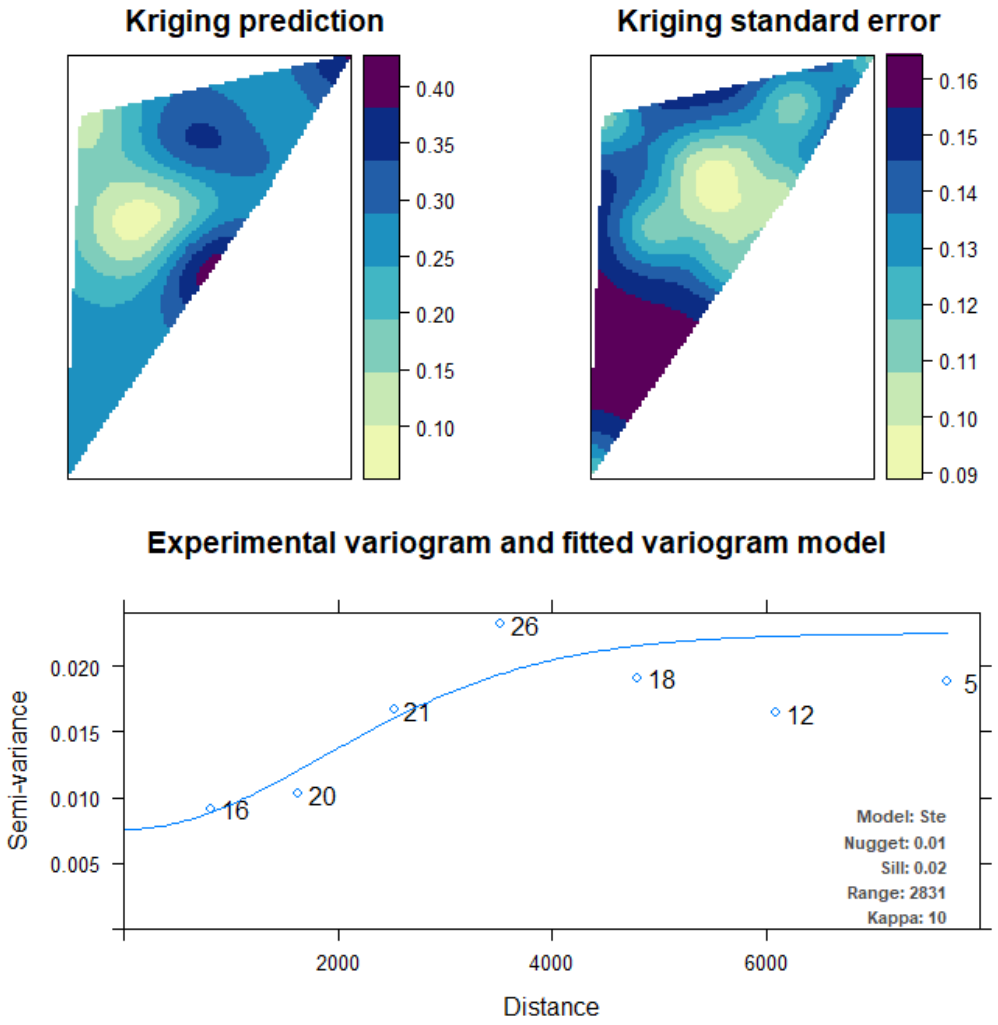

Fig. 2.9. The ordinary kriging prediction model for values of *Globodera pallida* egg viability showed most areas were estimated between 0.25 to 0.35 and the error measurement associated with the prediction map followed similar patterns as the *G. pallida* cyst values model. The Ste (Matern, M. Stein's parameterization) model was used to fit the experimental variogram for values of *G. pallida* egg viability with the following initial parameters: sill (0.02), range (2,831), nugget (0.01) and kappa (10). The Ste model for values of *G. pallida* egg viability showed a relatively strong spatial correlation, as illustrated by a curved line that marked the boundary between correlated and non-correlated values.

Chapter 3: Spatiotemporal Analysis and Dispersal Patterns of *Globodera pallida* in Idaho

Abstract

The potato cyst nematode *Globodera pallida* is a globally regulated potato pest. It was detected for the first time in the U.S. in the state of Idaho in 2006, and as of February 2019, the infestation is limited to 1,326 ha. *Globodera pallida* is a specialized obligate sedentary endoparasite that can survive in the soil for up to 30 years in the absence of its potato host. In highly infested fields, the nematode can reduce tuber yields up to 80% and is spread mainly through soil, tubers or farm equipment. The objectives of this study were to describe the spatiotemporal distribution of *G. pallida* in infested fields and to model its dispersal patterns in southeastern Idaho. We used geostatistical tools and simulation models for precise mapping and to describe the relationships between *G. pallida* incidence with the spatial configurations. We found that the nematode is spatially-clustered particularly around the edges of the fields, and that the dispersal patterns of *G. pallida* followed the direction of cultivation. We found that the absence of potato in the field contributed in stopping the nematode reproduction, and the use of chemical fumigants and biofumigant cover crops contributed in a significant reduction of the viability of the eggs in time and space. We observed a process of a non-linear decline in the prevalence of cysts as the distance separation from the primary infestation focus increased. A power-law model was used to fit *G. pallida* dispersal capabilities. The main goal of this study is to provide information on *G. pallida* distribution to policymakers, stakeholders, potato growers and researchers to facilitate common understandings on the challenges and opportunities for controlling this pest in Idaho.

Introduction

Phytopathogenic nematodes represent a considerable threat for food security worldwide. Around 4,100 species of plant-parasitic nematodes have been identified and they cause between $80 and $118 billion per year in crop losses (Koenning et al., 1999; Sasser and Freckman, 1987). *Globodera pallida* (Behrens, 1975; Stone, 1972), one of the most destructive plant-parasitic nematodes, is a globally regulated potato pest. *Globodera pallida* and *Globodera rostochiensis* (Wollenweber, 1923; Skarbilovich, 1959), both potato cyst nematodes (PCN), co-evolved with potato and other native *Solanum* species in the Andean Region of South America (Picard et al., 2004). Recent survey data revealed that *G. rostochiensis* is present in 68 countries and *G. pallida* in 48 (CABI, 2018). *Globodera pallida* is a specialized obligate sedentary endoparasite that can survive in the soil for up to 30 years in the absence of its potato host (Turner, 1996). In highly infested fields, *G. pallida* can reduce tuber yields up to 80% and is spread mainly through soil, tubers or farm equipment (Talavera et al., 1998; Vasyutin and Yakovleva, 1998).

Globodera pallida was found in southeastern Idaho in 2006 in two potato fields in Bingham County (Hafez et al., 2007; USDA-APHIS, 2019). The United States Department of Agriculture's Animal and Plant Health Inspection Service (USDA-APHIS) and the Idaho State Department of Agriculture (ISDA) have listed *G. pallida* as a quarantine pest for Idaho under Title 7 CFR 301.86 Federal Regulation. USDA-APHIS and ISDA have implemented a containment and eradication program to prevent *G. pallida* spread to other potato fields. In fields infested with *G. pallida*, the program outlines: (i) restrictions on the movement of soil and plant materials; (ii) prohibition of planting potato and other solanaceous crops; and (iii) sanitation procedures for farm equipment. Chemical application with the nematicide Telone II (1,3-dichloropropene) is being conducted in infested fields as part of the *G. pallida* eradication program and *Solanum sisymbriifolium* 'litchi tomato' is under field scale trials in infested fields (USDA-APHIS, 2019). The regulated area includes portions of northern Bingham and southern Bonneville Counties and is currently limited to 3,057 hectares, of which 1,326 ha are fields infested with *G. pallida* (USDA-APHIS, 2019). USDA-APHIS have issued a list of regulated articles: (i) *G. pallida*; (ii) *G. pallida* host crops (eggplant

[*Solanum melongena*], pepper [*Capsicum* spp.], tomatillo [*Physalis philadelphica*], tomato [*Solanum esculentum*]); (iii) root crops; (iv) garden and dry beans (*Phaseolus* spp.) and peas (*Pisum* spp.); (v) all nursery stock; (vi) soil, compost, humus, muck, peat and manure; (vii) hay, straw and fodder; and (viii) any equipment or conveyance used in an infested or associated field that can carry soil if move out of the field. USDA-APHIS provides steps for deregulating *G. pallida* infested fields: (i) no viable eggs detected (collected eggs are testing for viability); (ii) three rounds of greenhouse bioassay of field cysts to confirm absence of reproduction; and (iii) in-field bioassay where fields can be released from quarantine status after three more negative viability surveys after harvests of a susceptible crop. As of February 2019, 22 fields (969 ha) have passed step 1 (no viable eggs found) and 18 fields (720 ha) have passed step 2 (no reproduction) (USDA-APHIS, 2019).

In a globalized and more integrated world, international trade represents an important invasion pathway for non-native plant pests. Pest invasion consists of several phases (Ferris et al., 2003): (i) entry of the organism; (ii) establishment through local reproduction; (iii) integration into the local environment; and (iv) spread. Because of these risks, international trade agreements and phytosanitary measures were established and re-enforced to minimize risks of accidental introduction of plant pests to non-native areas. The International Plant Protection Convention (IPPC) defines ‘quarantine pest’ as ‘a pest of potential economic importance to the area endangered thereby and not yet present there, or present but not widely distributed and being officially controlled’ (FAO-IPPC, 2017). In order to avoid severe economic losses due to the entry of non-native plant diseases, a comprehensive understanding of the spatio-temporal and dispersal patterns of the pathogens is warranted to better manage and control disease epidemics that could potentially devastate our food provision and energy resources.

Georeferenced or geostatistical data denote the locations and time periods when events are recorded from a continuous surface occupying a fixed subset, D, of two-dimensional space (R^2) and where the attribute value ($Z[s_i]$) is a random vector at location s_i in D (Cressie, 1993). Spatial data comprised all surfaces that share a common border or have a direct transport connection with neighbors, which could capture interaction flows between the areas (Haining, 2003). Space-time events possess an intrinsic continuity or structure

which enable the formulations of predictive models, and the concept of spatial continuity is often referred to as 'Tobler's First Law of Geography' where 'Everything is related to everything else, but near things are more related than distant things' (Tobler, 1970). The concept of spatial continuity is translated in the spatial context as follows (Haining, 2003): (i) if the attribute values of one point location are similar to another location (spatial dependence), this process is known as a positive spatial autocorrelation; and (ii) as the distance separation of observations increases such autocorrelation will tend to weaken and the attribute values will appear to be spatially-independent, this process is known as negative spatial autocorrelation.

Exploratory spatial data analysis provides a collection of visual and essential mapping tools to detect and assess spatial patterns and to formulate hypotheses. The Akima interpolation method is a mathematical model based on a piecewise function composed of a set of polynomials each of degree three and is a continuously differentiable sub-spline interpolation (Akima, 1970, 1991). Data from next neighbor is used to determine the coefficients of the interpolation polynomial. The ordinary kriging is used as a probabilistic interpolator to estimate the value of a random variable, z, at one or more unsampled points. The kriging estimate of variable z at point x_0, $\hat{z}(x_0)$, is a linear weighted sum of n observations surrounding the estimate and provides minimum mean-squared error values at unsampled locations (Cressie, 1993; Haining, 2003). Experimental variograms represent a description of the spatial continuity of the data and is calculated using a measure of variability between pairs of points at various distances (Matheron, 1963). Moran's *I* is used to measure spatial autocorrelation based on both point locations and attribute values simultaneously (Moran, 1950). The null hypothesis for Moran's *I* test is the absence of spatial autocorrelation ($P > 0.05$), which means the attribute values are randomly distributed among the locations in the given study area. Spatial analysis applied to plant-parasitic nematodes has been used to develop accurate sampling methods in fields (Dinardo-Miranda and Fracasso, 2009; Francl, 1986), determine ecological patterns of nematode distribution (Porazinska et al. 2012), and to support the use of site-specific management in nematode infested fields (Avendaño et al. 2003). Evans et al. (2003) used spatial analysis to target 'hot spots' of PCN infestations for additional treatment with fumigant, thereby reducing the cost

of chemicals applied and minimizing possible environmental damage. Contina et al. (2018) used spatial analysis to determine the regional spatial pattern of *G. pallida* in Idaho and to assess the effectiveness of the control and eradication measures.

The distribution or dispersal of plant pathogens in a field illustrates a certain increasing or decreasing trends, known as dispersal gradient, when plotting against the distance from the original source of infestation (Gregory, 1968; Mundt et al., 2009; Severns et al., 2019). There are two basic types of biological dispersal: (i) density-independent or passive dispersal that depends on humans, animal and environmental factors for dispersal, as in the case of plant-parasitic nematodes (Nathan, 2001); and (ii) density-dependent or active dispersal that depends on factors such as local population size, resource competition and environmental conditions, as in the case of some plant-parasitic fungi (Bowler and Benton, 2005). Discontinuous dispersal in infested fields may result in establishment of isolated pest foci from the main infestation focus using short-distance dispersal mechanism facilitated by passive transportation (human activities). The combination of long- and short-distance dispersal (LDD and SDD) mechanisms is considered as stratified dispersal and consisted of (Hengeveld, 1989): (i) establishment of new foci far from the moving population front; (ii) growth and development of individual foci; and (iii) fusion of foci that contributes to the advance of population front. Choi et al. (2017) reported that the pine wood nematode, *Bursaphelenchus xylophilus*, invasion consisted in a jumping type of dispersal and the formation of new patches which later expanded and merged, supporting the existence of a stratified dispersal pattern for *B. xylophilus*. Madden et al. (2007) categorized the disease dispersal gradient as: (i) primary gradient, where all infestations are originating at the initial inoculum source or focus (primary spread of the disease), which occurs for monocyclic diseases; and (ii) secondary gradient, where infections are due to inoculum produced beyond the initial inoculum source (secondary spread of the disease), which occurs for polycyclic diseases.

Non-linear and mechanistic models of disease dispersal have been developed to capture the determinants of spatiotemporal disease spread. The negative exponential and power law are the most widely used contact distribution models in plant disease epidemiology (Madden et al., 2007; Mundt, 1989). Both models explain a process of a non-

linear decline in inoculum prevalence as distance increases, however for the power-law model, the gradient is steeper near the source and shallower far from the source, compared with the exponential model (Madden et al., 2007). Power-law models were used in plant nematology for estimating sampling surveys in infested fields (Duncan et al., 1989; McSorley et al., 1985), determining the aggregation of several nematode species in soil (Boag and Topham, 1984), and classifying soil nematode communities in urban landscapes (Park et al., 2013). Plant disease dispersal models convey important information on: (i) the spatial behavior of non-native pests; (ii) the identification of vulnerable area; and (iii) the provision of a framework for predicting and controlling pest invasions as well as enabling early detection and eradication programs.

The objectives of this study were to describe the spatiotemporal distribution of *G. pallida* in infested fields and to model its dispersal patterns in southeastern Idaho. We proceeded in characterizing the distribution of *G. pallida* in infested fields during the first year of detection and after application of fumigants and planting of non-host crops in subsequent years. As the distribution and abundance of invasive species is often correlated with human activities and land use practices, we simulated the spatial spread of *G. pallida* in potato fields using the invasive species distribution models (ISDM) to compute a negative exponential dispersal pattern (Hattab et al., 2017; Meentemeyer et al., 2008). We calculated the distance separation between the main *G. pallida* inoculum source focus from the rest of the foci in fields and between fields, and we fitted a power-law model to the distribution of foci in order to estimate SDD and LDD parameters for *G. pallida*. Finally, we concluded our study by discussing the implications of understanding the spatiotemporal and dispersal patterns of *G. pallida*, as well as, comparing and exploring the strength and limitations of our models. The results of this study would contribute to identify vulnerable areas and enable a provisional framework for prediction and control.

Materials and Methods

Data collection. Data point locations of fields infested with *G. pallida* in southeastern Idaho with the associated number of cysts and the values of egg viability were collected by USDA-APHIS from 2006 to 2014 (Fig. 3.1; Table 3.1 and 3.2). The sampling system used by USDA-APHIS consisted in dividing each infested field into grids of dimensions $20\ m \times 20\ m$. For each grid, 2.27 kg soil was collected in a full-field sampling scheme during the first year of detection to determine the location of the infestation foci, and 9.07 kg soil was collected in infested grids after each application of fumigants and planting of non-host crops in subsequent years. The soil taxonomy associated with the infested fields are mostly inside the Bannock series, and consists of deep, well-drained soils formed in medium textured alluvium over gravel and sand (NCSS, 2002). The taxonomic class is coarse-loamy over sandy or sandy-skeletal, mixed, superactive, frigid Aridic Calcixerolls (NCSS, 2002).

The identity of *G. pallida* was confirmed by morphological and molecular methods (Skantar et al. 2007). *Globodera pallida* cysts were extracted from soil samples using the USDA cyst extraction method (USDA-APHIS, 2009). The viability of *G. pallida* eggs was assessed using Meldola Blue as the staining agent (Ogiga and Estey, 1974). The values of *G. pallida* cysts were transformed with $\log_{10}$ (cysts/kg soil + 1) to standardize the variance and the values of egg viability was expressed in percentage. The data collected is represented as a set of marked points illustrated in algebraic terms as following:

$$y = \{(x_1, m_1), \ldots, (x_n, m_n)\}$$

where x_i are the point centroid of each grid, represented as Easting and Northing and expressed in meters, and m_i are the number of cysts collected or the values of egg viability.

Deterministic spatial modeling. The Akima interpolation model was used to build a raster-based map of *G. pallida* distribution in infested fields. The Akima method is a mathematical model based on a continuously differentiable sub-spline interpolation function composed of a set of cubic polynomials (Akima, 1970, 1991). Data from next neighbor is used to determine the coefficients of the interpolation polynomial. The model is defined as follows:

For a set of data points:

$$s_i = s(x_i), \quad 1 \leq i \leq k$$

The interpolation function is defined as:

$$s(x) = a_0 + a_1(x - x_i) + a_2(x - x_i)^2 + a_3(x - x_i)^3, \quad x_i \leq x \leq x_i + 1$$

where $a_0, a_1, a_2, and\ a_3$ are the coefficients of the interpolation polynomial for each interval $[x_i,\ x_{i+1}]$. The Akima spline interpolation is characterized by its non-linearity and is less affected by outliers.

Stochastic spatial modeling. The ordinary kriging was used as a probabilistic interpolator to estimate the value of a random variable, z, at one or more unsampled points. The kriging estimate of variable z at point x_0, $\hat{z}(x_0)$, is a linear weighted sum of n observations surrounding the estimate (Stein, 1999):

$$\hat{z}(x_0) = \sum_{i=1}^{n} \lambda_i z(x_i)$$

where λ_i are the weights and $z(x_i)$ is the known value of variable z at sampling site x_i.

We estimated the index of dispersion (D) by calculating the average variance-to-mean ratio, as defined by:

$$D = \frac{\sigma^2}{\mu}$$

where σ^2 is the estimated variance and μ is the estimated mean of cysts from the kriging interpolation output. The index of dispersion was used to determine whether the distribution of *G. pallida* cysts in the fields were clustered or dispersed compared to the randomness associated with a Poisson process. The index of dispersion ranges from 0 to 1, where: (i) $(D = 0)$ represents a constant distribution (not dispersed); (ii) $0 < D < 1$ represents a binomial distribution (under-dispersed or clustered); (iii) $D = 1$ represents a Poisson distribution (uniformly dispersed); and (iv) $D > 1$ represents a negative binomial distribution (over-dispersed).

Kriging, as a probabilistic interpolator, relies on an experimental variogram to measure the spatial correlation of the random function $\hat{z}(x_0)$ (Stein, 1999). The variogram is defined by calculating the semivariance as a function of distance:

$$\gamma(d) = \frac{1}{2}\sum\{[\hat{z}(x_1) - \hat{z}(x_2)]^2\}$$

The semivariance increases with increasing lag distance (monotonic increasing), which indicates that at short distances the values of $\hat{z}(x)$ correlates with space (spatial dependence), but as the lag distance increases, they become increasingly uncorrelated (spatial independence). If the spatial dependence varies along with spatial directions, anisotropy, the process is modeled using directional variograms, as defined by:

$$\gamma(d,\theta) = \left(\frac{1}{2}N(d,\theta)\right)\sum_{i=1}^{N(d,\theta)}[\hat{z}(x_1) - \hat{z}(x_2+h,\theta)]^2$$

where θ represents the directional angles along the point locations.

Spatial autocorrelation. Spatial autocorrelation represents the relationship between nearby spatial units. The concept is best summarized by Tobler's first law of geography 'near things are more related than distant things' (Tobler, 1970). Moran's *I* was used as a measure of spatial autocorrelation based on both point locations and attribute values simultaneously (Moran, 1950). The goal of Moran's *I* is to find the correlation of one variable with itself regarding a spatial weight matrix. The null hypothesis for Moran's *I* test is the absence of spatial autocorrelation ($P > 0.05$), which means the attribute values are randomly distributed among the locations in the given study area. Moran's *I* coefficient is computed using the formula:

$$I = \frac{n}{S_0}\frac{\sum_{i=1}^{n}\sum_{j=1}^{n}w_{i,j}(y_i-\bar{y})(y_j-\bar{y})}{\sum_{i=1}^{n}(y_i-\bar{y})^2}$$

Where y_i are the observations, $w_{i,j}$ represents the distance weight (distance matrix), n is the number of observations and $S_0 = \sum_{i=1}^{n}\sum_{j=1}^{n}w_{i,j}$. Moran's *I* coefficient (observed values) ranges from -1 to + 1, where -1 is negative spatial autocorrelation, 0 is absence of spatial autocorrelation and + 1 is positive spatial autocorrelation.

Invasive species distribution modeling. ISDM was used as a spatial simulation to characterize the spread of *G. pallida* in a potato field and to produce risk maps of occurrence likelihood in the absence of control measures. The force of invasion (F_i) was calculated as a negative exponential dispersal kernel using the formula (Meentemeyer et al., 2008):

$$F_i = \Sigma_{k=1}^{N} exp\left(\frac{-d_{ik}}{a}\right)$$

where d_{ik} is the Euclidean distance between each *G. pallida* initial foci of invasion k in a target area i. The parameter a represents the form of the dispersal kernel where low values of a indicate high dispersal limitation and high values indicate low dispersal limitation.

In this study, we established that *G. pallida* dispersal capabilities and limitations are closely related to the level of human activities in the fields, and represent the form of the dispersal kernel. We defined human activities as the labors required for soil preparations with equipment and machinery, field planting and maintenance, and other types of labors that require transit in the fields. *Globodera pallida* dispersal is characterized as density-independent or passive transmission that requires human intervention to move cyst-infested soils from contaminated to non-contaminated areas.

***Globodera pallida* dispersal and inoculum gradients.** The distance separation between the primary inoculum focus of *G. pallida* in fields and secondary foci (SDD) was calculated using a distance-based matrix, and the same method was used to estimate distance separation between the most infested field and less infested fields (LDD), as illustrated in algebraic terms:

$$d_{ij} = d(\{X_i\},\{X_j\}) = \|X_i - X_j\|^2$$

where d_{ij} is the pairwise distances between major inoculum focus X_i and minor foci X_j , and are arranged in a matrix. A power-law model (Gregory model) was used to fit the distribution prevalence of *G. pallida* cysts over increasing distances (Gregory, 1968; Madden et al., 2007):

$$Y = a_P s^{-b_p}$$

where a_P and b_P are parameters and s is the distance separation from the inoculum focus. The model describes a non-linear decline in inoculum prevalence as distance increases with a steeper gradient near the inoculum source and a shallower gradient far from the source, along with a fat-tail distribution.

Data analysis and modeling. The software R version 3.5.2 was used as a modeling language environment for data exploration and spatial analysis in this study (R Core Team, 2018). Centroid coordinates of field grids were projected into Easting and Northing coordinate system using the spatial reference EPSG:3524 NAD83 in the package ‘sp’. Akima interpolation algorithm was performed using the packages ‘akima’ and ‘fields’ (Akima,

1970, 1991). Ordinary kriging and the variogram modeling were performed using the packages ‘gstat’ and ‘automap’. The ‘automap’ package automatically fits a variogram to the data and provides initial estimates for the sill (variance), range (distance at which the variogram reaches the sill), nugget (error measurement) and kappa (a smoothing parameter). A kriging prediction and a standard error maps were also generated in this procedure. Moran’s *I* was estimated using the packages ‘ape’ and ‘ncf’. ISDM was computed using the packages ‘iSDM’ and ‘raster’ (Hattab, 2017). SDD and LDD distributions were plotted and model-fitted using the packages ‘ggplot2’, ‘MASS’, ‘plyr’ and ‘nls2’.

Results

The use of spatial interpolation to predict and map the distribution of *G. pallida* cysts in infested fields revealed the invasion patterns of the nematode. The Akima interpolation method showed that *G. pallida* cysts are spatially-clustered particularly around the northside corners of the fields. In the first year of *G. pallida* detection in Idaho, we analyzed the nematode distribution in six infested fields (Bin001, Bin025, Bin026, Bin054, Bin068 and Bon064), and we found the presence of multiple infestation foci with high level of cyst densities in soil (Fig. 3.2 and 3.3). The number of infestation foci per field were: (i) Bin001, 173; (ii) Bin025, 1,493; (iii) Bin026, 317; (iv) Bin054, 76; (v) Bin068, 22; and (vi) Bon064, 151. The level of cyst densities per kilogram of soil per foci and associated standard error were: (i) Bin001, 3.17 ± 0.56; (ii) Bin025, 36.07 ± 2.39; (iii) Bin026, 13.49 ± 1.83; (iv) Bin054, 22.38 ± 7.74; (v) Bin068, 5.91 ± 3.34; and (vi) Bon064, 5.73 ± 1.77. Bin025 was the most highly infested field ($P < 0.05$), with major concentration of foci and cysts located in its northern sides, followed by a diffusion wave of infestation toward the southeast corners, with some pioneered-foci advancing toward the center of the field. Similar dispersal patterns were observed for Bin026 and Bin054. Bin001 showed the least concentration of cysts in soil, but with higher level of scattered-infestation foci than Bin068. We found that the dispersal patterns of *G. pallida* followed the direction of cultivation in the fields, and oriented toward North/South direction for most fields, except Bon064 which was East/West.

Kriging interpolation methods use both mathematical and statistical tools to predict the incidence of *G. pallida* cysts at all locations within the study area, and additionally provide prediction errors of the quality of the interpolation based on the spatial autocorrelation among the cyst data points. Ordinary lognormal kriging prediction showed similar distribution patterns of *G. pallida* cysts in the fields, spatially-aggregated with high cyst densities level in soil, and was associated with low-level of kriging standard errors (Fig. 3.4). We found higher level of cyst concentration near the entrance of the fields, when comparing satellite imagery with kriging maps for most of the infested fields, which indicated potential contamination by agricultural equipment. We calculated the index of dispersion to determine whether the distribution of cysts in the fields were clustered or dispersed compared to the randomness associated with a Poisson process and were for: (i) Bin001, 0.17; (ii) Bin025, 0.08; (iii) Bin026, 0.34; (iv) Bin054, 0.24; (v) Bin068, 0.71; and (vi) Bon064, 0.29. The results showed that the index of dispersion were between $0 < D < 1$ indicating that the distribution of *G. pallida* cysts in the fields was under-dispersed or clustered, and pointing to a binomial distribution. Bin025 showed the highest degree of nematode clustering, particularly in the northern part of the field, and Bin068 showed the lowest degree of nematode clustering, with a pioneered-wave of dispersion oriented toward northeast.

We studied the spatial continuity of *G. pallida* cysts for each field using experimental and fitted variogram models. The experimental variograms measured the variability between pairs of cyst data points at various distances and fitted a non-linear model to the coefficients. The results showed the presence of spatial dependence associated with different distance ranges, where the incidence of *G. pallida* cysts in the fields correlated with space (Fig. 3.5). The experimental variograms for all fields were fitted using the Ste model (Matern, M. Stein's parameterization), except for Bin054 were a Spherical model was fitted (Table 3.2). The distance ranges of spatial dependence were (in meters): (i) Bin001, 119; (ii) Bin025, 2,526; (iii) Bin026, 45; (iv) Bin054, 63; (v) Bin068, 68); and (vi) Bon064, 21. Bon064 showed the lowest range of spatial continuity because of the increased-level of variabilities in the repartition of cyst densities over the surface area of the field. Bin025 illustrated an unbounded variogram (intrinsic process), where it increased indefinitely with increasing

distances (over 500 m of range), mostly because of the vast and continuous extent of the field infestation by *G. pallida* cysts. We investigated the orientation of spatial dependence in the fields by using directional variograms and were computed using eight directions (north, northeast, east, southeast, south, southwest, west and northwest). We found that the spatial dependence was the same in all directions for all fields (isotropic process), except for Bin025, where spatial dependence reached a distance range of 200 m when oriented toward southeast and northwest directions of the field (anisotropic process) (Fig. 3.6). We computed the Moran's *I* to the test for the presence of spatial autocorrelation and to determine the relationship of cyst distribution between nearby locations. We found a significant positive spatial autocorrelation for all fields ($P = 0$), which indicated that nearby cysts incidence are related each other, and further confirmed the presence of cyst clustering process in the fields (Table 3.3).

After the detection of *G. pallida*, potato was not allowed to grow in infested fields and was replaced by two seasons of biofumigant cover crops, and the fields were treated with agrochemical fumigants. We conducted a spatiotemporal mapping analysis of Bin025 to determine the fluctuations of *G. pallida* cysts collected during monitoring surveys in the northern part of this field. We found no significant increase in the number of cysts collected during the first monitoring surveys in 2009 and 2010 ($P > 0.05$) (Fig. 3.7; Table 3.4). However, we found significant decrease in the number of cysts collected during the first monitoring surveys in 2011 and 2012 compared to previous years ($P < 0.05$) (Fig. 3.7; Table 3.4). The results indicated that there were no *G. pallida* cysts production in Bin025, as the nematode was unable to reproduce and multiply in the absence of its potato host. We conducted similar analysis to Bin026, and we compared the fluctuations of both the number of cysts collected and the viability of the eggs over the years, ranging from 2009 to 2012. We found significant reduction of the number of cysts collected in 2012, at approximately 23%, compared to previous years ($P < 0.05$), and we also found that the viability of eggs in the field reached 0% in 2012 (Fig. 3.8; Table 3.5). The results indicated similar trends oriented towards a constant decrease in the number of cysts collected in the fields, as well as a sudden reduction in the viability of eggs compared to previous years. While the absence of the potato

host contributed in stopping the nematode reproduction, the use of chemical fumigations and biofumigant cover crops contributed in the reduction of the viability of the eggs.

We modeled the force of invasion of *G. pallida* using ISDM to simulate the dispersal capabilities of the nematode in Bin025, using the raster layer data generated in the kriging procedure for 2007. We randomly placed thirty infestation foci over the field, and ISDM simulated the expansion of the foci using a negative exponential dispersal patterns under nine probability dispersal kernels that reflected the intensity of human activities. As the dispersal kernel increased, the results showed the occurrence of a stratified dispersal mechanism, which consisted in the growth and development of individual *G. pallida* foci, and the fusion of foci that contributed to the advance of the infestation wave front (Fig. 3.9).

We estimated the distance separation between the primary *G. pallida* cysts concentration focus in the field from the rest of the infestation foci, and we calculated the percentage of cyst prevalence relative to the primary focus of infestation. We observed a process of a non-linear decline in the prevalence of cysts as the distance separation from the primary infestation focus increased (Fig. 3.10). The decline in the prevalence of cysts, at a rate between 35% and 48%, presented a very steep gradient near the primary infestation focus and shallower far from it, which indicated the presence of a travelling wave of infestation. A power-law model was fitted over the distribution of cyst prevalence to describe the SDD pattern of *G. pallida* in the fields. The model exhibited a fat-tailed distribution as the distance separation from the primary infestation focus increased (Fig. 3.10). The model parameters for the estimates of the power-model were significant ($P < 0.001$) and the coefficients of correlation between the observed and the model prediction values were: (i) Bin001, 0.52; (ii) Bin025, 0.44; (iii) Bin026, 0.47; (iv) Bin054, 0.76; (v) Bin068, 0.93; and (vi) Bon064, 0.86. We modeled the LDD pattern of *G. pallida* between fields by calculating the distance separation between the most infested field (Bin025) from the rest of the infested fields. We observed similar results in the LDD pattern of the nematode compared to SDD with a fat-tailed distribution as the distance separation from Bin025 increased (Fig. 3.11). The model parameters for the estimates was significant ($P < 0.004$) and the coefficient of correlation was 0.99.

Discussion

Our study has provided a comprehensive analysis on the spatiotemporal and dispersal characteristics of *G. pallida* in Idaho. The patchy distribution of the cysts in the fields is well-documented in the literature and has a biological explanation (Been and Schomaker, 2000; Schomaker and Been, 1999). *Globodera pallida* spreading is defined as density-independent or passive dispersal that depends on human activities in the field for short- and long-distance scattering. This nematode most probably arrived via agricultural equipment contaminated with cyst-infested soils and was distributed irregularly in the field. We observed that the dispersal of *G. pallida* followed the direction of cultivation, as illustrated in our spatial interpolation maps, and was spatially-stratified. The discontinuous stratified dispersal mode consisted in the establishment of an infestation focus, the growth and development of individual foci and the fusion of foci in time (Hengeveld, 1989). Been and Schomaker (2000) reported that that the distribution of PCN in the field was spatially-aggregated and continuous potato growing would cause the infestation foci to increase in size.

The discontinuous distribution of *G. pallida* in the field could potentially be explained by the presence of a biotic component that might have negatively impacted the nematode reproduction in certain areas in the field (Eberlein et al., 2016). Several cosmopolitan antagonistic microbes are known to reduce and suppress *G. pallida* reproduction rate (Contina et al., 2017; Dandurand et al., 2016). Soil texture and pore size influence the migration of plant-parasitic nematodes to the roots. Rode (1962) showed that the migration of juveniles *G. rostochiensis* to the potato roots was greatest in sandy soil, intermediate in loamy soil, and least in clay soil. The potential presence of microvariations in soil texture might influence the spatial arrangement of *G. pallida* in the field. The patchy distribution could also be explained by the occurrence of genetic variation in *G. pallida* that could foster the development of metapopulations in different sections across and between fields (Folkertsma et al., 2001; Picard et al., 2004). However, Picard and Plantard (2006) showed that genetic differentiation occurred among infested fields with *G. pallida* at a distance more than 50 km of separation, where the process of isolation by distance (IBD) favorized the development of genetic variations. Contina et al. (2018) showed that the fields

infested with *G. pallida* in Idaho are spatially aggregated as an ellipsoidal-shaped cluster around a radius of 12 km, which is well below the critical distance separation for the occurrence of IBD genetic variations.

The use of geostatistical tools allows precise mapping and describes the relationship between attribute variables and the spatial configurations. In our study, we showed that the incidence of *G. pallida* cysts in the field was correlated with space. We found that the spatial dependence was the same in all directions for all fields (isotropic process), except for Bin025, where spatial dependence reached a distance range of 200 m when oriented toward southeast and northwest directions of the field (anisotropic process). Spatial autocorrelation is an important approach for improving sampling efficiency and inference (Dinardo-Miranda and Fracasso, 2009; Francl, 1986; Wang et al., 2012), determine ecological patterns of nematode distribution (Porazinska et al. 2012), and to support the use of site-specific management in nematode infested fields (Avendaño et al. 2003). Spatial autocorrelation provides a glimpse of undergoing process of clustering and dispersal limitations of nematode that could be facilitate by pedogenic processes occurring in the field. Evans et al. (2003) used gaussian and spherical variograms to determine the ranges of spatial autocorrelation of *G. pallida* in field plots, and built kriging prediction maps to identify 'hot spots' of nematode infestations for treatment with fumigant.

We examined the spatiotemporal distribution of *G. pallida* cysts and the viability of eggs during the years of control and eradication using chemical fumigants and biofumigants cover crops. We found that the absence of potato in the field contributed in stopping the nematode reproduction, and the use of chemical fumigations and biofumigant cover crops contributed in the reduction of the viability of the eggs in time. The enforcement of quarantine regulation in Idaho greatly contributed in restricting *G. pallida* infested fields to a small area of 1,267 ha (USDA-APHIS, 2018). As PCN can suppress potato yields by more than 10%, the benefits of excluding these nematodes from potato growing areas in the U.S. are estimated to be $300 million annually (Dwinell and Lehman, 2004; Hockland et al., 2006). Hodda and Cook (2009) estimated, in the absence of PCN regulation, the economic losses for Australian agriculture could exceed $370 million. Schomaker and Been (2006) estimated that the mortality rate of *G. rostochiensis* and *G. pallida*, in the absence of the host,

was greater in the first year after potato crop (69%) than in subsequent years (20-30%), and the population decline was independent of nematode population density. Through quarantine, fumigation and regular soil testing, PCN invasions were stopped and the nematodes were eradicated before establishment in Israel (EPPO, 1987), Australia (EPPO, 2010) and Finland (EPPO, 2012).

The proliferation of *G. pallida* in soil can reach the dramatic size of 35.66 eggs/g soil as observed in 2010 for Bin025. *Globodera pallida* produces only one infection cycle per crop cycle and causes the development of a monocyclic epidemic, characterized by a rapid linear-increased number of cysts in soil. *Globodera pallida* cysts can survive in soil for up to 30 years in the absence of potato, and are able to disperse passively across space by human activities in the fields (Schomaker and Been, 1999; Turner, 1996). The initial nematode density in soil represents a fundamental component of disease intensity over time and space. In our study, both SDD and LDD of *G. pallida* followed a process of a non-linear decline in the prevalence of cysts as the distance separation from the primary infestation focus increased, and a power-law model was able to capture the parameters and significance of this process. Similarly, invasive species modeling approaches predict a traveling wave of conquest which is amplified in space and time by the species reproductive capacity, generation time, and dispersal ability (Mundt et al., 2009). The power-law model illustrates a fat-tailed distribution typical for LDD of plant pathogens that will contribute in time to the advance of the infestation fronts to uninfested areas (Gregory 1968; Madden et al., 2007). Recent findings showed that the rising soil temperature due to climate change could increase PCN adult female nematodes survival rate in soil (Skelsey et al., 2018), and as more nematodes reach their final life stage, the surge of inoculum in soil would reinforce the traveling wave of infestation, aggravating the epidemic and would certainly complicate the task for phytosanitary agencies.

This study provides detailed information of the extent of *G. pallida* in Idaho and characterizes the spatiotemporal distribution of this invasive nematode in the fields. The tools and methods developed can be expanded to include the influences of pedogenic variations on the incidence of nematode propagules in the soil, as well as enabling monitoring and evaluation of the control and eradication program. The outputs of this study should contribute

to the eradication efforts of this nematode from Idaho, and should certainly inform regulators, policymakers and potato growers on the progress of controlling this invasive pest.

Literature Cited

Akima, H. 1970. A new method of interpolation and smooth curve fitting based on local procedure. J. ACM 17:589-602.

Akima, H. 1991. A method of univariate interpolation that has the accuracy of a third-degree polynomial. J. ACM Trans. Math. Software 17:341-366.

Avendaño, F., Schabenberger, O., Pierce, F. J., and Melakeberhan, H. 2003. Geostatistical analysis of field spatial distribution patterns of soybean cyst nematode. Agron. J. 95:936-948.

Been, T. H., and Schomaker, C. H. 2000. Development and evaluation of sampling methods for fields with infestation foci of potato cyst nematodes (*Globodera rostochiensis* and *G. pallida*). Phytopathology 90:647-656.

Behrens, E. 1975. *Globodera Skarbilovic*, 1959, eine selbstaendige Gattung in der Unterfamilie Heteroderinae Skarbilovic, 1947 (Nematoda: Heteroderidae). Vortragstagung zu aktuellen Problemen der Phytonematologie am 29/5/1975 in Rostock. Manuskriptdruck der Vortraege. Rostock, 1975:12-26.

Boag, B., and Topham, P. B. 1984. Aggregation of plant-parasitic nematodes and Taylor's Power Law. Nematologica 30:348-357.

Bowler, D. E., and Benton, T. G. 2005. Causes and consequences of animal dispersal strategies: Relating individual behavior to spatial dynamics. Biol. Rev. 80:205-225.

CABI. 2018. *Globodera pallida* (white potato cyst nematode). Online publication. Centre for Agriculture and Biosciences International. https://www.cabi.org/ISC/datasheet/27033.

Choi, W. I., Jung, H. J., Kim, D. S., Lee, D. S., Lee, C. Y., Nam, Y., Ki, J. B., and Park, Y. S. 2017. Dispersal patterns of Pine wilt disease in the early stage of its invasion in South Korea. Forests 8:411-421.

Contina, J. B., Dandurand, L. M., and Knudsen, G. R. 2017. Use of GFP-tagged *Trichoderma harzianum* as a tool to study the biological control of the potato cyst nematode *Globodera pallida*. Appl. Soil Ecol. 115:31-37.

Contina, J. B., Dandurand, L. M., and Knudsen, G. R. 2018. A spatial analysis of the potato cyst nematode *Globodera pallida* in Idaho. Phytopathology 108:988-1001.

Cressie, N. A. C. 1993. Statistics for spatial data. Wiley, New York.

Dandurand, L. M., and Knudsen, G. R. 2016. Effect of the trap crop *Solanum sisymbriifolium* and two biocontrol fungi on reproduction of the potato cyst nematode *Globodera pallida*. Ann. Appl. Biol. 169:180-189.

Dinardo-Miranda, L. L., and Fracasso, J. V. 2009. Spatial distribution of plant-parasitic nematodes in sugarcane fields. Sci. Agric. 66:188-194.

Duncan, L. W., Ferguson, J. J., Dunn, R. A., and Noling, J. W. 1989. Application of Taylor's power law to sample statistics of *Tylenchulus semipenetrans* in Florida citrus. J. Nematol. 21:707-711.

Dwinell, L. D., and Lehman, P. S. 2004. Plant-parasitic nematodes which are exotic pests in agriculture and forestry. Pages 51-70 in: Biological Pollution: An Emerging Global Menace, K. O. Briton, ed. American Phytopathological Society Press, St Paul, Minnesota.

Eberlein, C., Heuer, H., Vidal, S., and Westphal, A. 2016. Microbial communities in *Globodera pallida* females raised in potato monoculture soil. Phytopathology 106:581-590.

EPPO. 1987. Non-occurrence of *Globodera rostochiensis* in Israel. Online publication. European and Mediterranean Plant Protection Organization (EPPO) reporting service no. 18. https://gd.eppo.int/reporting/article-5754.

EPPO. 2010. Eradication of potato cyst nematode (PCN) from Western Australia. Online publication. International Plant Protection Convention (IPPC). https://www.ippc.int/en/countries/australia/pestreports/2010/09/eradication-of-potato-cyst-nematode-pcn-from-western-australia/.

EPPO. 2012. Situation of *Globodera pallida* in Finland in 2011. Online publication. European and Mediterranean Plant Protection Organization (EPPO) reporting service no. 04. https://gd.eppo.int/reporting/article-1900.

Evans, K., Webster, R., Barker, A., Halford, P., and Russel, M. 2003. Mapping infestations of potato cyst nematodes and the potential for spatially varying application of nematicides. Prec. Agric. 4:149-162.

FAO-IPPC. 2017. Pest risk analysis for quarantine pests. Online publication. Food and Agriculture Organization of the United Nations – International Plant Protection Convention. http://www.fao.org/3/a-j1302e.pdf.

Ferris, H., Jetter, K. M., Zasada, I., Chitambar, J. J., Venette, R. C., Klonsky, K. M., and Becker, J. O. 2003. Risk assessment of plant-parasitic nematodes. Pages 99-119 in: Exotic pests and diseases: Biology and economics for biosecurity, D. A. Summer, ed. Iowa State University Press.

Folkertsma, R. T., van Koert, P., Rouppe van der Voort, J. N. A. M., de Groot, K. E., Kammenga, J. E., Helder, J., and Bakker, J. 2001. The effects of founding events and agricultural practices on the genetic structure of three metapopulations of *Globodera pallida*. Phytopathology 91:753-758.

Francl, L. J. 1986. Spatial analysis of *Heterodera glycines* populations in field plots. J. Nematol. 18:183-189.

Gregory, P. H. 1968. Interpreting plant disease dispersal gradients. Annu. Rev. Phytopathol. 6:189-212.

Hafez, S. L., Sundararaj, P., Handoo, Z. A., Skantar, L., Carta, K., and Chitwood, D. J. 2007. First report of the Pale Cyst Nematode, *Globodera pallida*, in the United States. Plant Dis. 91:325.

Haining, R. P. 2003. Spatial data analysis: Theory and practice. Cambridge University Press, Cambridge, UK.

Hattab, T., Garzón-López, C. X., Ewald, M., Skowronek, S., Aerts, R., Horen, H., Brasseur, B., Gallet-Moron, E., Spicher, F., Decocq, G., Feilhauer, H., Honnay, O., Kempeneers, P., Schmidtlein, S., Somers, B., Van De Kerchove, Rocchini, D., and Lenoir, J. 2017. A unified framework to model the potential and realized distributions of invasive species within the invaded range. Divers. Distrib. 23:806-819.

Hengeveld, R. 1989. Dynamics of biological invasions. Chapman and Hall Ltd, New York.

Hockland, S., Inserra, R. N., Millar, L., and Lehman, P. S. 2006. International plant health: Putting legislation into practice. Pages 328-343 in: Plant Nematology. R. N. Perry and M. Moens, eds. CAB International, Oxfordshire, UK.

Hodda, M., and Cook, D. C. 2009. Economic impact from unrestricted spread of potato cyst nematodes in Australia. Phytopathology 99:1387-1393.

Koenning, S. R., Overstreet, C., Noling, J. W., Donald, P. A., Becker, J. O., and Fortnum, B. A. 1999. Survey of crop losses in response to phytoparasitic nematodes in the United States for 1994. J. Nematol. 31:587-618.

Madden, L. V., Hughes, G., and van den Bosch, F. 2007. The study of plant disease epidemics. The American Phytopathological Society, APS Press St. Paul, Minnesota.

Marks, R. J., and Brodie, B. B. 1998. Potato cyst nematodes: Biology, distribution and control. CABI, Wallingford, UK.

Matheron, G. 1963. Principles of geostatistics. Econ. Geol. 58:1246-1266.

McSorley, R., Dankers, W. H., Parrado, J. L., and Reynolds, J. S. 1985. Spatial distribution of the nematode community on Perrine marl soils. Nematropica 15:77-92.

Meentemeyer, R. K., Anacker, B. L., Mark, W., and Rizzo, D. M. 2008. Early detection of emerging forest disease using dispersal estimation and ecological niche modeling. Ecol. Appl. 18:377-390.

Moran, P. 1950. A Test for the Serial Independence of Residuals. Biometrika, 37:178-181.

Mundt, C. C. 1989. Use of the modified Gregory model to describe primary disease gradients of wheat leaf rust produced from area sources of inoculum. Phytopathology 79:241-246.

Mundt, C. C., Sackett, K. E., Wallace, L. D., Cowger, C., and Dudley, J. P. 2009. Long-distance dispersal and accelerating waves of disease: Empirical relationships. Am. Nat. 173:456-466.

Nathan, R. 2001. The challenges of studying dispersal. Trends Ecol. Evol. 16:481-483.

NCSS. 2002. Bannock series. Online publication. National Cooperative Soil Survey. https://soilseries.sc.egov.usda.gov/OSD_Docs/B/BANNOCK.html.

Ogiga, I. R., and Estey, R. H. 1974. The use of Meldola Blue and Nile Blue A for distinguishing dead from living nematodes. Nematologica 20:271-276.

Park, S. J., Taylor, R. A. J., and Grewal, P. S. 2013. Spatial organization of soil nematode communities in urban landscapes: Taylor's Power Law reveals life strategy characteristics. Appl. Soil Ecol. 64:214-222.

Picard, D., and Plantard, O. 2006. What constitutes a population for the plant parasitic nematode *Globodera pallida* in its native area (Peru)? Int. J. Parasitol. 36:115-122.

Picard, D., Plantard, O., Scurrah, M., and Mugniéry, D. 2004. Inbreeding and population structure of the potato cyst nematode (*Globodera pallida*) in its native area (Peru). Mol. Ecol. 13:2899-2908.

Porazinska, D. L., Giblin-Davis, R. M., Powers, T. O., and Thomas, W. K. 2012. Nematode spatial and ecological patterns from tropical and temperate rainforests. PLoS One 7:1-11.

R Core Team. 2018. R: A language and environment for statistical computing. R Foundation for statistical computing, Vienna, Austria. http://www.R-project.org/.

Rode, H. 1962. Untersuchungen uber das wandervermogen von Larven des Kartoffelnematoden (*Heterodera rostochiensis* Woll.) in Modellversuchen mit verschiedenen Bodenarten. Nematologica 7:74-82.

Sasser, J. N., and Freckman, D. W. 1987. A world perspective on nematology: The role of the society. Pages 7-14 in: Vistas on Nematology. J. A. Veech, and D. W. Dickson, eds. Society of Nematologists, Hyattsville, MD.

Schomaker, C. H., and Been, T. H. 1999. A model for infestation foci of potato cyst nematodes, *Globodera rostochiensis* and *G. pallida*. Phytopathology 89:583-590.

Schomaker, C. H., and Been, T. H. 2006. Plant growth and population dynamics. Pages 276-301 in: Plant Nematology. R. N. Perry and M. Moens, eds. CABI, Oxfordshire, UK.

Severns, P. M., Sackett, K. E., Farber, D. H., and Mundt, C. C. 2019. Consequences of long-distance dispersal for epidemic spread: Patterns, scaling, and mitigation. Plant Dis. 103:177-191.

Skantar, A. M., Handoo, Z. A., Carta, L. K., and Chitwood, D. J. 2007. Morphological and molecular identification of *Globodera pallida* associated with potato in Idaho. J. Nematol. 39:133-144.

Skarbilovich, T. S. 1959. On the structure of the nematodes of the order Tylenchida Thorne, 1949. Acta Parasitol. Polonica 15:117-132.

Skelsey, P., Kettle, H., MacKenzie, K., and Blok, V. 2018. Potential impacts of climate change on the threat of potato cyst nematode species in Great Britain. Plant Pathol. 67:909-919.

Stein, M. L. 1999. Interpolation of spatial data: Some theory for kriging. Springer Verlag, New York.

Stone, A. R. 1972. The round cyst species of *Heterodera* as a group. Ann. Appl. Biol. 71:280-283.

Talavera, M., Andreu, M., Valor, H., and Tobar, A. 1998. Nematodos fitoparásiticos en áreas productoras de patata de Motril y Salobreña. Invest. Agric. Prod. Prot. Veg. 13:87-95.

Tobler, W. R. 1970. A computer movie simulating urban growth in the Detroit region. Econ. Geogr. 46:234-240.

Turner, S. J. 1996. Population decline of potato cyst nematodes (*Globodera rostochiensis* and *G. pallida*) in field soils in Northern Ireland. Ann. Appl. Biol. 129:315-322.

USDA-APHIS. 2009. Pale potato cyst nematode national survey and diagnostic cyst sample forwarding protocols. Online publication. United States Department of Agriculture's Animal and Plant Health Inspection Service. https://www.aphis.usda.gov/plant_health/plant_pest_info/potato/downloads/pcndocs/PCN_NatlSurvey.pdf.

USDA-APHIS. 2019. Pale cyst nematode eradication program, 4th Quarter Report (October 1-December 31). Online publication. United States Department of Agriculture – Animal and Plant Health Inspection Service. https://www.aphis.usda.gov/aphis/ourfocus/planthealth/plant-pest-and-disease-programs/pests-and-diseases/sa_nematode/sa_potato/ct_pcn_programupdates.

USDA-NASS. 2012. Census of agriculture: Potatoes harvested. Online publication. United States Department of Agriculture's National Agricultural Statistics Service. https://www.nass. usda.gov/Publications/AgCensus/2012/Online_Resources/Ag_Atlas_Maps/Crops_and_Plants/Field_Crops_Harvested/12-M195-RGBDot1-largetext.pdf.

Vasyutin, A. S., and Yakovleva, V. A. 1998. *Globodera* in potatoes in Russia. Kartofel' I Ovoshchi 6:29-32.

Wang, J. F., Stein, A., Gao, B. B., Ge, Y. 2012. A review of spatial sampling. Spat. Stats. 2:1-14.

Wollenweber, H. W. 1923. Krankheiten und BeschSdigungen der Kartoffel. Arb. Forsch. Inst. Kartof. 7:1-56.

Table 3.1. Sampling of fields infested with *Globodera pallida* and the impact of eradication measures on eggs viability.

Field[a]	Area (ha)	Sampling coverage	Number of grids	Sampling size kg soil/grid	Year	Total sampled soil (kg)	Total cysts collected	Cysts/kg soil	Eggs/g soil	Average eggs viability (%)
Bin001	18.29	Full-field	469	2.27	2007	1,065	6,410	6.02	0.60	12.46
		Monitoring grids	76	9.07	2009	2,068	67,116	32.46	3.25	1.02
					2010	1,379	54,538	39.55	3.96	0.28
					2011	1,379	54,054	39.20	3.92	0.13
					2012	689	13,155	19.09	1.91	0.00
					2014	689	14,093	20.45	2.04	0.00
Bin025	89.52	Full-field	555	2.27	2007	1,260	277,496	220.23	22.02	20.03
		Monitoring grids	59	9.07	2009	1,605	471,074	293.50	29.35	0.36
					2010	1,070	381,545	356.58	35.66	0.21
					2011	535	121,494	227.04	22.70	0.00
Bin026	55.08	Full-field	1,410	2.27	2007	3,201	8,347	2.61	0.26	17.69
		Monitoring grids	97	9.07	2009	2,639	54,881	20.80	2.08	0.22
					2010	1,760	44,864	25.49	2.55	0.18
					2011	1,760	37,277	21.18	2.12	0.02
					2012	880	16,211	18.43	1.84	0.00

[a] Direction of cultivation was North/South.

Table 3.2. Sampling of fields infested with *Globodera pallida* and the impact of eradication measures on eggs viability.

Field[a]	Area (ha)	Sampling coverage	Number of grids	Sampling size kg soil/grid	Year	Total sampled soil (kg)	Total cysts collected	Cysts/kg soil	Eggs/g soil	Average eggs viability (%)
Bin054	57.91	Full-field	1,466	2.27	2007	3,328	3,861	1.16	0.12	33.31
		Monitoring grids	62	9.07	2009	1,687	32,180	19.08	1.91	0.58
			60		2010	1,088	23,227	21.35	2.13	0.16
			60		2011	1,088	18,595	17.09	1.71	0.14
Bin068	57.87	Full-field	1,485	2.27	2008	3,371	295	0.09	0.009	9.32
		Monitoring grids	22	9.07	2009	599	1,671	2.79	0.28	3.17
					2010	399	853	2.14	0.21	0.74
					2011	200	216	1.08	0.11	0.00
Bon064	60.91	Full-field	1,505	2.27	2007	3,416	1,964	0.57	0.06	36.08
		Monitoring grids	74	9.07	2009	2,014	10,913	5.42	0.54	0.68
					2010	1,342	9,318	6.94	0.69	0.48
					2011	1,342	6,310	4.70	0.47	0.30

[a] Direction of cultivation was North/South for all fields except Bon064 which was East/West.

Table 3.3. Parameters of the variogram models for each field infested with *Globodera pallida*.

Field	Model	Nugget	Sill	Range	kappa
Bin001	Ste	0	0.08	119	0.30
Bin025	Ste	0.02	1.4	2,526	0.40
Bin026	Ste	0	0.15	45	0.40
Bin054	Spherical	0	0.04	63	-
Bin068	Ste	0	0.01	68	0.20
Bon064	Ste	0	0.03	21	0.80

Table 3.4. Moran's *I* values for each field infested with *Globodera pallida*.

Field	Observed	Expected	Standard deviation	*P*-value
Bin001	0.01	-2.14×10^{-03}	2.81×10^{-03}	0
Bin025	0.16	-4.20×10^{-04}	7.02×10^{-04}	0
Bin026	0.03	-7.07×10^{-04}	1.08×10^{-03}	0
Bin054	0.02	-6.81×10^{-04}	8.91×10^{-04}	0
Bin068	0.002	-6.74×10^{-04}	5.42×10^{-04}	2.38×10^{-08}
Bon064	0.009	-6.60×10^{-04}	7.20×10^{-04}	0

Table 3.5. Temporal fluctuations of *Globodera pallida* cysts collected in Bin025.

Year	Average cysts/kg soil
2009	74.85 ± 5.56a[a]
2010	89.70 ± 7.06a
2011	56.76 ± 4.39b
2012	50.93 ± 3.76b

[a] Same letter indicates that the means (±standard error) are not significant $P > 0.05$.

Table 3.6. Temporal fluctuations of *Globodera pallida* cysts and viability of eggs in Bin026.

Year	Average cysts/kg soil	Average viability of eggs (%)
2009	5.09 ± 0.45ac[a]	$0.03 \pm 5.00 \times 10^{-05}$ a
2010	6.44 ± 0.38b	$0.20 \pm 2.00 \times 10^{-04}$ b
2011	5.61 ± 0.36ab	$0.02 \pm 3.40 \times 10^{-05}$ a
2012	4.65 ± 0.32c	0.00 ± 0.00 a

[a] Same letter indicates that the means (±standard error) are not significant $P > 0.05$.

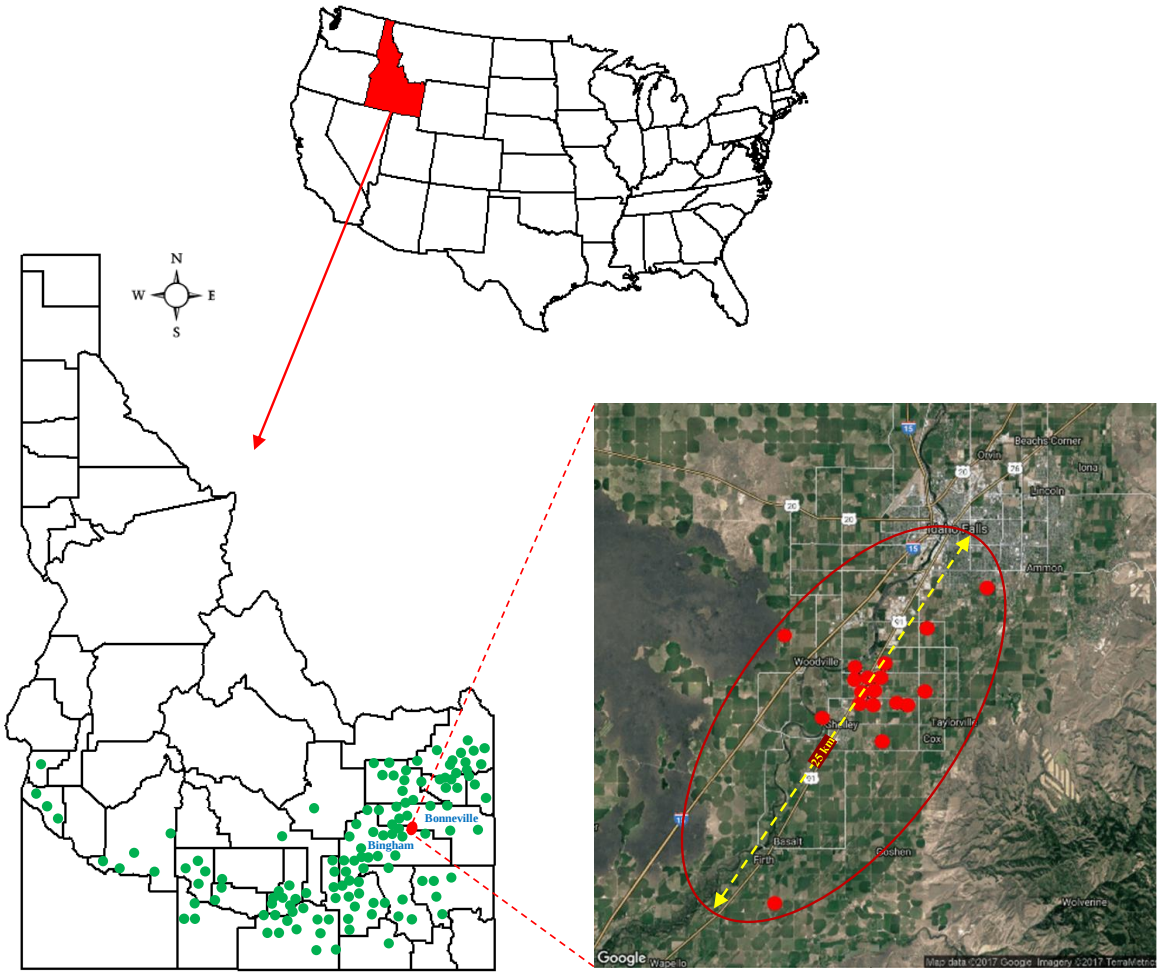

Fig. 3.1. Map of the state of Idaho (left) and location of the potato fields infested with *Globodera pallida* in southeastern Idaho (right). In green are the distribution of potato fields along the Snake River (USDA-NASS, 2012) and in red are the fields infested with *G. pallida* (Contina et al., 2018; USDA-APHIS, 2018). The infestation area spans over a diameter of 25 km and encompasses the Counties of Bonneville and Bingham.

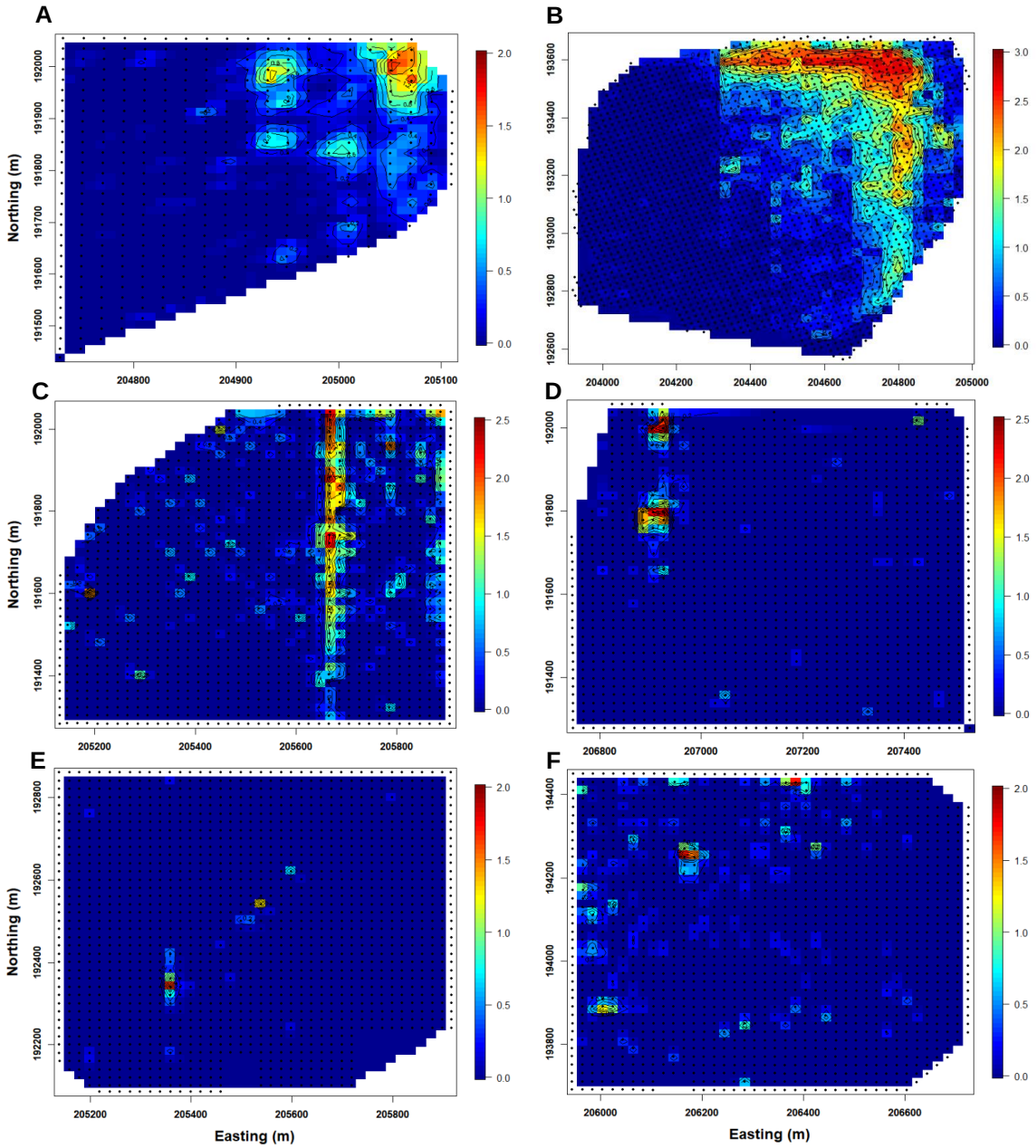

Fig. 3.2. Spatial Akima interpolation maps of *Globodera pallida* cysts in infested fields using USDA-APHIS full-field sampling data at a rate of 57 kg soil/ha (2.27 kg soil per grid [400 m^2]) during the initial *G. pallida* detection in Idaho. **A.** Bin001; **B.** Bin025; **C.** Bin026; **D.** Bin054; **E.** Bin068; **F.** Bon064. The number of cysts are log10-transformed per kg soil per grid.

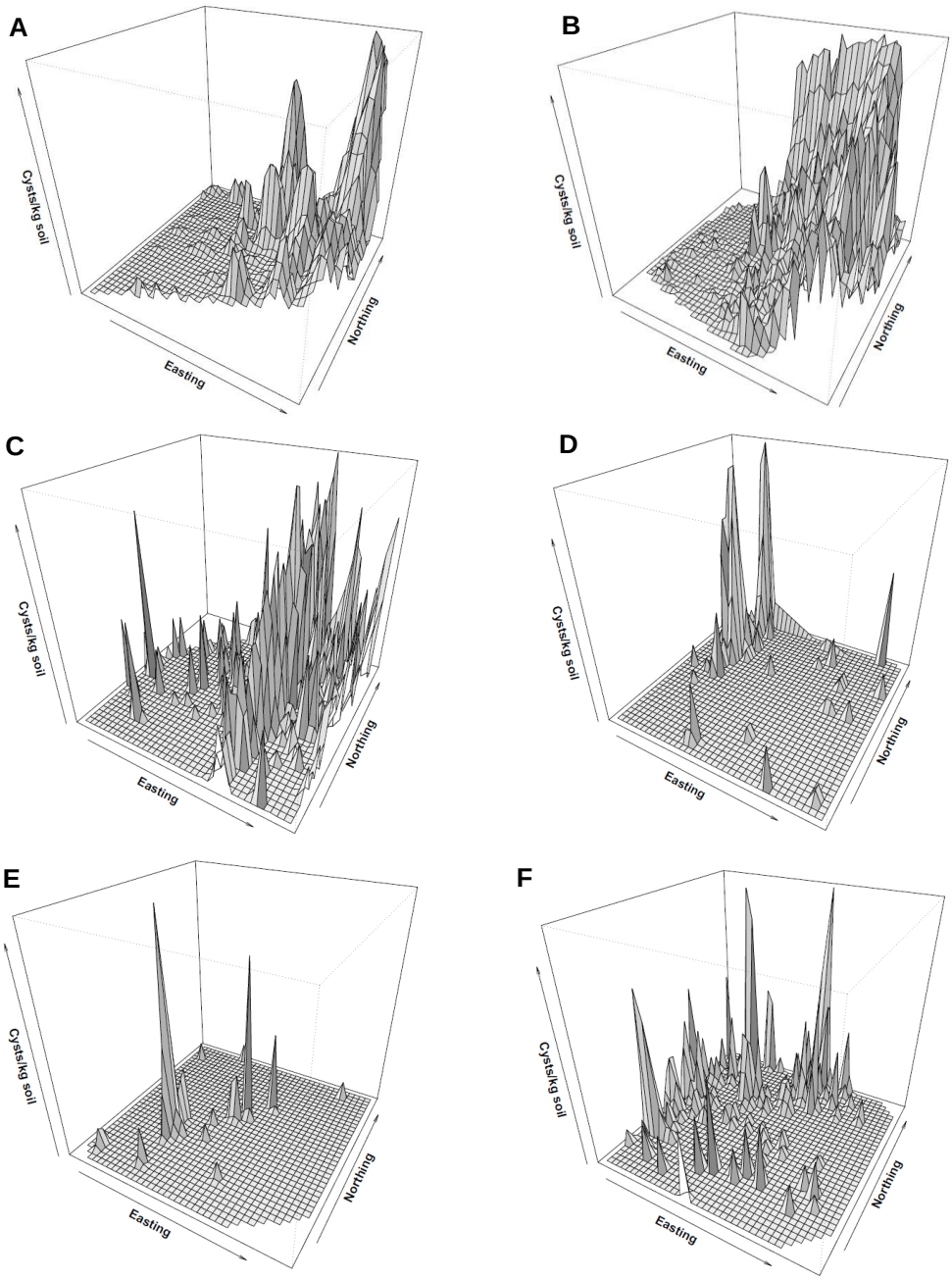

Fig. 3.3. 3D simulation of *Globodera pallida* cysts distribution in infested fields using the Akima interpolation method. **A.** Bin001; **B.** Bin025; **C.** Bin026; **D.** Bin054; **E.** Bin068; **F.** Bon064. The number of cysts are log10-transformed per kg soil per grid.

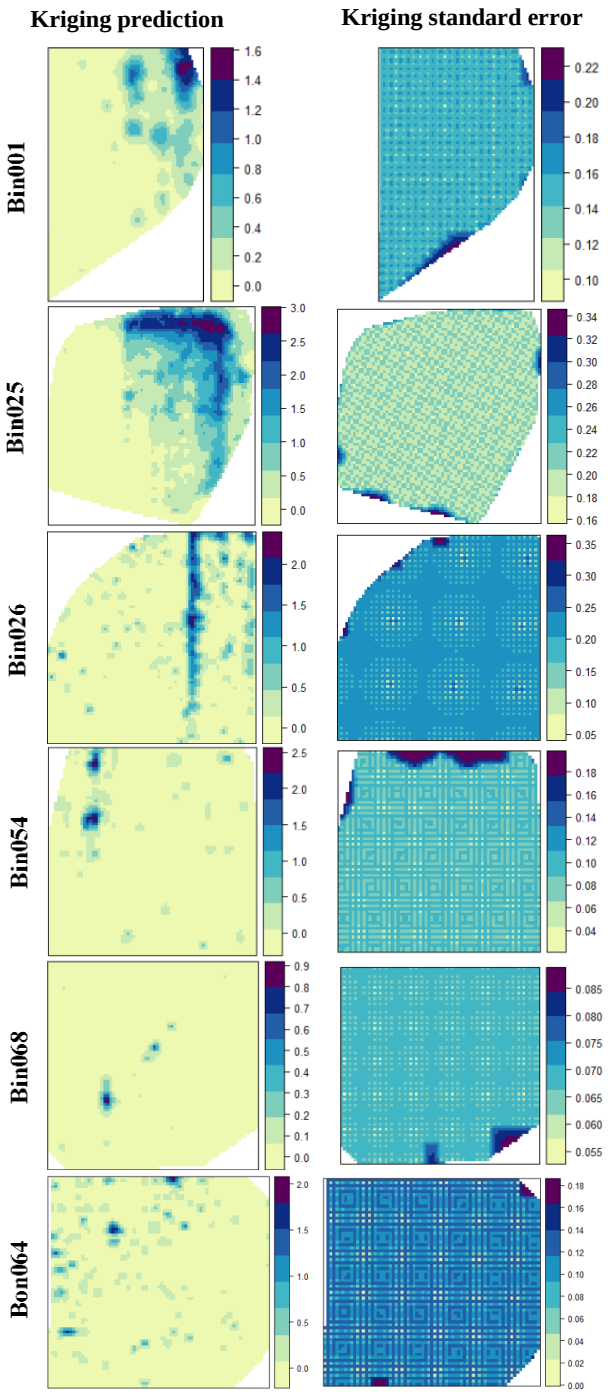

Fig. 3.4. Spatial interpolation maps using kriging algorithms to calculate the distribution of *Globodera pallida* cysts in infested fields using USDA-APHIS full-field sampling data at a rate of 57 kg soil/ha (2.27 kg soil per grid [400 m^2]) during the initial *G. pallida* detection in Idaho.

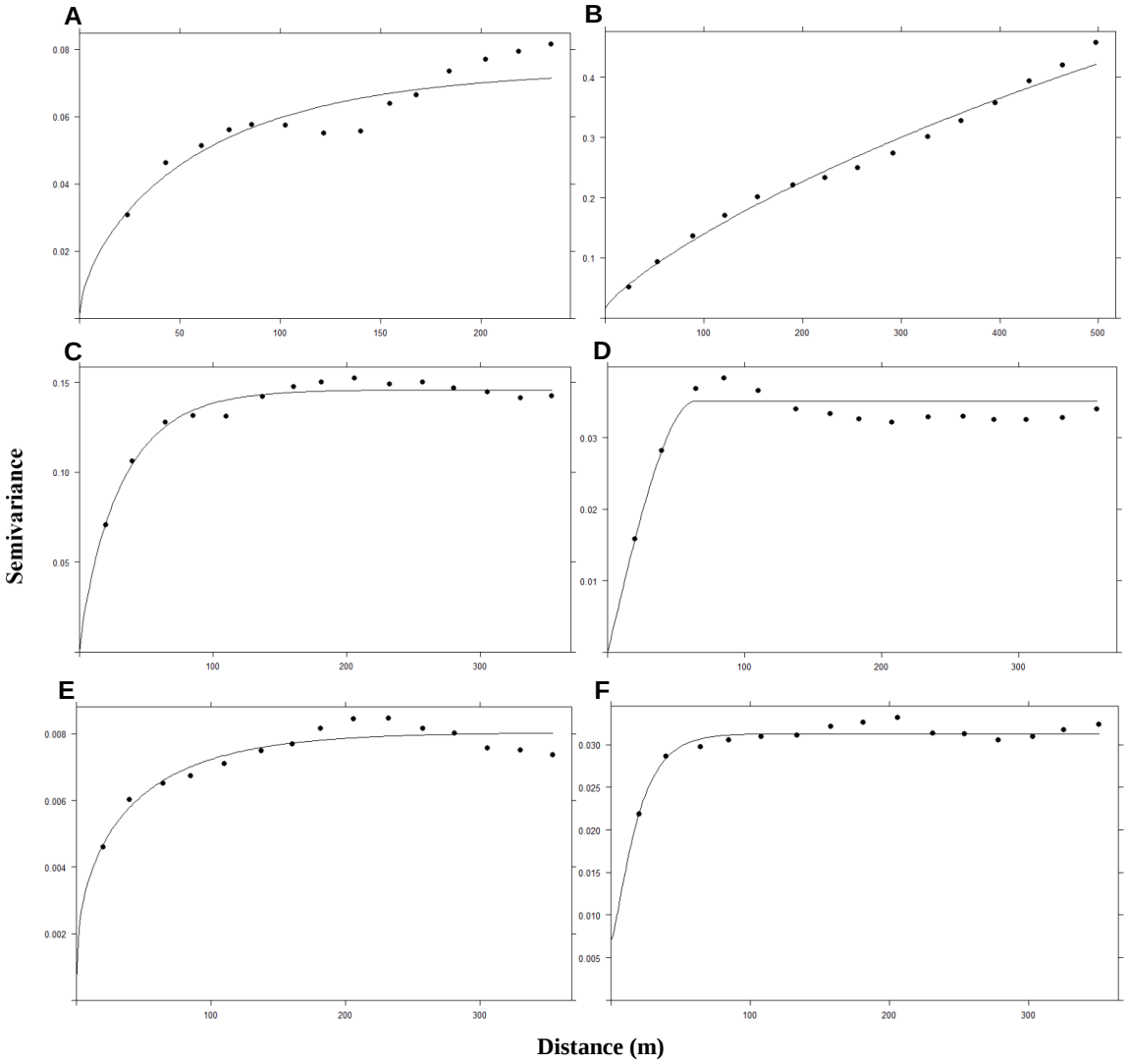

Fig. 3.5. Experimental variogram and fitted variogram model. **A.** Bin001 (model: Ste, nugget: 0, sill: 0.08, range: 119, kappa: 0.3). **B.** Bin025 (model: Ste, nugget: 0.02, sill: 1.4, range: 2,526, kappa: 0.4). **C.** Bin026 (model: Ste, nugget: 0, sill: 0.15, range: 45, kappa: 0.4). **D.** Bin054 (model: Spherical, nugget: 0, sill: 0.04, range: 63). **E.** Bin068 (model: Ste, nugget: 0, sill: 0.01, range: 68, kappa: 0.2). **F.** Bon064 (model: Ste, nugget: 0, sill: 0.03, range: 21, kappa: 0.8).

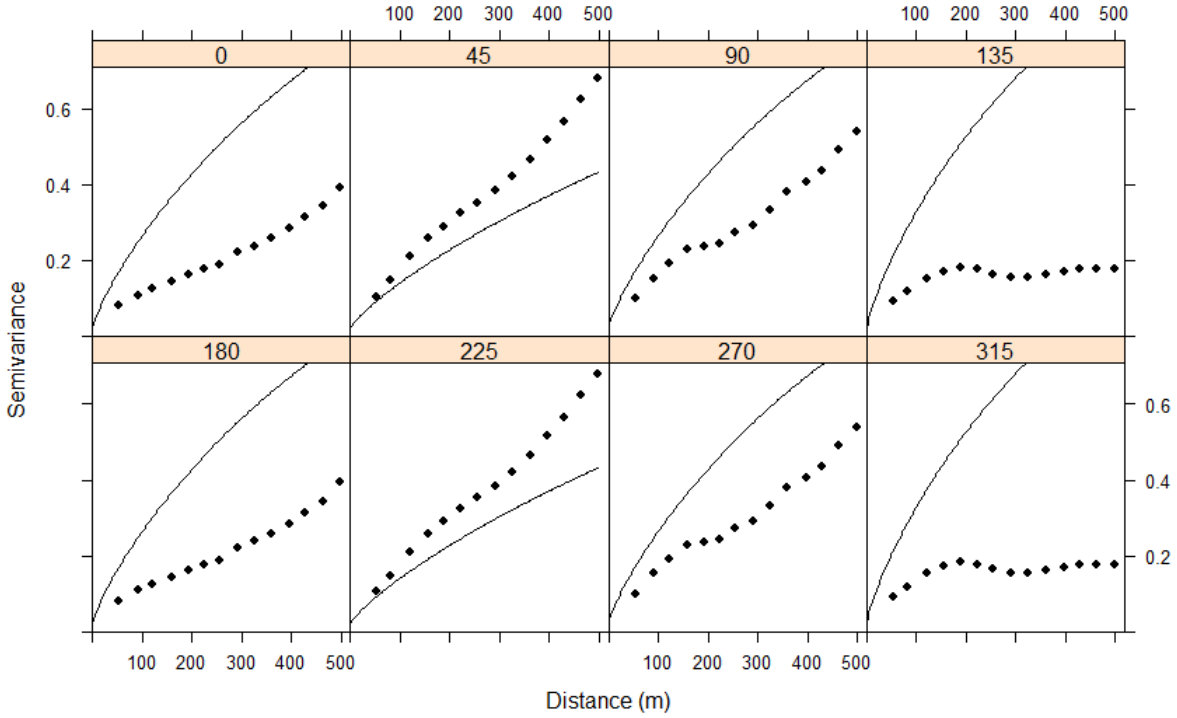

Fig. 3.6. Directional variograms for Bin025 showing the presence of anisotropic process in the spatial distribution of *Globodera pallida* in the field. The directional variograms were computed using eight directions (north [0], northeast [45], east [90], southeast [135], south [180], southwest [225], west [270], and northwest [315]). Spatial dependence reached a distance range of 200 m when oriented toward southeast and northwest directions of the field.

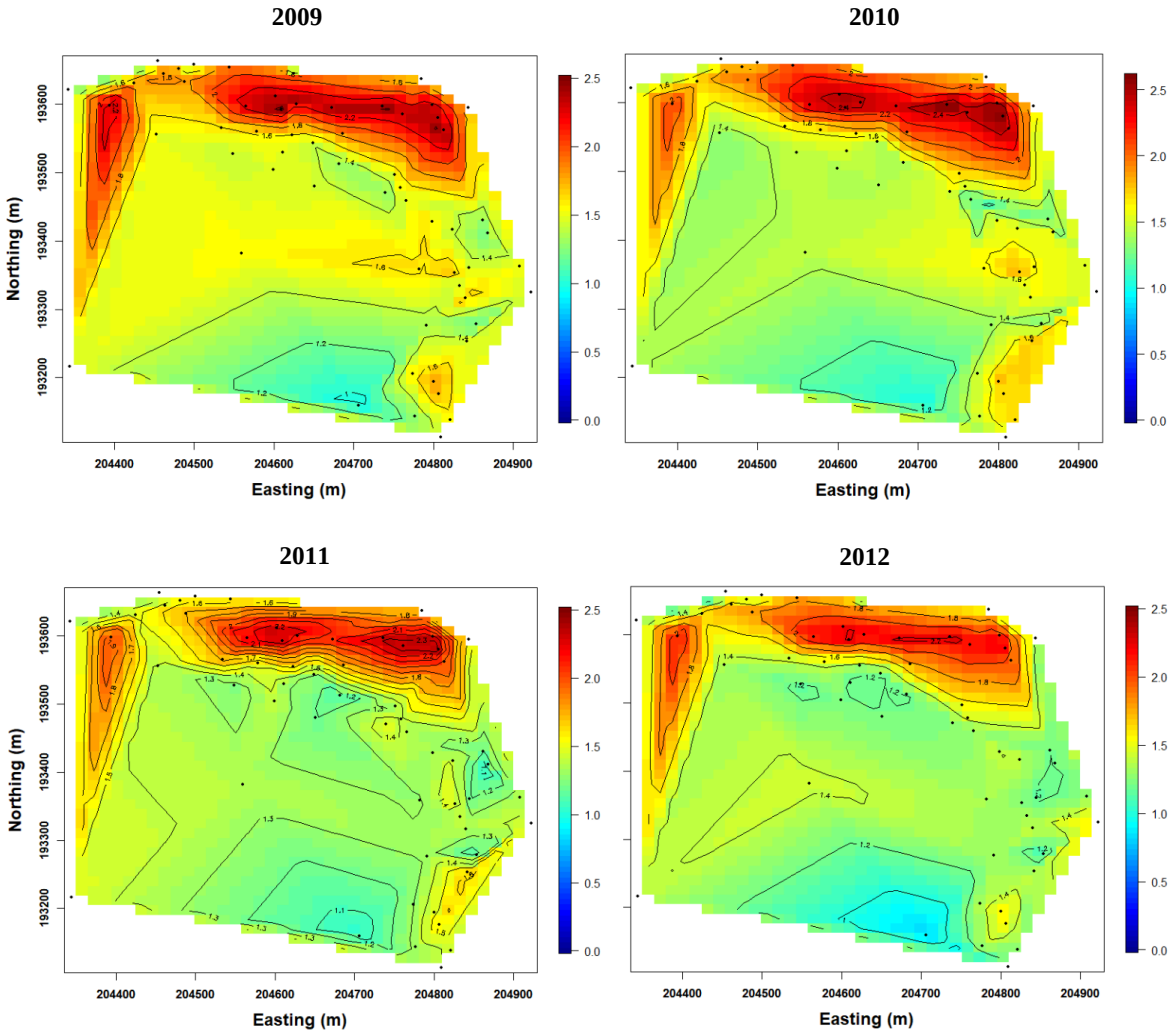

Fig. 3.7. Spatiotemporal fluctuations of *Globodera pallida* cysts number for Bin025 during sampling of the monitoring grids using USDA-APHIS part-field sampling data at a rate of 227 kg soil/ha (9.07 kg soil per grid [400 m^2]).

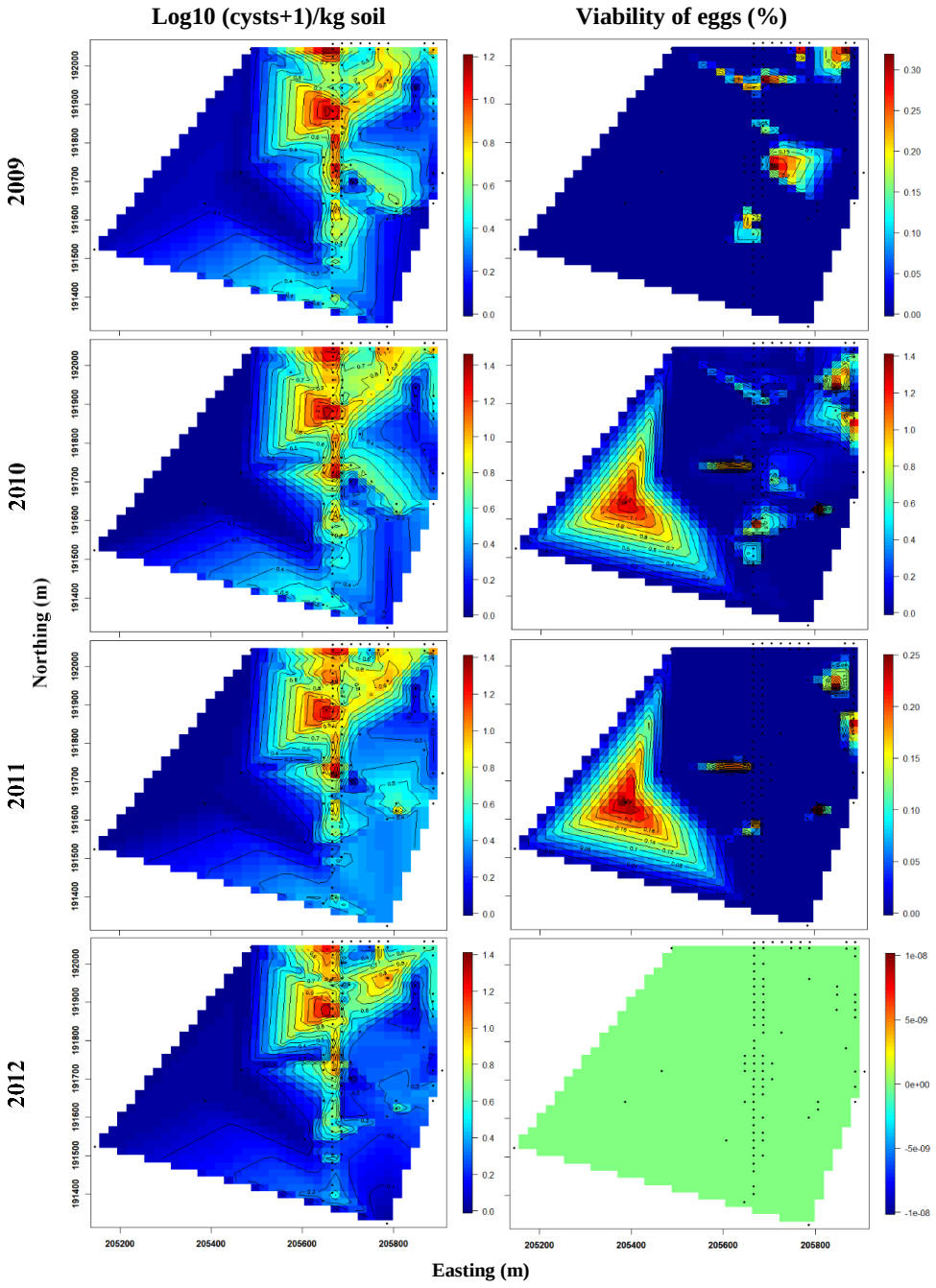

Fig. 3.8. Spatiotemporal fluctuations of *Globodera pallida* cysts number and viability of eggs for Bin026 during sampling of the monitoring grids using USDA-APHIS part-field sampling at a rate of 227 kg soil/ha (9.07 kg soil per grid [400 m2]).

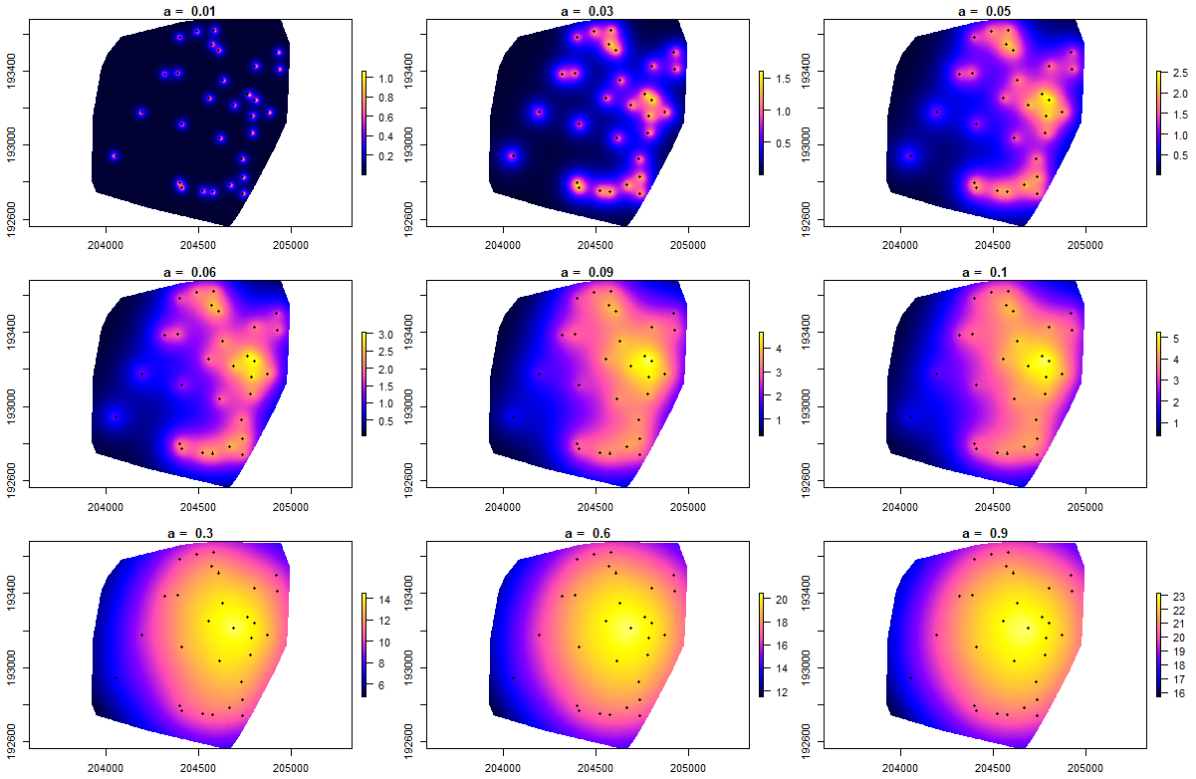

Fig. 3.9. Simulations of *Globodera pallida* spreading in Bin025 field in the absence of control measures using the invasive species distribution models (ISDM) to compute a negative exponential dispersal patterns with different probability kernel density function.

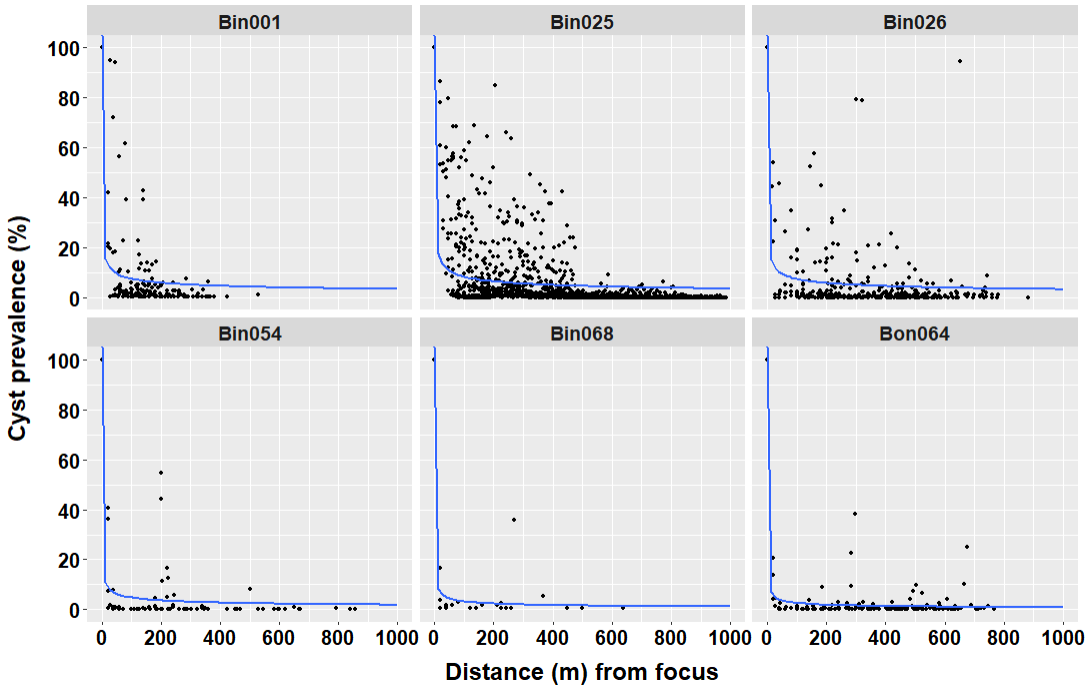

Fig. 3.10. A power-law model was fitted into the distribution of cyst prevalence for each field to explain the short-distance dispersal pattern of *G. pallida*. The model parameters were: Bin001 ($y = 37.49 \times x^{-0.35}, P < 0.001, r = -0.52$); Bin025 ($y = 44.76 \times x^{-0.36}, P < 0.001, r = -0.44$); Bin026 ($y = 36.80 \times x^{-0.35}, P < 0.001, r = -0.47$); Bin054 ($y = 30.35 \times x^{-0.40}, P < 0.001, r = -0.76$); Bin068 ($y = 25.92 \times x^{-0.45}, P < 0.001, r = -0.93$); and Bon064 ($y = 23.91 \times x^{-0.48}, P < 0.001, r = -0.86$).

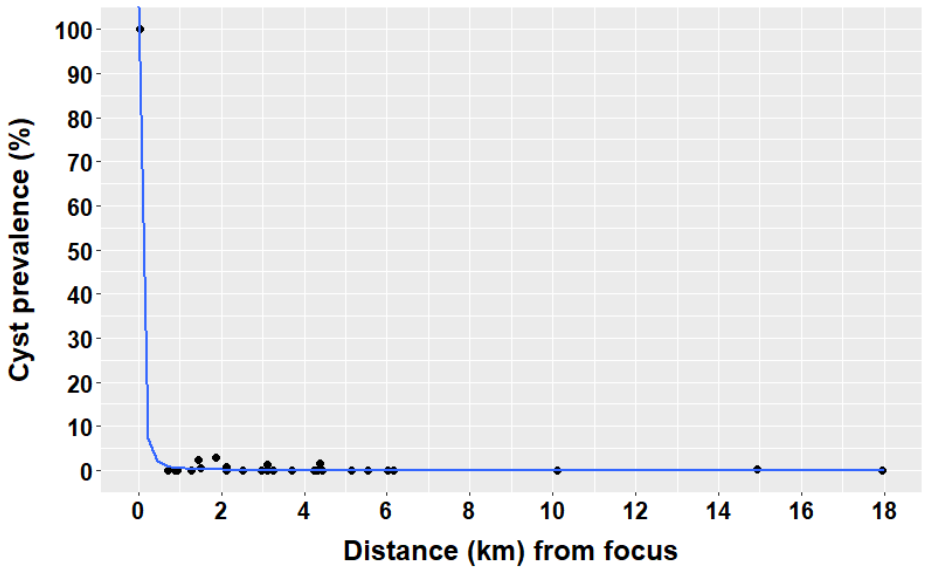

Fig. 3.11. A power-law model was fit into the distribution of cyst prevalence to explain the long-distance dispersal pattern of *Globodera pallida*. The model parameters were: $y = 0.53 \times x^{-1.75}, P < 0.004, r = -0.99$.

Chapter 4: A Predictive Risk Model Analysis of the Potato Cyst Nematode *Globodera pallida* in Idaho

Abstract

Globodera pallida is a major nematode pest of potato (*Solanum tuberosum*) and is of great economic importance for the potato industry. Assessing potato yield loss caused by the Idaho *G. pallida* population under field conditions was not performed due to its quarantine status in Idaho where it is prohibited by regulatory statutes to grow potato in any infested fields. The experimental data came from three trials that were conducted under greenhouse conditions. A predictive risk model analysis was performed to: (i) determine the effect of the Idaho population of *G. pallida* on potato yield; (ii) estimate reproduction rate from different initial nematode densities; and (iii) simulate potato yield losses in Idaho field conditions by integrating the coefficients of potato yield into the SUBSTOR-DSSAT crop simulation model. Experiments were conducted under greenhouse conditions using five initial *G. pallida* soil infestation levels (0, 10, 20, 40 and 80 eggs/g soil). The coefficients of potato yield achieved under each initial nematode density were integrated into the SUBSTOR-DSSAT potato growth simulation model. The model showed that tuber weight reached a maximum yield of 96 ton/ha in non-infested soil. Based on the greenhouse trials, the model predicted a minimum yield of 12 and 58 ton/ha in trial 1 and trial 2/3 respectively, when initial nematode density was 80 eggs/g soil. In trial 1, tuber weight was significantly reduced by 44% at 40 eggs/g soil and by 87% at 80 eggs/g soil, and 20% at 40 eggs/g soil and by 39% at 80 eggs/g soil in trial 2/3. The outputs of this study should facilitate common understandings between regulators, policymakers and potato growers on the challenges and opportunities for controlling this economically important pest in Idaho.

Introduction

The potato cyst nematode *Globodera pallida* (Behrens, 1975; Stone, 1972) is a globally regulated and an economically important potato pest (CABI, 2018; Hodda and Cook, 2009). *Globodera pallida* and *Globodera rostochiensis* (Wollenweber, 1923; Skarbilovich, 1959), both potato cyst nematodes, co-evolved with potato and other native *Solanum* species in the Andean Region of South America (Grenier et al., 2001; Picard et al., 2004). Potato cyst nematodes were first observed on potato roots in Germany in 1881, before spreading worldwide (CABI, 2018; Grenier et al., 2001; Wollenweber, 1923). According to recent survey data, *G. rostochiensis* has been detected in 68 countries and *G. pallida* in 48 (CABI, 2018).

Globodera pallida is a specialized obligate sedentary endoparasite that can survive in the soil for up to 30 years in the absence of its potato host (Turner, 1996). The major plant hosts of *Globodera* spp. are restricted to Solanaceae, in particular potato, tomato and aubergine (Mai, 1952; Roberts and Stone, 1981). *Globodera pallida* is spread mainly through soil, tubers or farm equipment contaminated with cysts (Evans and Stone, 1977). In highly infested fields, *G. pallida* can reduce tuber yields up to 80% (Talavera et al. 1998; Vasyutin and Yakovleva, 1998). In Europe, where resistant varieties are available, potato cyst nematodes have been estimated to reduce potato production by 9% annually (Turner and Rowe, 2006). In the UK, potato cyst nematodes are the second most economically important potato pest after late blight, costing £26 million per year in potato yield loss (Twining et al., 2009). In the UK, following the widespread planting of potato cultivars resistant to only *G. rostochiensis*, an increase in *G. pallida* infestations was observed (Minnis et al., 2002). Potato cyst nematodes are found in 64% of the potato fields in the UK, with *G. pallida* found in over 90% of infestations (Minnis et al., 2002).

In the United States, *G. pallida* was found in southeastern Idaho in 2006 in two potato fields in Bingham County (Hafez et al., 2007). The U.S. Department of Agriculture's Animal and Plant Health Inspection Service (USDA-APHIS) and the Idaho State Department of Agriculture (ISDA) have listed *G. pallida* as a quarantine pest for Idaho under Title 7 CFR 301.86 Federal Regulation. USDA-APHIS and ISDA have implemented a containment and eradication program to prevent *G. pallida* spread to other potato fields. In fields infested with

G. pallida, the program outlines: (i) restrictions on the movement of soil and plant materials; (ii) prohibition of planting potato and other solanaceous crops; and (iii) sanitation procedures for farm equipment. Chemical application with the nematicide Telone II (1,3-dichloropropene) is being conducted in infested fields as part of the *G. pallida* eradication program and *Solanum sisymbriifolium* 'litchi tomato' is under field scale trials in infested fields (USDA-APHIS, 2018). The regulated area includes portions of northern Bingham and southern Bonneville Counties and is currently limited to 3,057 hectares, of which 1,326 ha are fields infested with *G. pallida* (USDA-APHIS, 2019).

Idaho is the largest producer, packer and processor of potatoes in the U.S. with a production value of $1.19 billion in 2017 (USDA-NASS, 2018). In 2017, the U.S. value of potato production is estimated to $4.56 billion, and Japan, Canada, Mexico and South Korea are the top customers of U.S. potatoes (USDA-NASS, 2018). The presence of *G. pallida* in Idaho constitutes a considerable threat for the potato industry and resistance to this nematode in russet-type potato cultivars is currently unavailable for the U.S. (Whitworth et al., 2018). However, the extent of *G. pallida* in Idaho is limited to a small area with low nematode population levels and represents less than 1% of annual potato production areas. Contina et al. (2018) showed that the fields infested with *G. pallida* in Idaho are spatially aggregated as an ellipsoidal-shaped cluster around a radius of 12 km. *Globodera pallida* spread followed a contagion effect scenario, where infested fields contributed to the infestation of nearby fields, probably through soil contaminated agricultural equipment (Contina et al., 2018). The presence of *G. pallida* in Idaho is unlikely to be associated with new introductions from outside the state (Contina et al., 2018). USDA-APHIS quarantine and eradication programs are monitoring the presence of *G. pallida* in potato fields through intensive soil sampling and testing at regular time intervals. Research on the control of *G. pallida* in Idaho is focused on developing resistant potato varieties, trap crops, biofumigants and biocontrol agents (Contina et al., 2017; Dandurand and Knudsen, 2016; Dandurand et al., 2017; Whitworth et al., 2018).

Quantitative research on plant nematode disease epidemics are focused on: (i) modeling the relationship between initial (P_i) and final (P_f) egg densities; and (ii) evaluating the impacts of nematode infection on host growth (Brodie, 1996; Ferris, 1985; Jones et al., 1967; Jones and Kempton, 1978; LaMondia and Brodie, 1986; Seinhorst, 1965; Seinhorst and Ouden, 1971). Potato cyst nematodes produce only one infection cycle per crop cycle

and cause the development of monocyclic disease. In monocyclic epidemics, the initial nematode inoculum represents a fundamental component of disease intensity over time (Seinhorst, 1965). The early stages of monocyclic epidemics are characterized by a linear model, and a reduction in the initial inoculum or the rate of infection will result in a reduction of the disease level by the same proportion at any time throughout the epidemic (Madden et al., 2007). Pylypenko (1999) reported a linear relationship for *G. rostochiensis*; for a resistant potato cultivar, 55 eggs per gram soil were associated with a 3.3% yield loss, whereas a 37.7% yield loss was observed for susceptible variety; but populations of 121 eggs per gram soil were associated with losses of 16.9% and 63.3%, respectively.

The main objective of crop disease modeling is to capture and understand the determinants of epidemic development in order to develop comprehensive disease management and control programs. The pathogen reproduction rate, considered as a measure of disease risk, provides quantitative information on the disease development and provides a basis for developing disease control programs that will reduce crop losses and disease incidence (Madden and Nutter, 1995; Savary et al., 2006). The goals of disease management and control (Nutter, 2001; Zadoks, 1985) are to: (i) eliminate or reduce the initial pathogen inoculum; (ii) reduce the disease infection rate; and (iii) reduce the time of pathogen-host interactions to reduce disease intensity.

Risk in plant disease is considered as the probability of occurrence of a disease incidence or severity (Luo et al., 1998; Teng and Yuen, 1991). The information can be obtained from the probability distribution where the mean and its deviation can be estimated (Luo et al., 1998), and from Monte-Carlo simulation (Teng and Yuen, 1991). Simulation modeling using crop growth model provides detailed analysis and prediction of risk of yield losses (Luo et al., 1998; Teng and Savary, 1992). The Decision Support System for Agrotechnology Transfer (DSSAT) was developed by the International Benchmark Sites Network for Agrotechnology Transfer (IBSNAT) to facilitate the application of crop models into agronomic research (Jones et al., 1998, 2003). DSSAT integrates growth models for over 40 different crops and is supported by a cluster of applications for weather, soil, genetic, crop management, and observational experimental data with example data sets for all growth models (Hoogenboom et al., 2017). The Simulation of Underground Bulking Storage Organs

(SUBSTOR) potato crop model, incorporated into DSSAT, has been tested and validated under a wide range of environmental conditions (Griffin et al., 1993; Raymundo et al., 2017).

There is a need to integrate crop pest into crop growth models for a comprehensive approach to disease management and control strategies. Jones et al. (1985) integrated the effects of soybean looper (*Pseudoplusia includens*), corn earworm (*Heliothis* spp.) and southern green stinkbug (*Nezara virdula* L.) in the SOYGRO model. Bourgeois (1989) developed a cercospora late leaf spot model and combined it with the Peanut Growth (PNUTGRO) model. Willocquet et al. (2002) coupled crop growth model simulating rice yield response to multiple pest injuries for tropical Asia. However, extensive research efforts are required to incorporate pest models into crop growth models. Collecting data on pest initial inoculum, infection rates, damage quantifications and population genetics composition is a difficult task. Nevertheless, this approach for connecting pest models with crop models will extend the practical applications of crop models to wide-ranging problems (Batchelor et al., 1993; Boote et al., 1983; Donatelli et al., 2017).

This study is focused on investigating the risk of potato yield losses caused by *G. pallida* as a result of initial nematode densities using the potato growth model in the SUBSTOR-DSSAT crop simulation system. Assessing potato yield loss caused by the Idaho *G. pallida* population was not performed under field conditions due to its quarantine status in Idaho where it is prohibited by regulatory statutes to grow potato in any infested fields. The experimental data came from two trials, using five different *G. pallida* initial nematode densities in soil that were conducted in greenhouse environment. The objectives of this study were to: (i) determine the effect of *G. pallida* initial nematode densities on potato yield; (ii) determine the nematode reproduction rate; and (iii) simulate the risk of potato yield losses in Idaho field conditions by integrating the coefficients of potato yield into the SUBSTOR-DSSAT crop simulation model. The main goal of this study is to inform policymakers, stakeholders and the public in general of the threats posed by *G. pallida* for the U.S. potato industry.

Materials and Methods

Propagation of *G. pallida* and plant material culture. Cysts were obtained from infested potato fields in Shelley, Idaho, and were propagated on the susceptible potato cultivar 'Désirée' under greenhouse conditions of 18˚C ± 2˚C and 16:8-h light: dark period (Contina et al., 2017; Dandurand and Knudsen, 2016; Dandurand et al., 2017; Kooliyottil et al., 2016). After 16 weeks of growth, *G. pallida* cysts were recovered from soil using the USDA cyst extraction method (USDA-APHIS, 2009), and stored at 4˚C prior experimental use. The identity of *G. pallida* was assessed and confirmed by morphological and molecular methods (Skantar et al., 2007). Cysts, with 50% hatching rate, 90% egg viability and 300 eggs/cyst, were surfaced-sterilized in a solution of 0.3% NaOCl for 5 min and rinsed thoroughly with sterile distilled water. Cysts were placed inside a sterile nylon mesh bags (McMaster Carr, Elmhurst, IL) with a 250 µm of mesh opening. The nylon mesh was sealed along the edges with a hand sealer (Sealer 8" F-200, Sealer sales Inc., Northridge, CA), and were placed in sterile distilled water for hydration for 3 days before adding to soil. Potato plants (*Solanum tuberosum*) 'Désirée' cv, classified as certified disease free (from the Nuclear Potato Seed Program, University of Idaho), were grown from tissue culture plantlets in standard media (Murashige and Skoog, 1962) for 4 weeks prior to transplanting.

Effect of *G. pallida* initial inoculum densities on potato yield. Three trials were conducted using Prosser fine sandy loam soil, which was air-dried and sieved through a 5-mm mesh. A 2:1 sand: soil mixture (56% sand, 35% silt, 8% clay, pH 7.0) was autoclaved twice for 90 min at 121˚C prior to experimental use. A 15-cm diameter size Terra Cotta clay pot (The Home Depot, Atlanta, GA) was used and each clay pot contained 1.5 kg soil mix. There were five different levels of *G. pallida* initial nematode densities (0, 10, 20, 40 and 80 eggs/g soil), as treatments. The initial *G. pallida* densities used in this study represent the upper-level of nematode densities associated with yield loss showed by the Seinhorst model for potato cyst nematode (Seinhorst and Den Ouden, 1971; Ward et al., 1985). Treatments included 10 replicates and were arranged in a completely randomized block design. Pots were maintained under greenhouse conditions of 18˚C ± 2˚C, 60% relative humidity and 16:8-h light: dark period. Pots were watered twice daily in the amount of 100 ml of water and

fertilized once a week using Jack's classic garden fertilizer 20-20-20 (JR Peters Inc., Allentown, PA) applied at a rate of 0.5 g/ l water.

Potato growth and nematode reproduction assessments. After 12 weeks, potato above-ground (top), roots and tubers were weighted as fresh and dry in a scale, and were expressed in gram (Thermo Fisher Scientific, Waltham, MA). Cysts were extracted from soil using the USDA cyst extraction method (USDA-APHIS, 2009). Extracted cysts were crushed in 100 µl of sterile distilled water and eggs were counted under a dissecting microscope (Leica M80, Leica Microsystems, Wetzlar, Germany). Nematode reproduction rate (*Rf*) was calculated based on the ratio of the final egg population density (*Pf*) over the initial egg population density (*Pi*) per gram of soil.

SUBSTOR-DSSAT potato crop simulation models. The SUBSTOR-potato model inputs are daily weather data, soil profile parameters, cultivar parameters and crop management information (Singh et al., 1998). The model simulates the daily dynamics of phenology, biomass and yield accumulation. There are five phenological stages in the model (Griffin et al., 1993; Singh et al., 1998): (i) pre-planting; (ii) planting to sprout germination; (iii) sprout germination to emergence; (iv) emergence to tuber initiation; and (v) tuber initiation to maturity. The SUBSTOR-potato models are designed to simulate growth and development under (Singh et al., 1998): (i) non-limiting conditions; (ii) water limited conditions; or (iii) water and nitrogen limited conditions.

All growth stages are affected by temperature in root and tuber growth (*RTFSOIL*). Tuber initiation (*TI*) is a function of daylength and temperature and is also influenced by plant nitrogen level and soil water deficit (Griffin et al., 1993; Singh et al., 1998). The model uses potato cultivar coefficient (*P2*) and photoperiod (*PHPER*) to determine the relative daylength factor for tuber initiation (*RDLFTI*), and is defined as:

$$RDLFTI = (1 - P2) + 0.00694 \times P2 \times (24 - PHPER)^2$$

The model estimates a tuber induction index (*TII*) at the beginning of emergence, and is defined as:

$$TII = (RTFTI \times RDLFTI) + 0.5 \times [1 - AMIN1\ (SWDF2, NDEF2)]$$

where, *AMIN1* (*SWDF2, NDEF2*) simulates water stress (*SWDF2*) or nitrogen deficiency (*NDEF2*).

Potato growth in the model is maintained by the carbohydrate resource from the seed

piece (*SEEDAV*) during the pre-emergence phase, and continues to support post-emergence growth up to a plant leaf area (*PLA*) of 400 cm^2 per plant (Griffin et al., 1993; Singh et al., 1998). In the post-emergence vegetative growth stage, potential photosynthetic carbohydrate assimilation (*PCARB*) is defined as:

$$PCARB = RUE \times \frac{PAR}{PLANTS} \times \left(1 - e^{(-k \times LAI)}\right)$$

where, *RUE* is the solar radiation, *PAR* is the percentage of incoming radiation, *k* is an extinction coefficient and *LAI* is the leaf area index.

The actual daily carbohydrate accumulation (*CARBO*) is calculated as:

$$CARBO = PCARB \times AMIN1\ (PRFT, SWDF1, NDEF1) + 0.5 \times DDEADLF$$

where, *PRFT* is the effects of non-optimal temperature on *CARBO* and *DDEADLF* is the carbohydrate translocation in senesced leaves prior to abscission.

The potential tuber growth (*PTUBGR*) is a function of maximum tuber growth rate (*G3*) and temperature, and is defined as:

$$PTUBGR = G3 \times \frac{RTFSOIL}{PLANTS}$$

The actual tuber growth (*GROTUB*) is influenced by water and nitrogen stress, and tuber sink strength (*TIND*) as:

$$GROTUB = PTUBGR \times AMIN1\ (SWDF2, NDEF2) \times TIND$$

The potential leaf expansion (*PLAG*) is estimated by the genetic coefficient for maximum leaf expansion (*G2*), a temperature factor (*RTFVINE*), water and nitrogen stress, and is expressed as:

$$PLAG = G2 \times \frac{RTFVINE}{PLANTS} \times AMIN1\ (SWDF2, NDEF2)$$

Weather data for southeastern Idaho was obtained from AgriMet Cooperative Agricultural Weather Network for the Pacific Northwest Region (AgriMet, 2018). Ashton, ID weather station (AHTI) was used to generate the following weather parameters from 1988 to 2017: (i) minimum daily air temperature (˚F); (ii) maximum daily air temperature (˚F); (iii) daily precipitation (in); and (iv) daily global solar radiation (langleys). AHTI weather data was saved as a text file and WeatherMan, a DSSAT application, was used to import the data into DSSAT weather database. Prior to import, WeatherMan converted the units for temperature in Celsius (˚C), rain in millimeter (mm) and solar radiation in megajoule per

square meter (MJ/m^2). We used a pre-built simulation model in DSSAT based on validated data from a potato growth experiment conducted in Hermiston, OR (OSBO 8801) (Hoogenboom et al., 2017; Jones et al., 2003), and was modified to include the southeastern Idaho weather data (AHTI) and sandy loam soil data from Aberdeen, ID. The genetic coefficients for the potato cultivar 'Désirée' used in DSSAT included (Hoogenboom et al., 2017; Jones et al., 2003): (i) daily leaf expansion rate (*G2*) 2000 cm^2/m^2; (ii) daily potential tuber growth rate (*G3*) 25.0 g/m^2; (iii) index that suppresses tuber growth during the period that immediately follows tuber induction (*PD*) 0.9; (iv) tuber initiation sensitivity to photoperiods (*P2*) 0.6; and (v) temperature for tuber initiation 16˚C.

Integrating yield coefficients to SUBSTOR-DSSAT potato crop model. Potato yield coefficient was calculated by comparing yields in *G. pallida* non-infested with infested soil, and can be expressed by:

$$Y_{coeff} = 1 - \left[\frac{(Y_0 - Y_n)}{Y_0}\right]$$

where, (Y_{coeff}) is the potato yield coefficient, (Y_0) is the yield in *G. pallida* non-infested soil and (Y_n) is the yield in infested soil at different levels of *G. pallida* initial nematode densities (n). The expression $\left[\frac{(Y_0 - Y_n)}{Y_0}\right] \times 100$ represents the percentage of yield loss.

The application of yield coefficient to crop model variables can be expressed by:

$$Y_{ij} = Y_i \times Y_{coeff}$$

where, (Y_{ij}) is the potential potato yield after *G. pallida* damage and (Y_i) is the potential yield without *G. pallida* damage.

The coupling points for yield coefficients in the potato crop model, as defined in the DSSAT v.4.7.0 software (Hoogenboom et al., 2017; Jones et al., 2003), were: (i) above-ground weight (*CWAD*), expressed as kilogram dry-matter per hectare (kg[dm]/ha); (ii) root weight (*RWAD*) (kg[dm]/ha); (iii) tuber dry weight (*UWAD*) (kg[dm]/ha) and fresh weight (*UYAD*) (ton[fm]/ha); and (iv) total plant weight (*TWAD*) (kg[dm]/ha).

Data analysis. Statistical data analyses were performed using R version 3.5.2 (R Core Team, 2018). Analysis of variance and generalized linear models were performed to analyze the effect of *G. pallida* initial nematode densities on potato growth parameters with significant differences occurring at level of $P \leq 0.05$. Tukey's HSD test was performed to

compare the mean differences for each level of initial nematode density with significant differences occurring at level of $P \leq 0.05$. Linear regression analyses were performed to model the relationship between initial nematode densities (predictors) and potato growth parameters (responses). Pearson correlation coefficient was used to assess the strength of the regression models with significant differences occurring at level of $P \leq 0.05$. A Bayesian analysis was performed to generates a sample from the posterior distribution of a linear regression model with Gaussian errors using Gibbs sampling in a random univariate Markov Chain Monte Carlo simulation (MCMC) with 10,000 sampling size per chain (Martin et al., 2011). A generalized additive model (GAM) was performed to model the relationship between dry root weight and *G. pallida* reproduction rate using a non-linear smooth function to model and capture the non-linearities in the data (Hastie and Tibshirani, 1990). The following R packages were used: (i) 'agricolae' for performing a Tukey's HSD comparison test; (ii) 'ggplot2' for plotting DSSAT simulation output; (iii) 'MCMCpack' for performing a Bayesian inference using posterior simulation; and (iv) 'mgcv' for fitting a GAM model to the data by using a Gauss-Seidel backfitting algorithm method.

Results

Potato growth assessment. For potato growth and *G. pallida* reproduction assessments, no significant differences as determined by the analysis of variance, were detected between trial 2 and trial 3 ($P > 0.05$), therefore experimental data from both trials were combined (trial 2/3). In trial 1, fresh and dry top weights were significantly reduced by 73% and 81%, respectively, when *G. pallida* initial nematode densities were at 80 eggs/g soil compared to non-infested soil ($P \leq 0.05$) (Table 4.1). Dry root weight significantly decreased by 88% at 80 eggs/g soil compared to non-infested soil ($P \leq 0.05$) (Table 4.1). Fresh tuber weight was significantly reduced by 44% at 40 eggs/g soil and by 87% at 80 eggs/g soil, and dry tuber weight was significantly reduced by 34% at 40 eggs/g soil and by 86% at 80 eggs/g soil compared to non-infested soil ($P \leq 0.05$) (Table 4.1). Overall, total dry plant weight decreased significantly by 43% at 40 eggs/g soil and by 84% at 80 eggs/g soil compared to non-infested soil ($P \leq 0.05$) (Table 4.1). Tubers produced per plant showed a propensity to increase in number at 10, 20 and 40 eggs/g soil, with a significant 30% increase in the

number of tubers at 20 eggs/g soil ($P \leq 0.05$), however the number of tubers was significantly reduced by 54% at 80 eggs/g soil compared to non-infested soil ($P \leq 0.05$) (Table 4.2). Furthermore, fresh tuber weight per unit was significantly reduced by 30% at 40 eggs/g soil and by 79% at 80 eggs/g soil, and dry tuber weights per unit was significantly reduced by 31% at 40 eggs/g soil and 82% at 80 eggs/g soil compared to non-infested soil ($P \leq 0.05$) (Table 4.2).

In trial 2/3, no significant weight reductions were observed for fresh and dry top at any level of *G. pallida* initial nematode densities, and no significant dry root weight reduction was detected compared to non-infested soil ($P > 0.05$) (Table 4.1). However, fresh tuber weight was significantly reduced by 20% at 40 eggs/g soil and by 39% at 80 eggs/g soil, and dry tuber weight was significantly reduced by 20% at 40 eggs/g soil and by 42% at 80 eggs/g soil compared to non-infested soil ($P \leq 0.05$) (Table 4.1). Overall, total dry plant weight decreased significantly by 36% at 80 eggs/g soil compared to non-infested soil ($P \leq 0.05$) (Table 4.1). Tubers produced per plant showed a propensity to increase in number at 10 and 20 eggs/g soil, with a significant 19% increase in the number of tubers at 20 eggs/g soil ($P \leq 0.05$), before dropping at 40 and 80 eggs/g soil (Table 4.2). Furthermore, fresh tuber weight per unit was significantly reduced by 30% at 40 eggs/g soil and by 39% at 80 eggs/g soil, and dry tuber weight per unit was significantly reduced by 28% at 40 eggs/g soil and by 42% at 80 eggs/g soil compared to non-infested soil ($P \leq 0.05$) (Table 4.2).

***Globodera pallida* reproduction assessment.** Trial 1 showed significant increased proliferation of *G. pallida* cysts in dry potato roots for each increasing level of initial nematode densities in soil ($P \leq 0.05$) (Table 4.3): (i) 1,903 cysts/g root at 10 eggs/g soil; (ii) 1,572 cysts/g root at 20 eggs/g soil; (iii) 2,699 cysts/g root at 40 eggs/g soil; and (iv) 36,933 cysts/g root at 80 eggs/g soil. Similar increased proliferation patterns of *G. pallida* cysts were observed in soil (Table 4.3): (i) 0.80 cysts/g soil at 10 eggs/g soil; (ii) 0.95 cysts/g soil at 20 eggs/g soil; and (iii) 1.19 cysts/g soil at 40 eggs/g soil; however, at 80 eggs/g soil the number of cysts per gram of soil was lowered to 0.56. The number of eggs per cyst decreased significantly at each increasing level of initial nematode densities ($P \leq 0.05$) (Table 4.3): (i) 588 eggs/cyst at 10 eggs/g soil; (ii) 535 eggs/cyst at 20 eggs/g soil; (iii) 465 eggs/cyst at 40 eggs/g soil; and (iv) 324 eggs/cyst at 80 eggs/g soil. *Globodera pallida* reproduction rate (final population/initial population, *Pf/Pi*) decreased significantly at each increasing level of

initial nematode densities in soil ($P \leq 0.05$) (Table 4.3): (i) 47.25 at 10 eggs/g soil; (ii) 25.51 at 20 eggs/g soil; (iii) 14.18 at 40 eggs/g soil; and (iv) 2.45 at 80 eggs/g soil.

Trial 2/3 showed significant increased proliferation of *G. pallida* cysts in dry potato roots for each increasing level of initial nematode densities in soil ($P \leq 0.05$) (Table 4.3): (i) 562 cysts/g root at 10 eggs/g soil; (ii) 1,090 cysts/g root at 20 eggs/g soil; (iii) 1,263 cysts/g root at 40 eggs/g soil; and (iv) 2,292 cysts/g root at 80 eggs/g soil. Similar increased proliferation patterns of *G. pallida* cysts were observed in soil (Table 4.3):(i) 0.48 cysts/g soil at 10 eggs/g soil; (ii) 0.73 cysts/g soil at 20 eggs/g soil; (iii) 0.79 cysts/g soil at 40 eggs/g soil; and (iv) 0.89 cysts/g soil at 80 eggs/g soil. The number of eggs per cyst decreased significantly at each increasing level of initial nematode densities ($P \leq 0.05$) (Table 4.3): (i) 439 eggs/cyst at 10 eggs/g soil; (ii) 424 eggs/cyst at 20 eggs/g soil; (iii) 389 eggs/cyst at 40 eggs/g soil; and (iv) 368 eggs/cyst at 80 eggs/g soil. *Globodera pallida* reproduction rate (*Pf/Pi*) decreased significantly at each increasing level of initial nematode densities in soil ($P \leq 0.05$) (Table 4.3): (i) 19.90 at 10 eggs/g soil; (ii) 14.43 at 20 eggs/g soil; (iii) 7.52 at 40 eggs/g soil; and (iv) 4.10 at 80 eggs/g soil.

Modeling the relationship between *G. pallida* initial nematode densities and potato growth parameters. Trial 1 showed strong and significant negative linear relationships between initial nematode densities in soil (predictors) and potato growth parameters (response variables) ($P < 0.001$) (Table 4.4). Pearson correlation coefficient (R^2), a measure of strength in linear relationships, were for: fresh top (0.47), dry top (0.47), dry root (0.52), fresh tuber (0.61), dry tuber (0.60) and total dry plant (0.56). Bayesian regression analysis, a method to measure the posterior probability distributions in linear relationships, for total dry plant showed that the 97.5% confidence interval was for (Fig. 4.1; Table 4.5): (i) the intercept (15.96 and 19.80); (ii) the initial nematode densities (-0.23 and -0.14); and (iii) the residual error variance σ^2 (15.15 and 34.13).

Trial 2/3 also showed a significant negative linear relationship between initial nematode densities in soil and potato growth parameters ($P < 0.001$) (Table 4.4). Pearson correlation coefficient (R^2) were for: fresh top (0.03), dry top (0.05), dry root (0.10), fresh tuber (0.20), dry tuber (0.20) and total dry plant (0.20). Bayesian regression analysis for total dry plant showed that the 97.5% confidence interval was for (Fig. 4.2; Table 4.5): (i) the

intercept (22.18 and 25.85); (ii) the initial nematode densities (-0.16 and -0.07); and (iii) the residual error variance σ^2 (31.34 and 54.98).

Modeling the relationship between *G. pallida* initial nematode densities and nematode reproduction rate. Trial 1 showed a strong and significant negative linear relationship between initial nematode densities and nematode reproduction rate ($R^2 = 0.60$, $P < 0.001$) (Table 4.6). Similar results were observed for trial 2/3 ($R^2 = 0.52$, $P < 0.001$) (Table 6). A generalized additive model (GAM) was performed to model the relationship between dry root weight and *G. pallida* reproduction rate using a non-linear smooth function to model and capture the non-linearities in the data. Trial 1 showed a positive and significant non-linear relationship between dry root weight and *G. pallida* reproduction rate with a correlation coefficient $r = 0.91$ ($P < 0.001$) (Fig. 4.3). Similar results were observed in trial 2/3 with a correlation coefficient $r = 0.34$ ($P = 0.01$) (Fig. 4.3).

SUBSTOR-DSSAT potato growth simulation and *G. pallida* impact assessment. The coefficients of potato yield achieved under each initial nematode density for each potato growth parameters were integrated into the SUBSTOR-DSSAT potato growth simulation model (Table 4.7). The model simulated the potential yield for potato dry top, dry root, fresh and dry tubers, and total dry plant for each *G. pallida* initial nematode densities under Idaho weather and field conditions. In trial 1, 103 days after planting (DAP), potato dry top reached a maximum yield of 6,427 kg/ha under *G. pallida* non-infested soil and reached a minimum yield of 1,221 kg/ha at *G. pallida* initial nematode density of 80 eggs/g soil (Fig. 4.4A.). From 149 to 168 DAP, potato dry root reached a maximum yield of 1,804 kg/ha in non-infested soil and reached a minimum yield of 217 kg/ha at initial nematode density of 80 eggs/g soil (Fig. 4.4B). At 149 DAP, potato dry and fresh tubers reached a maximum yield of 19,145 kg/ha and 96 ton/ha, respectively, in non-infested soil and reached a minimum yield of 2,680 kg/ha and 12 ton/ha, respectively, at initial nematode density of 80 eggs/g soil (Fig. 4.5AB). At 148 DAP, potato total dry plant reached a maximum yield of 23,911 kg/ha in non-infested soil and reached a minimum of 3,826 kg/ha at 80 eggs/g soil (Fig. 4.6). In trial 2/3, similar potato yields are reported under *G. pallida* non-infested soil, corresponding to each potato growth parameters. At *G. pallida* initial nematode density of 80 eggs/g soil, the following minimum potato yields were observed (Fig. 4.7AB; 4.8AB; 4.9): (i) dry top (5,399

kg/ha); (ii) dry root (1,137 kg/ha); (iii) dry tuber (11,104 kg/ha); (iv) fresh tuber (58 ton/ha); and (v) total dry plant (15,303 kg/ha).

Discussion

Soil infested with *G. pallida* caused significant potato yield loss in the susceptible cultivar 'Désirée' and severely hindered potato growth development. Our study showed that fresh tuber yield losses in 'Désirée' reached between 87% and 39% when initial nematode density (*Pi*) was 80 eggs/g soil and between 44% and 20% at 40 eggs/g soil, compared to non-infested soil. Our greenhouse results coincided within the range of potato yield losses observed in other studies conducted in highly infested field plots planted with susceptible potato cultivars (Brown and Sykes, 1983; Schomaker and Been, 2006; Talavera et al. 1998; Trudgill et al., 1996; Trudgill et al., 2014; Vasyutin and Yakovleva, 1998). We observed severe stunting, limited root development and chlorosis in potato plants when *Pi* was 80 eggs/g soil, coinciding with similar phenotypic observations recorded by other studies conducted in highly infested soils (Evans, 1982; Trudgill and Cotes, 1983). In the second trial of our study, we observed a slight increase of potato biomass at *G. pallida* initial nematode densities of 10 eggs/g soil, however at 40 and 80 eggs/g soil we observed significant biomass reductions. We observed a slight increase in the number of tubers at 20 and 40 eggs/g soil, however the size of the tubers was considerably smaller compared to non-infested soil. Seinhorst and Den Ouden (1971) indicated that if potato cyst nematodes stimulate the growth of the plant directly, the growth stimulation would be inversely proportional to the density of the nematode in soil and would only have an effect at small initial nematode densities, as observed in the second trial. They also showed that at small nematode densities, potato growth was not significantly reduced, and only was significant at high nematode densities in soil, as observed in our study.

In our study, the relationship between *Pi* and potato yield showed a negative linear interaction, indicating significant yield losses as *Pi* increased in soil. Modeling the interactions between *Pi* and yield provide additional tools for maximizing long term yield under resistant and partially resistant cultivars and controlling the extent of field infestations. Numerous linear models for explaining the interaction between *Pi* and yield have been

developed for resistant and non-resistant potato cultivars. Elston et al. (1991) developed an inverse linear model to summarize the relationship between *Pi* of *G. pallida* and the yield of partially resistant potatoes. Trudgill et al. (1996) developed a curvilinear relationship between PCN population density and yield in field trials, and showed that the slope of the curve was influenced by environmental factors, including soil type and by differences in cultivar damage tolerance.

We observed significant increase of *G. pallida* reproduction rate, reaching almost 50 times the amount of eggs initially applied in soil. Whitehead (1991) showed a *G. pallida* reproduction rate of 21.7 in the susceptible 'Désirée' cultivar in infested fields. Phillips et al. (1991) reported the maximum *G. pallida* reproduction rate for the following potato cultivars: (i) 'Maris Piper'(non-resistant) 44.4; (ii) 'Morag' (moderate resistance) 44.3; (iii) 'Fiona' (low level of resistance) 29.1; (iv) '11233' (moderate resistance) 26.2; (v) 'Vantage' 9.6 (high resistance); and (vi) '12243' (low level of resistance) 12.4. Greco et al. (1982) reported *G. pallida* reproduction rates of 128, 58 and 65 in the susceptible 'Sieglinde' cv at initial nematode density of 6,856 eggs/g soil in three separate microplots experiment. Whitehead (1977) estimated that if each gram of soil contains one *G. pallida* nematode egg, then they could be 3.30×10^9 eggs/g soil per hectare, in the top 40 cm of the soil profile. The reproduction rate of *G. pallida* decreased, as the initial nematode densities in soil increased, due to the reduction of the root system and infection court, leading to a density-dependent population dynamic, as observed in our trials (Phillips et al., 1991; Seinhorst and Den Ouden, 1971; Trudgill et al., 1996). Jones and Kempton (1978) showed that the nematode sex ratio, the number of eggs produced by the female and the host crop growth limitations were the main mechanisms for the density-dependent regulation of *G. rostochiensis* population growth.

The integration of crop growth simulation models to crop pest disease models provides valuable predictions of potential crop yields under disease and real farm conditions, and represents a tool to assess potential pest risks for agricultural production and food security (Batchelor et al., 1993; Bourgeois, 1989; Boote et al., 1983; Donatelli et al., 2017; Jones et al., 1985). The DSSAT software application program includes database management programs for soil, weather, crop management and experimental data, and the databases are used for precision management, gene-based modeling and breeding selection, water use,

greenhouse gas emissions, and long-term sustainability through the soil organic carbon and nitrogen balances. However, DSSAT database programs for assessing the direct impact of crop pests on yields, estimating the economic impact of yield losses and predicting the level of pathogen populations in soil sampling remain unavailable. To remediate for the lack of crop disease components in DSSAT, we generated coefficients of potato attainable yields under different *G. pallida* initial infestation levels in soil from greenhouse trials, and integrated them into the SUBSTOR-DSSAT crop management and experimental database to simulate the impact of *G. pallida* in potato yield. From the simulation, we were able to estimate significant fresh tuber yield losses between 84 and 38 ton/ha in the susceptible 'Désirée' cv when *Pi* was 80 eggs/g soil and to evaluate the overall potato plant growth. To our knowledge, this is the first time that DSSAT was used to simulate the impact of *G. pallida* on potato yield.

Numerous PCN models and simulation platforms, based on many years of field trials, were directly developed to evaluate the impact on yields, determine the economic threshold, estimating soil sampling methods and nematode probability detection, and to assess the effectiveness of nematicides, trap crops and resistant cultivars on nematode population dynamics in the field (Been et al., 2005; Jones and Kempton, 1980; Moxnes and Hausken, 2007; Schomaker and Been, 2006; Ward et al., 1985). Been et al. (2005) developed NemaDecide, a decision support system for the management of PCN, based on the results from 50 years of Dutch quantitative nematological research that had been structured into stochastic models and integrated in a software package. NemaDecide was used as a quantitative information system to enable growers to estimate risks of yield losses, to determine population development, to estimate the probability of detection of nematode foci by soil sampling, to calculate the cost/benefit of control measures and to provide adequate advice for growers to optimize financial returns.

In this study, we observed significant differences in potato growth and *G. pallida* reproduction rate between trial 1 and trial 2/3. Trial 1 was conducted in Fall (September-November 2017), while trial 2/3 was conducted in Spring (March-June 2018). In trial 1, we observed a high *G. pallida* reproduction rate coinciding with a high potato growth reduction, however in trial 2/3, *G. pallida* reproduction rate was reduced, and a low potato growth reduction was observed. Although greenhouse conditions were kept constant for both trials,

we concluded that temporal difference between the trials might be the source of variation in the results obtained. Temporal differences might affect the potato plant photoperiod experienced during *G. pallida* development, and also might influence nematode breaking of diapause. Evans (1987) showed that *Globodera* spp. undergo a diapause stage in which juvenile development within egg remains dormant until favorable hatching conditions are reached. Ellenby (1958) found that *G. rostochiensis* produced fewer females on potato roots in short days than in long days. Evans et al. (1975) reported that *G. rostochiensis* and *G. pallida* distinct distributions in the Andes were related to the effects of daylength on the hosts. Franco and Evans (1979) observed that *Globodera* spp. from Europe tended to produce more cysts on plants grown in 16-hr days, however *G. rostochiensis* from Peru produced more cysts on plants grown in 12-hr days. Hominick (1986) showed that the breaking of nematode diapause was attributed to photoperiod signals passed to the developing *G. rostochiensis* females and eggs by the plant. Hominick et al. (1985) observed diapause in *G. rostochiensis* and recorded a low rate of hatch in the fall and winter after harvest, and a faster rate of hatch the following spring and summer. Temporal temperature conditions might also explain the variations in the results obtained. Franco (1979) reported that *G. pallida* is better adapted to temperatures between 10˚ and 18˚C, and more cysts and eggs per plant were produced at lower temperatures. Similar temperature conditions and nematode reproduction were also reported for *Globodera spp.* (Martin, 1965; Oostenbrink, 1967).

Due to *G. pallida* high reproduction rate and considerable impact on potato yield, this pest can rapidly spread via contaminated farm equipment or plant materials in the absence of an effective biosecurity regulation (Hodda and Cook, 2009). *Globodera pallida* produces only one infection cycle per crop cycle and causes the development of monocyclic disease. The early stages of monocyclic epidemics are characterized by a linear model, and a reduction in the initial inoculum or the rate of infection will result in a reduction of the disease level (Madden et al., 2007). The enforcement of quarantine regulation in Idaho greatly contributed in restricting *G. pallida* infested fields to a small area of 1,326 ha (USDA-APHIS, 2019). The benefits of excluding these nematodes from potato growing areas in the U.S. are estimated to be $300 million annually (Dwinell and Lehman, 2004; Hockland et al., 2006). Hodda and Cook (2009) estimated, in the absence of potato cyst nematodes regulation, the economic losses for Australian agriculture could exceed $370

million. Schomaker and Been (2006) estimated that the mortality rate of *G. rostochiensis* and *G. pallida*, in the absence of the host, was greater in the first year after potato crop (69%) than in subsequent years (20-30%), and the population decline was independent of nematode population density. When non-host crops were cultivated for 2 or 3 years consecutively, potato yield increased by 2.7 and 3.4 times, and *G. pallida* populations declined by 54% and 91%, respectively (Samaliev, 1998). In the absence of potato crop, *G. pallida* rapid reproduction rate will stop, reducing its probability to spread across the containment line. As the reproduction rate comes to a halt, control measures will achieve better results for the eradication of the remaining viable nematode eggs in the fields. The use of nematicides contributes to the reduction of initial nematode densities in soil, however the high cost, inherent toxicity, and potential environmental damage of many nematicides have limited or prohibited their use (Haydock et al., 2006; Schneider et al., 2003). One of the most important environmental problems associated with nematicide usage is groundwater contamination (Cohen, 1996). Furthermore, models showed that sufficient *G. pallida* eggs are likely to survive in the soil after nematicide applications, leading to a resurgence of large nematode populations in subsequent potato crop cycle (Trudgill et al., 2003). Resistance in potato russet-type varieties suitable for U.S. producers is currently unavailable. Breeding resistance for *G. pallida*, with integration into a crop rotation scheme (non-host and trap crops), can provide a viable alternative to nematicides and will favor a long-term sustainable control of *G. pallida* in the field (Dandurand and Knudsen, 2016; Dandurand et al., 2017; Whitworth et al., 2018). Gurr (1992) reported that resistance may offer more effective control of *G. pallida* than chemical treatment.

We acknowledge some limitations in our risk simulation model in terms of its evaluation and validation using real field data. Because of the quarantine status of *G. pallida* in Idaho, this study could not be performed in potato field conditions. Furthermore, there are no recorded field data on *G. pallida* associated-potato yield losses for Idaho, which in most cases are used to establish the robustness of a risk model by comparing observed data with the simulated model. However, the simulation model in this study provides ample information on the potential risk of significant potato yield losses caused by *G. pallida* for the potato industry. This study provides valuable simulation data for agricultural economist to model the economic impact of this pest for Idaho potato production, and contributes to the

growing demands by decision-makers for the integration of disease model into crop growth simulation platform. This study is especially oriented toward potato growers affected by the presence of this nematode in their fields. The tools and methods used in this study can be expanded to include the impact of various control methods on *G. pallida* population dynamics and potato growth, as well as to estimate the risk impact of climate change for potato production. The outputs of this study should facilitate common understandings between regulators, policymakers and potato growers on the challenges and opportunities for controlling this economically important potato pest in Idaho.

Literature Cited

AgriMet. 2018. AgriMet historical archive weather data access. Online database. AgriMet Cooperative Agricultural Weather Network for the Pacific Northwest Region. https://www.usbr.gov/pn/agrimet/webarcread.html.

Batchelor, W. D., Jones, J. W., Boote, K. J., and Pinnschmidt, H. O. 1993. Extending the use of crop models to study pest damage. Trans. ASAE 36:551-558.

Been, T. H., Schomaker, C. H., and Molendijk, L. P. G. 2005. NemaDecide: A decision support system for the management of potato cyst nematodes. Pages 143-155 in: Potato in progress: Science meets practice, A. J. Haverkort, and P. C. Struik, eds. Wageningen Academic Publishers, Netherlands.

Behrens, E. 1975. *Globodera Skarbilovic*, 1959, eine selbstaendige Gattung in der Unterfamilie Heteroderinae Skarbilovic, 1947 (Nematoda: Heteroderidae). Vortragstagung zu aktuellen Problemen der Phytonematologie am 29/5/1975 in Rostock. Manuskriptdruck der Vortraege. Rostock, 1975:12-26.

Boote, K. J., Jones, J. W., Mishoe, J. W., and Berger, R. D. 1983. Coupling pests to crop growth simulators to predict yield reductions. Phytopathology 73:1581-1587.

Bourgeois, G. 1989. Interrelationships between late leafspot disease and Florunner peanut: A modeling approach. Ph.D. Diss., University of Florida, Gainesville.

Brodie, B. B. 1996. Effect of initial nematode density on managing *Globodera rostochiensis* with resistant cultivars and nonhosts. J. Nematol. 28:510-519.

Brown, E. B., and Sykes, G. B. 1983. Assessment of the losses caused to potatoes by the potato cyst nematodes *Globodera rostochiensis* and *G. pallida*. Ann. Appl. Biol. 103:271-276.

CABI. 2018. *Globodera pallida* (white potato cyst nematode). Online publication. Centre for Agriculture and Biosciences International. https://www.cabi.org/ISC/datasheet/27033.

Cohen, S. Z. 1996. Pesticides in ground water in the United States: Monitoring, modeling, and risks from the U.S. perspective. J. Environ. Sci. Health B. 31:345-352.

Contina, J. B., Dandurand, L. M., and Knudsen, G. R. 2017. Use of GFP-tagged *Trichoderma harzianum* as a tool to study the biological control of the potato cyst nematode *Globodera pallida*. Appl. Soil Ecol. 115:31-37.

Contina, J. B., Dandurand, L. M., and Knudsen, G. R. 2018. A spatial analysis of the potato cyst nematode *Globodera pallida* in Idaho. Phytopathology 108:988-1001.

Dandurand, L. M., and Knudsen, G. R. 2016. Effect of the trap crop *Solanum sisymbriifolium* and two biocontrol fungi on reproduction of the potato cyst nematode *Globodera pallida*. Ann. Appl. Biol. 169:180-189.

Dandurand, L. M., Morra, M. J., Zasada, I. A., Phillips, W. S., Popova, I., and Harder, C. 2017. Control of *Globodera* spp. using *Brassica juncea* seed meal and seed meal extract. J. Nematol. 49:437-445.

Donatelli, M., Magarey, R. D., Bregaglio, S., Willocquet, L., Whish, J. P. M., and Savary, S. 2017. Modelling the impacts of pests and diseases on agricultural systems. Agric. Syst. 155:213-224.

Dwinell, L. D., and Lehman, P. S. 2004. Plant-parasitic nematodes which are exotic pests in agriculture and forestry. Pages 51-70 in: Biological Pollution: An Emerging Global Menace, K. O. Briton, ed. American Phytopathological Society Press, St Paul, Minnesota.

Ellenby, C. 1958. Day length and cyst formation in the potato root eelworm *Heterodera rostochiensis* Woll. Euphytica 3:81-90.

Elston, D. A., Phillips, M. S., and Trudgill, D. L. 1991. The relationship between initial population density of potato cyst nematode *Globodera pallida* and the yield of partially resistant potatoes. Revue Nématol. 14:221-229.

Evans, A. A. F. 1987. Diapause in nematodes as a survival strategy. Pages 180-187 in: Vistas on Nematology. J. A. Veech and J. A. Dickson, eds. Society of Nematologists, Hyattsville, MD.

Evans, K. 1982. Effects of infestation with *Globodera rostochiensis* (Wollenweber) Behrens Ro1 on the growth of four potato cultivars. Crop Prot. 1:169-179.

Evans, K., Franco, J., and De Scurrah, M. 1975. Distribution of species of potato cyst nematodes in South America. Nematologica 21:365-369.

Evans, K., and Stone, A. R. 1977. A review of the distribution and biology of the potato cyst nematodes *Globodera rostochiensis* and *G. pallida*. Int. J. Pest Manag. 23:178-189.

Ferris, H. 1985. Population assessment and management strategies for plant-parasitic nematodes. Agric. Ecosyst. Env. 12:285-299.

Franco, J. 1979. Effect of temperature on hatching and multiplication of potato cyst nematodes. Nematologica 25:237-244.

Franco, J., and Evans, K. 1979. Effects of daylength on the multiplication of potato cyst nematode (*Globodera* spp.) populations. Nematologica 25:184-190.

Greco, N., Di Vito, M., Brandonisio, A., Giordano, I., and De Marinis, G. 1982. The effect of *Globodera pallida* and *G. rostochiensis* on potato yield. Nematologica 28:379-386.

Grenier, E., Fournet, S., Petit, E., and Anthoine, G. 2010. A cyst nematode 'species factory' called the Andes. Nematology 12:163-169.

Griffin, T. S., Johnson, B. S., and Ritchie, J. T. 1993. SUBSTOR-potato v. 2.0: A simulation model for potato growth and development. Department of Agronomy and Soil Science, College of Tropical Agriculture and Human Resources, University of Hawaii, Honolulu.

Gurr, G. M. 1992. Control of potato cyst nematode (*Globodera pallida*) by host plant resistance and nematicide. Ann. Appl. Biol. 121:167-173.

Hafez, S. L., Sundararaj, P., Handoo, Z. A., Skantar, L., Carta, K., and Chitwood, D. J. 2007. First report of the Pale Cyst Nematode, *Globodera pallida*, in the United States. Plant Dis. 91:325.

Hastie, T. J., and Tibshirani, R. 1990. Generalized additive models. Chapman and Hall, London, UK.

Haydock, P. P. J., Woods, S. R., Grove, I. G., and Hare, M. C. 2006. Chemical control of nematodes. Pages 392-408 in: Plant Nematology. R. N. Perry and M. Moens, eds. CAB International, Oxfordshire, UK.

Hockland, S., Inserra, R. N., Millar, L., and Lehman, P. S. 2006. International plant health: Putting legislation into practice. Pages 328-343 in: Plant Nematology. R. N. Perry and M. Moens, eds. CAB International, Oxfordshire, UK.

Hodda, M., and Cook, D. C. 2009. Economic impact from unrestricted spread of potato cyst nematodes in Australia. Phytopathology 99:1387-1393.

Hominick, W. M. 1986. Photoperiod and diapause in the potato cyst nematode *Globodera rostochiensis*. Nematologica 32:408-418.

Hominick, W. M., Forrest, J. M. S., and Evans, A. A. F. 1985. Diapause in *Globodera rostochiensis* and variability in hatching trials. Nematologica 31:159-170.

Hoogenboom, G., Porter, C. H., Shelia, V., Boote, K. J., Singh, U., White, J. W., Hunt, L. A., Ogoshi, R., Lizaso, J. I., Koo, J., Asseng, S., Singels, A., Moreno, L. P., and Jones, J. W. 2017. Decision Support System for Agrotechnology Transfer (DSSAT) version 4.7. DSSAT Foundation, Gainesville, Florida.

Jones, F. G. W., and Kempton, R. A. 1978. Population dynamics, population models and integrated control. Page 333 in: Plant Nematology. J. F. Southey, ed. M.A.F.F. A.S. Publication G.D./1 H.M. Stationary Office, London.

Jones, F. G. W., and Kempton, R. A. 1980. Forecasting crop damage by nematodes: Nematode population dynamics. EPPO Bulletin 10:169-180.

Jones, F. G. W., Parrott, D. M., and Ross, G. J. S. 1967. The population genetics of the potato cyst nematode, *Heterodera rostochiensis*: Mathematical models to simulate the effects of growing eelworm-resistant potatoes bred from *Solanum tuberosum* ssp. *andigena*. Ann. Appl. Biol. 60:151-171.

Jones, J. W., Hoogenboom, G., Porter, C. H., Boote, K. J., Batchelor, W. D., Hunt, L. A., Wilkens, P. W., Singh, U., Gijsman, A. J., and Ritchie, J. T. 2003. The DSSAT cropping system model. Europ. J. Agronomy 18:235-265.

Jones, J. W., Mishoe, J. W., Wilkerson, G. G., Stimac, J. L., and Boggess, G. 1985. Integration of soybean crop and pest models. In: R. E. Frisbie, and P. L. Adkisson, eds. Symposium sponsored by the Consortium for Integrated Pest Management and USDA/CSRS.

Jones, J. W., Tsuji, G. Y., Hoogenboom, G., Hunt, L. A., Thornton, P. K., Wilkens, P. W., Imamura, D. T., Bowen, W. T., and Singh, U. 1998. Decision support system for agrotechnology transfer: DSSAT v. 3.0. Pages 157-177 in: Understanding Options for Agricultural Production. G. Y. Tsuji, G. Hoogenboom, and P. K. Thornton, eds. Kluwer Academic Publishers, Dordrecht, the Netherlands.

Kooliyottil, R., Dandurand, L. M., Govindan, B. N., and Knudsen, G. R. 2016. Microscopy method to compare cyst nematode infection of different plant species. Adv. Biosci. Biotechnol. 7:311-318.

LaMondia, J. A., and Brodie, B. B. 1986. Effects of initial nematode density on population dynamics of *Globodera rostochiensis* on resistant and susceptible potatoes. J. Nematol. 18:159-165.

Luo, Y., Teng, P. S., Fabellar, N. G., and TeBeest, D. O. 1998. Risk analysis of yield losses caused by rice leaf blast associated with temperature changes above and below for five Asian countries. Agric. Ecosystems Environ. 68:197-205.

Madden, L. V., Hughes, G., and van den Bosch, F. 2007. The study of plant disease epidemics. The American Phytopathological Society, APS Press St. Paul, Minnesota.

Madden, L. V., and Nutter, F.W. 1995. Modeling crop losses at field scale. Can. J. Plant Pathol. 17:174-185.

Mai, W. F. 1952. Susceptibility of *Lycopersicon* species to the golden nematode. Phytopathology 42:461.

Martin, A. 1965. Investigaciones sobre el nematodo dorado de la papa *Heterodera rostochiensis* Woll. Informe Anual E.E.A. La Molina, Perú.

Martin, A. D., Quinn, K. M., and Park, J. H. 2011. MCMCpack: Markov Chain Monte Carlo in R. J. Stat. Soft. 42:1-21.

Minnis, S. T., Haydock, P. P. J., Ibrahim, S. K., and Grove, I. G. 2002. Potato cyst nematodes in England and Wales: Occurrence and distribution. Ann. Appl. Biol. 102:187-195.

Moxnes, J. F., and Hausken, K. 2007. The population dynamics of potato cyst nematodes. Ecol. Model. 207:339-348.

Murashige, T., and Skoog, F. 1962. A revised medium for rapid growth and bioassays with tobacco tissue cultures. Physiol. Plant. 15:473-497.

Nutter, F. W. 2001. Disease assessment terms and concepts. Pages 312-323 in: Encyclopedia of Plant Pathology. O. C. Maloy, and T. D. Murray, eds. John Wiley and Sons, Inc., New York.

Oostenbrink, M. 1967. Studies on the emergence of encysted *Heterodera* larvae. Meded. Rijksf. Landb. Gent. 32:503-539.

Phillips, M. S., Hackett, C. A., and Trudgill, D. L. 1991. The relationship between the initial and final population densities of the potato cyst nematode *Globodera pallida* for partially resistant potatoes. J. Appl. Ecol. 28:109-119.

Picard, D., Plantard, O., Scurrah, M., and Mugniéry, D. 2004. Inbreeding and population structure of the potato cyst nematode (*Globodera pallida*) in its native area (Peru). Mol. Ecol. 13:2899-2908.

Pylypenko, L. A. 1999. The interrelations in a system parasite-host plant at the globoderosis. PhD Diss. National Agrarian University, Kyiv, Ukraine.

R Core Team. 2018. R: A language and environment for statistical computing. R Foundation for statistical computing, Vienna, Austria. http://www.R-project.org/.

Raymundo, R., Asseng, S., Prassad, R., Kleinwechter, U., Concha, J., Condori, B., Bowen, W., Wolf, J., Olesen, J. E., Dong, Q., Zotarelli, L., Gastelo, M., Alva, A., Travasso, M., Quiroz, R., Arora, V., Graham, W., Porter, P. 2017. Performance of the SUBSTOR-potato model across contrasting growing conditions. Field Crops Res. 202:57-76.

Robert, P. A., and Stone, A. R. 1981. Host ranges of *Globodera* species within *Solanum* subgenus *Leptostemonum*. Nematologica 27:172-189.

Samaliev, H. 1998. Influence of crop rotation on population density of *Globodera pallida* (Nematoda: Heteroderidae) on potato. Rasteniev'dni Nauki 35:239-242.

Savary, S., Teng, P. S., Willocquet, L., and Nutter, F. W. 2006. Quantification and modeling of crop losses: A review of purposes. Ann. Rev. Phytopathol. 44:89-112.

Schneider, S. M., Rosskopf, E. N., Leesch, J. G., Chellemi, D. O., Bull, C. T., Mazzola, M. 2003. USDA-ARS research on alternatives to methyl bromide: Pre-plant and post-harvest. Pest Mange. Sci. 59:814-826.

Schomaker, C. H., and Been, T. H. 2006. Plant growth and population dynamics. Pages 276-301 in: Plant Nematology. R. N. Perry and M. Moens, eds. CABI, Oxfordshire, UK.

Seinhorst, J. W. 1965. The relation between nematode density and damage to plants. Nematologica 11:137-154.

Seinhorst, J. W., and Den Ouden, H. 1971. The relation between density of *Heterodera rostochiensis* and growth and yield of two potato varieties. Nematologica 17:347-369.

Singh, U., Matthews, R. B., Griffin, T. S., Ritchie, J. T., Hunt, L. A., and Goenaga, R. 1998. Modeling growth and development of root and tuber crops. Pages 129-156 in: Understanding Options for Agricultural Production. G. Y. Tsuji, G. Hoogenboom, and P. K. Thornton, eds. Kluwer Academic Publishers, Dordrecht, The Netherlands.

Skantar, A. M., Handoo, Z. A., Carta, L. K., and Chitwood, D. J. 2007. Morphological and molecular identification of *Globodera pallida* associated with potato in Idaho. J. Nematol. 39:133-144.

Skarbilovich, T. S. 1959. On the structure of the nematodes of the order Tylenchida Thorne, 1949. Acta Parasitol. Polonica 15:117-132.

Stone, A. R. 1972. The round cyst species of *Heterodera* as a group. Ann. Appl. Biol. 71:280-283.

Talavera, M., Andreu, M., Valor, H., and Tobar, A. 1998. Nematodos fitoparásiticos en áreas productoras de patata de Motril y Salobreña. Invest. Agric. Prod. Prot. Veg. 13:87-95.

Teng, P. S., and Savary, S. 1992. Implementing the systems approach in pest management. Agric. Syst. 40:237-264.

Teng, P. S., and Yuen, J. E. 1991. Epidemic models: Lesions from plant pathology. Pages 272-296 in: Risk Assessment in Genetic Engineering. M. A. Levin, and H. S. Strauss, eds. McGraw-Hill, New York.

Trudgill, D. L. 1986. Yield losses caused by potato cyst nematodes: A review of the current position in Britain and prospects for improvements. Ann. Appl. Biol. 108:181-198.

Trudgill, D. L., and Cotes, L. M. 1983. Tolerance of potato to potato cyst nematodes (*Globodera rostochiensis* and *G. pallida*) in relation to the growth and efficiency of the root system. Ann. Appl. Biol. 102:385-397.

Trudgill, D. L., Elliott, M. J., Evans, K., and Phillips, M. S. 2003. The white potato cyst nematode (*Globodera pallida*): A critical analysis of the threat in Britain. Ann. Appl. Biol. 143:73-80.

Trudgill, D. L., Evans, K., and Parrott, D. M. 1975. Effects of potato cyst nematodes on potato plants: Effects in a trial with irrigation and fumigation on the growth and nitrogen and potassium contents of a resistant and susceptible variety. Nematologica 21:169-182.

Trudgill, D. L., Phillips, M. S., and Elliott, M. J. 2014. Dynamics and management of the white potato cyst nematode *Globodera pallida* in commercial potato crops. Ann. Appl. Biol. 164:18-34.

Trudgill, D. L., Phillips, M. S., and Hackett, C. A. 1996. The basis of predictive modelling for estimating yield loss and planning potato cyst nematode management. Pestic. Sci. 47:89-94.

Turner, S. J. 1996. Population decline of potato cyst nematodes (*Globodera rostochiensis* and *G. pallida*) in field soils in Northern Ireland. Ann. Appl. Biol. 129:315-322.

Turner, S. J., and Rowe, J. A. 2006. Cyst nematodes. Pages 91-120 in: Plant Nematology, R. N. Perry and M. Moens, eds. CABI, Wallingford, UK.

Twining, S., Clarke, J., Cook, S., Ellis, S., Gladders, P., Ritchie, F., and Wynn, S. 2009. Pesticide availability for potatoes following revision of Directive 91/414/EEC: Impact assessments and identification of research priorities. Project Report 2009. Potato Council, Oxford, UK.

USDA-APHIS. 2009. Pale potato cyst nematode national survey and diagnostic cyst sample forwarding protocols. Online publication. United States Department of Agriculture's Animal and Plant Health Inspection Service. https://www.aphis.usda.gov/plant_health/plant_pest_info/potato/downloads/pcndocs/PCN_NatlSurvey.pdf.

USDA-APHIS. 2019. Pale cyst nematode eradication program, 4th Quarter Report (October 1-December 31). Online publication. United States Department of Agriculture's Animal and Plant Health Inspection Service. https://www.aphis.usda.gov/aphis/ ourfocus/planthealth/plant-pest-and-disease-programs/pests-and diseases /sa_nematode/sa_potato/ct_pcn_programupdates.

USDA-NASS. 2018. Crop values 2017 summary. Online publication. United States Department of Agriculture's National Agricultural Statistics Service. http://usda.mannlib.cornell.edu/ usda/current/CropValuSu/CropValuSu-02-23-2018.pdf.

Vasyutin, A. S., and Yakovleva, V. A. 1998. *Globodera* in potatoes in Russia. Kartofel' I Ovoshchi 6:29-32.

Ward, S. A., Rabbinge, R., and Den Ouden, H. 1985. Construction and preliminary evaluation of a simulation model of the population dynamics of the potato cyst nematode *Globodera pallida*. Neth. J. Plant Pathol. 91:27-44.

Whitehead, A. G. 1977. Vertical distribution of potato, beet and pea cyst nematodes in some heavily infested soils. Plant Pathol. 26:85-90.

Whitehead, A. G. 1991. The resistance of six potato cultivars to English populations of potato cyst nematodes *Globodera pallida* and *G. rostochiensis*. Ann. Appl. Biol. 118:357-369.

Whitworth, J. L., Novy, R. G., Zasada, I. A., Wang, X., Dandurand, L. M., and Kuhl, J. C. 2018. Resistance of potato breeding clones and cultivars to three species of potato cyst nematode. Plant Dis. 102:2120-2128.

Willocquet, L., Savary, S., Fernández, L., Elazegui, F. A., Castilla, N., Zhu, D., Tang, Q., Huang, S., Lin, X., Singh, H. M., and Srivastsava, R. K. 2002. Structure and validation of RICEPEST, a production situation-driven, crop growth model simulating rice yield response to multiple pest injuries for tropical Asia. Ecol. Model. 153:247-268.

Wollenweber, H. W. 1923. Krankheiten und BeschSdigungen der Kartoffel. Arb. Forsch. Inst. Kartof. 7:1-56.

Zadoks, J. C. 1985. On the conceptual basis of crop loss assessment: The threshold theory. Ann. Rev. Phytopathol. 23:455-473.

Table 4.1. Potato growth assessment for each level of *Globodera pallida* initial nematode densities (*Pi*) in soil.

Pi (eggs/g soil)	Fresh top	Dry top	Dry root	Dry tuber	Fresh tuber	Total dry plant
	Weight (g)					
	Trial 1					
0	46.68 ±4.20a[a]	8.39 ±1.05a	1.19 ±0.11a	9.22 ±0.45a	42.10 ±2.53a	18.80 ±1.23a
10	37.23 ±3.94a	5.74 ±0.93a	0.95 ±0.15a	8.30 ±0.90ab	35.93 ±3.83ab	15.00 ±1.50ab
20	38.79 ±2.83a	6.19 ±0.85a	0.93 ±0.07a	6.84 ±0.86ab	30.26 ±3.36ab	13.96 ±1.52ab
40	32.32 ±5.47a	4.76 ±1.21ab	0.78 ±0.11a	5.17 ±0.86b	23.51 ±3.84b	10.71 ±1.88b
80	12.41 ±6.04b	1.63 ±0.80b	0.14 ±0.05b	1.32 ±0.53c	5.58 ±2.28c	3.08 ±1.32c
	Trial 2					
0	37.65 ±3.94a	5.17 ±0.54a	1.42 ±0.16a	16.34 ±0.96a	73.29 ±3.97a	22.93 ±1.32a
10	40.82 ±3.58a	5.93 ±0.42a	1.43 ±0.11a	16.21 ±1.08a	73.47 ±4.52a	23.57 ±1.17a
20	37.50 ±3.06a	5.68 ±0.46a	1.19 ±0.11a	15.75 ±1.04a	70.46 ±4.42a	22.62 ±1.30a
40	34.25 ±3.50a	4.79 ±0.44a	1.09 ±0.10a	13.10 ±1.38ab	58.35 ±5.96b	18.98 ±1.77ab
80	32.71 ±3.75a	4.33 ±0.44a	0.90 ±0.13a	9.51 ±1.23b	45.02 ±5.45b	14.74 ±1.55b

[a] Same letter indicates that the means (±standard error) are not significant $P > 0.05$.

Table 4.2. Potato tuber growth assessment for each level of *Globodera pallida* initial nematode densities (*Pi*) in soil.

Pi (eggs/g soil)	# Tubers (unit)	Dry tuber	Fresh tuber
		Weight (g)/unit	
		Trial 1	
0	5.4 ±0.7ab[a]	1.99 ±0.26a	8.91 ±1.00a
10	6.4 ±1.5ab	2.30 ±0.95a	9.62 ±3.80a
20	7.0 ±1.3a	1.12 ±0.17ab	5.00 ±0.67b
40	6.2 ±1.4ab	1.37 ±0.54ab	6.23 ±2.44b
80	2.5 ±0.6b	0.36 ±0.16b	1.89 ±0.76c
		Trial 2	
0	6.55 ±0.64a	2.81 ±0.26a	12.78 ±1.24a
10	7.45 ±0.84ab	2.74 ±0.41a	12.79 ±1.99a
20	7.80 ±1.04b	2.68 ±0.31ab	11.96 ±1.33a
40	7.00 ±0.63ab	2.01 ±0.22bc	8.93 ±0.98b
80	6.45 ±0.80a	1.62 ±0.19c	7.79 ±0.95b

[a] Same letter indicates that the means (±standard error) are not significant $P > 0.05$.

TABLE 4.3. Impact of the initial nematode densities (*Pi*) of *Globodera pallida* in soil on final nematode densities (*Pf*) and reproduction rate (*Rf*).

Pi (eggs/g soil)	Cysts/g dry root	Cysts/g soil	Eggs/cyst	*Pf* (eggs/g soil)	*Rf* (*Pf*/*Pi*)
			Trial 1		
10	1,903 ±561a[a]	0.80 ±0.08ab	588 ±21a	473 ±52a	47.25 ±5.21a
20	1,572 ±150b	0.95 ±0.08ab	535 ±19ab	510 ±56a	25.51 ±2.79b
40	2,699 ±269c	1.19 ±0.18a	465 ±24b	567 ±94a	14.18 ±2.35c
80	36,933 ±16,328d	0.56 ±0.13b	324 ±22c	196 ±52b	2.45 ±0.65d
			Trial 2		
10	562 ±62a	0.48 ±0.04a	439 ±18a	199 ±16a	19.90 ±1.57a
20	1,090 ±148a	0.73 ±0.07ab	424 ±20ab	289 ±24ab	14.43 ±1.22b
40	1,263 ±173ab	0.79 ±0.10b	389 ±17ab	301 ±36ab	7.52 ±0.89c
80	2,292 ±558c	0.89 ±0.07b	368 ±14b	328 ±33b	4.10 ±0.41c

[a] Same letter indicates that the means (±standard error) are not significant $P > 0.05$.

Table 4.4. Linear relationships between the initial nematode densities (*Pi*) of *Globodera pallida* in soil and potato growth parameters.

Regression parameters	Fresh top	Dry top	Dry root	Fresh tuber	Dry tuber	Total dry plant
	Response variable (y) in gram as predicted by Pi (x) in eggs/g soil					
	Trial 1					
Equation	$log_{10}y = -0.01x + 1.74$	$log_{10}y = -0.007x + 0.94$	$y = -0.01x + 1.17$	$y = -0.44x + 40.75$	$y = -0.10x + 9.12$	$y = -0.18x + 17.88$
p-value	2.03e-08	2.03e-08	1.98e-09	1.03e-11	2.65e-11	2.50e-10
Adjusted R^2	0.47	0.47	0.52	0.61	0.60	0.56
	Trial 2					
Equation	$log_{10}y = -0.002x + 1.56$	$log_{10}y = -0.001x + 0.73$	$y = -0.006x + 1.41$	$y = -0.38x + 75.65$	$y = -0.09x + 16.92$	$y = -0.11x + 24.01$
p-value	0.04	0.01	7.90e-04	2.47e-06	1.73e-06	1.78e-06
Adjusted R^2	0.03	0.05	0.10	0.20	0.20	0.20

Table 4.5. Bayesian confidence interval for the linear relationship between total dry plant weight and *Globodera pallida* initial nematode densities (*Pi*) in soil.

Parameters	Trial	Confidence interval				
		2.5%	25%	50%	75%	97.5%
Intercept	1	15.96	17.24	17.90	18.53	19.80
Pi		-0.23	-0.20	-0.19	-0.17	-0.14
σ^2		15.15	19.28	22.05	25.48	34.13
Intercept	2	22.18	23.39	24.02	24.64	25.85
Pi		-0.16	-0.13	-0.11	-0.01	-0.07
σ^2		31.34	37.31	41.00	45.32	54.98

σ^2 represents the residual error variance.

Table 4.6. Linear relationships between the initial nematode densities (*Pi*) of *Globodera pallida* in soil and nematode reproduction parameters.

Regression parameters	Cysts/g soil	Final population (*Pf*)	Reproduction rate (*Rf*)
	Response variable (y) as predicted by *Pi* (x) in eggs/g soil		
	Trial 1		
Equation	$log_{10}y = -0.001x + 0.31$	$log_{10}y = -0.008x + 2.84$	$y = -0.56x + 43.30$
p-value	0.04	5.81e-05	2.20e-09
Adjusted R^2	0.08	0.33	0.60
	Trial 2		
Equation	$log_{10}y = 0.003x - 0.31$	$log_{10}y = 0.002x + 2.31$	$y = -0.21x + 19.40$
p-value	4.70e-04	0.01	2.61e-14
Adjusted R^2	0.14	0.06	0.52

Table 4.7. Coefficients of potato yields for each *Globodera pallida* initial nematode densities (*Pi*) in soil.

Pi (eggs/g soil)	Dry top	Dry root	Dry tuber	Fresh tuber	Total dry plant
	Trial 1				
0	1.00	1.00	1.00	1.00	1.00
10	0.68	0.80	0.90	0.85	0.80
20	0.74	0.78	0.74	0.72	0.74
40	0.57	0.66	0.56	0.56	0.57
80	0.19	0.12	0.14	0.13	0.16
	Trial 2				
0	1.00	1.00	1.00	1.00	1.00
10	1.15	1.01	0.99	1.01	1.03
20	1.10	0.84	0.96	0.96	0.99
40	0.93	0.77	0.80	0.80	0.83
80	0.84	0.63	0.58	0.61	0.64

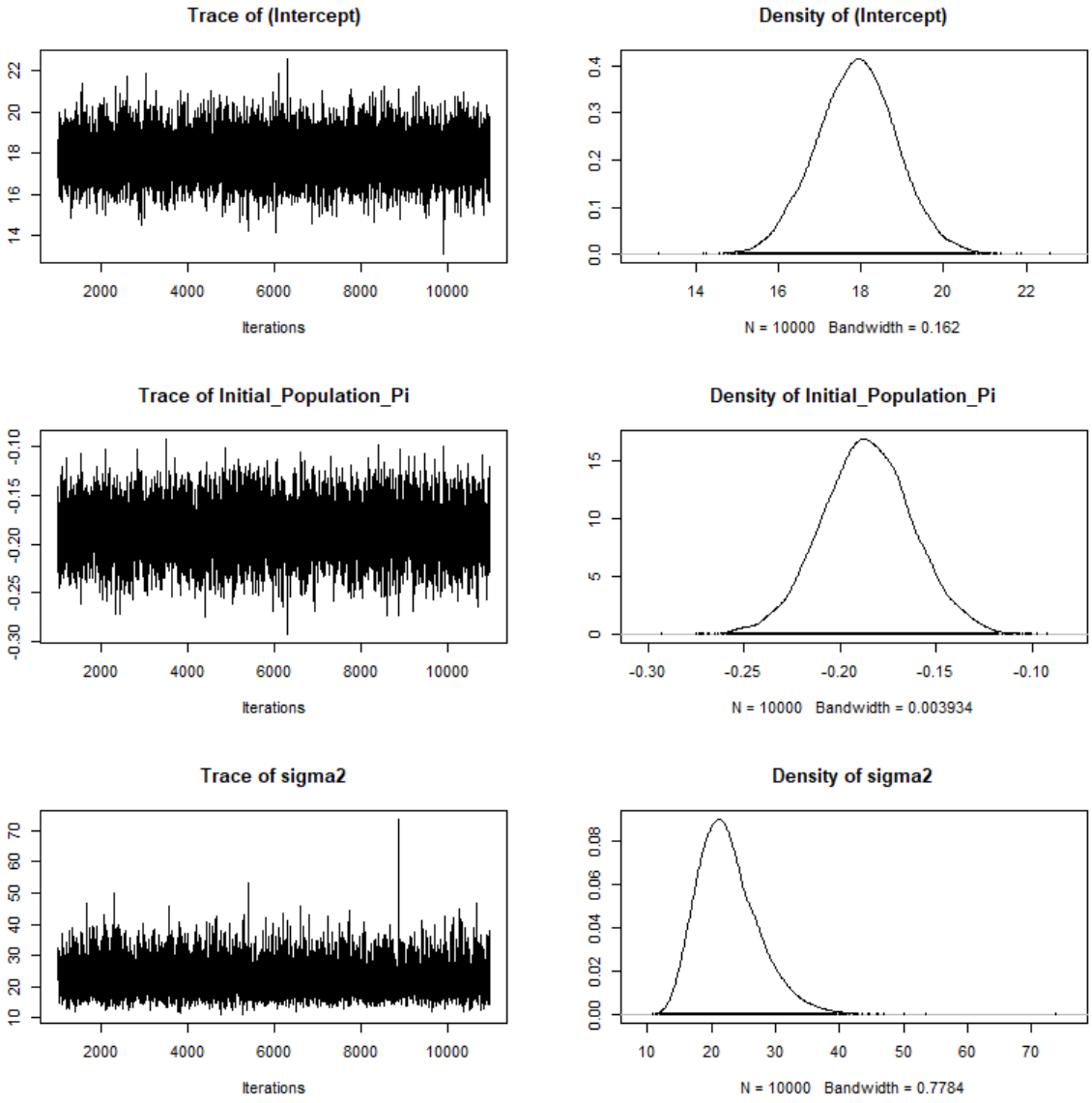

Fig. 4.1. Bayesian regression analysis for total dry plant weight in trial 1. The posterior probability distributions showed that the 97.5% confidence interval was for: (i) the intercept (15.96 and 19.80); (ii) the initial population densities (-0.23 and -0.14); and (iii) the residual error variance σ^2 (15.15 and 34.13).

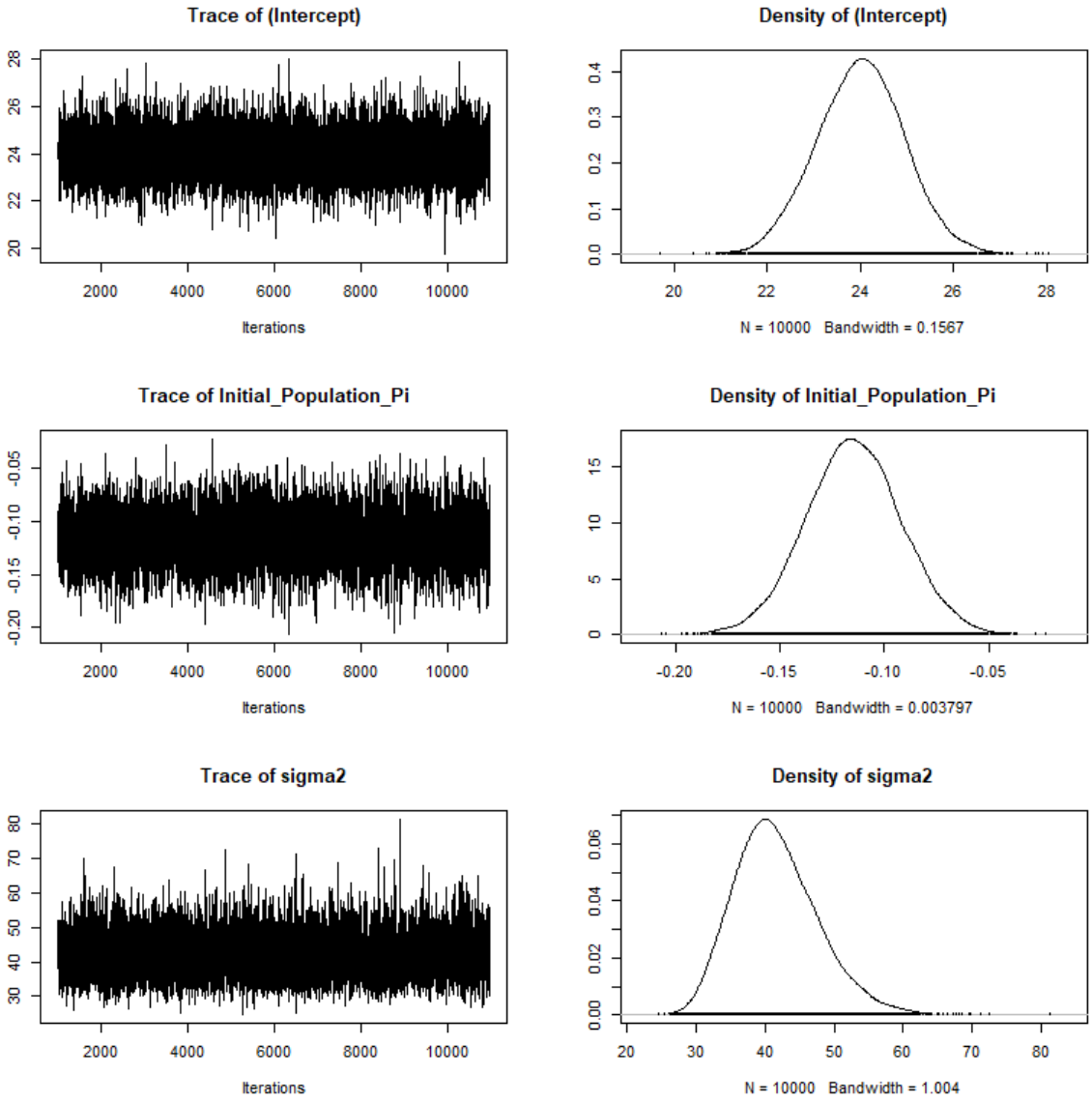

Fig. 4.2. Bayesian regression analysis for total dry plant weight in trial 2. The posterior probability distributions showed that the 97.5% confidence interval was for: (i) the intercept (22.18 and 25.85); (ii) the initial nematode densities (-0.16 and -0.07); and (iii) the residual error variance σ^2 (31.34 and 54.98).

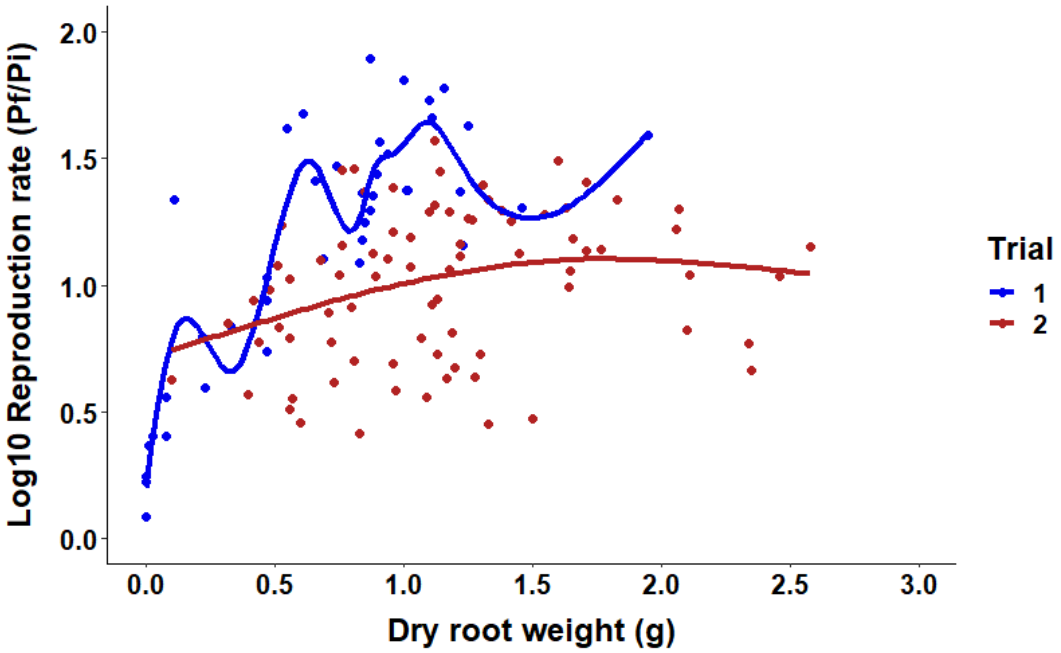

Fig. 4.3. A generalized additive model (GAM) was performed to model the relationship between dry root weight and *Globodera pallida* reproduction rate using a non-linear smooth function to model and capture the non-linearities in the data. Trial 1 showed a positive and significant non-linear relationship between dry root weight and *G. pallida* reproduction rate with a correlation coefficient $r = 0.91$ ($P < 0.001$). Similar results were observed in trial 2 with a correlation coefficient $r = 0.34$ ($P = 0.01$).

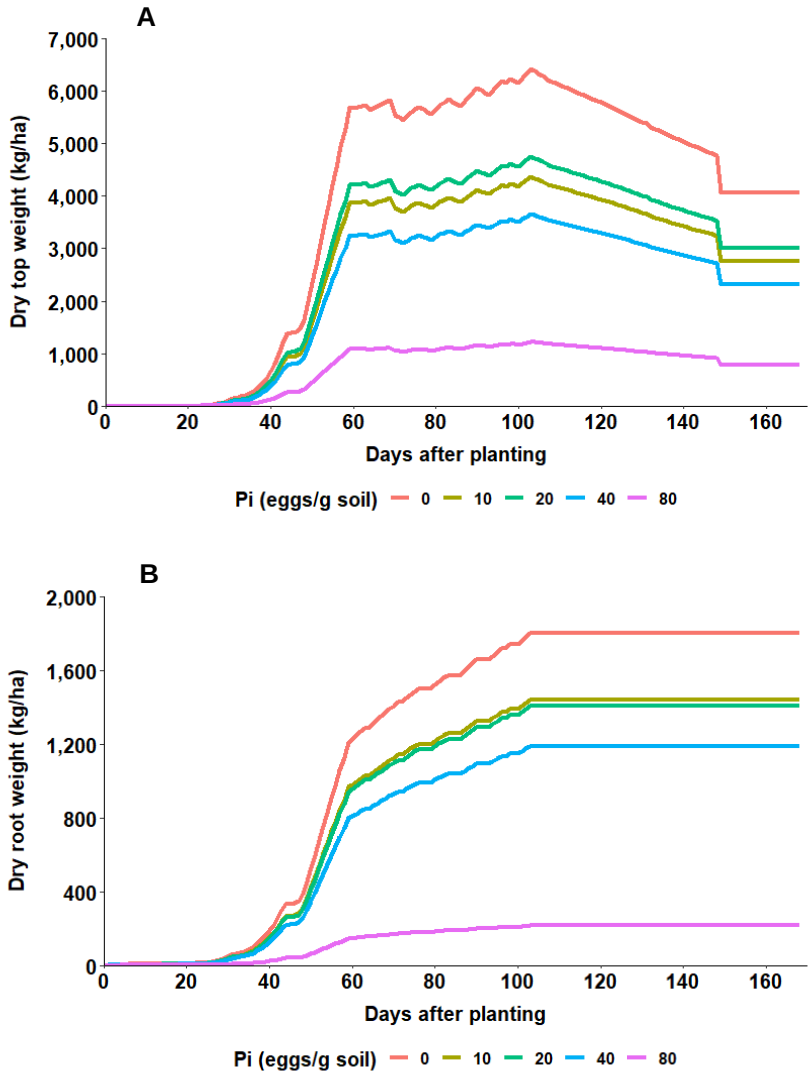

Fig. 4.4A. SUBSTOR-DSSAT potato growth simulation coupled with the impact of *Globodera pallida* initial nematode densities in soil for trial 1. After 103 days after planting (DAP), dry top reached a maximum yield of 6,427 kg/ha in non-infested soil and reached a minimum yield of 1,221 kg/ha at initial nematode density of 80 eggs/g soil. **B.** From 149 to 168 DAP, dry root reached a maximum yield of 1,804 kg/ha in non-infested soil and reached a minimum yield of 217 kg/ha at initial nematode density of 80 eggs/g soil.

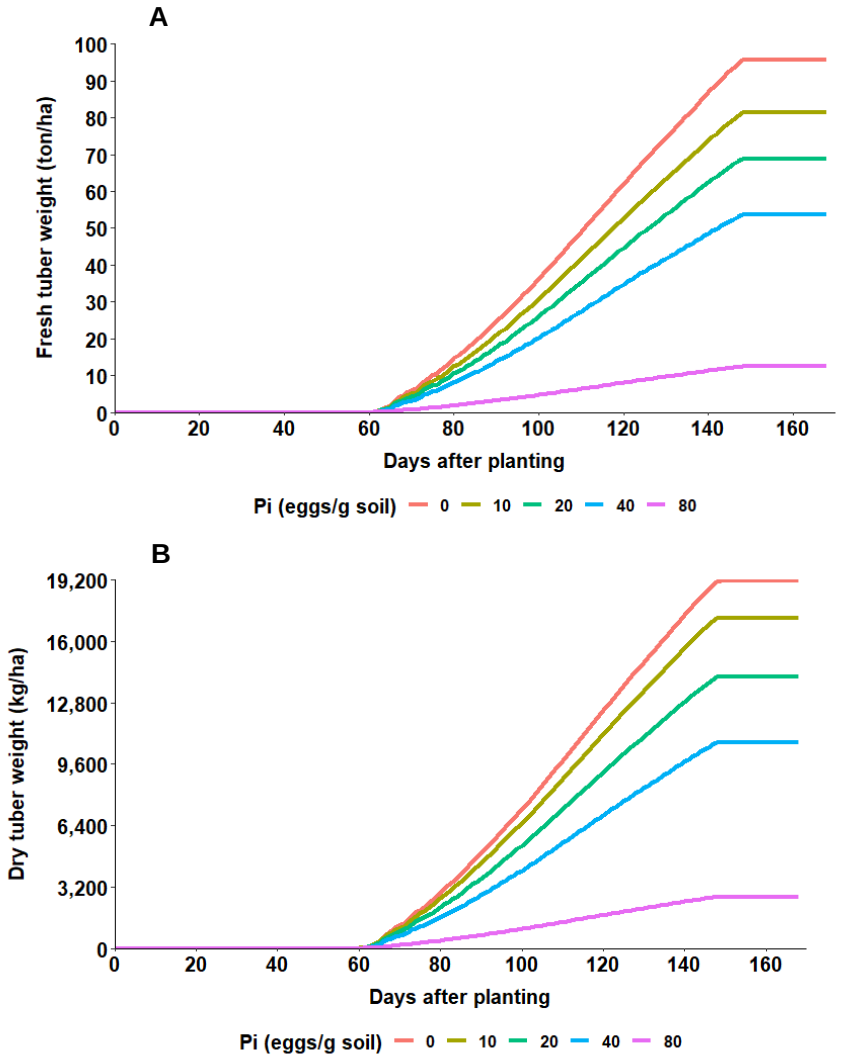

Fig. 4.5A.B. SUBSTOR-DSSAT potato growth simulation coupled with the impact of *Globodera pallida* initial nematode densities in soil for trial 1. At 149 days after planting, potato fresh and dry tubers reached a maximum yield of 96 ton/ha and 19,145 kg/ha, respectively, in non-infested soil and reached a minimum yield of 12 ton/ha and 2,680 kg/ha, respectively, at initial nematode density of 80 eggs/g soil.

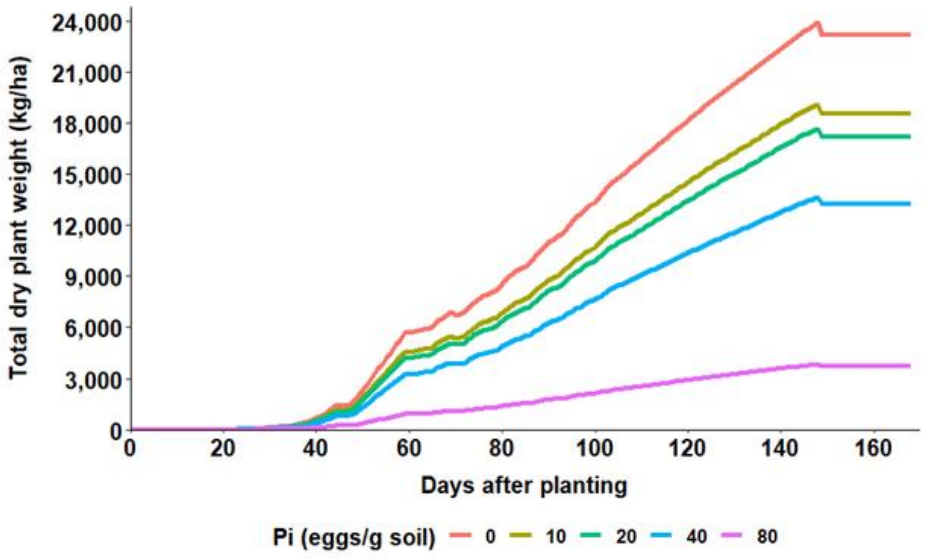

Fig. 4.6. SUBSTOR-DSSAT potato growth simulation coupled with the impact of *Globodera pallida* initial nematode densities in soil for trial 1. At 148 days after planting, total dry plant reached a maximum yield of 23,911 kg/ha in non-infested soil and reached a minimum of 3,826 kg/ha at 80 eggs/g soil.

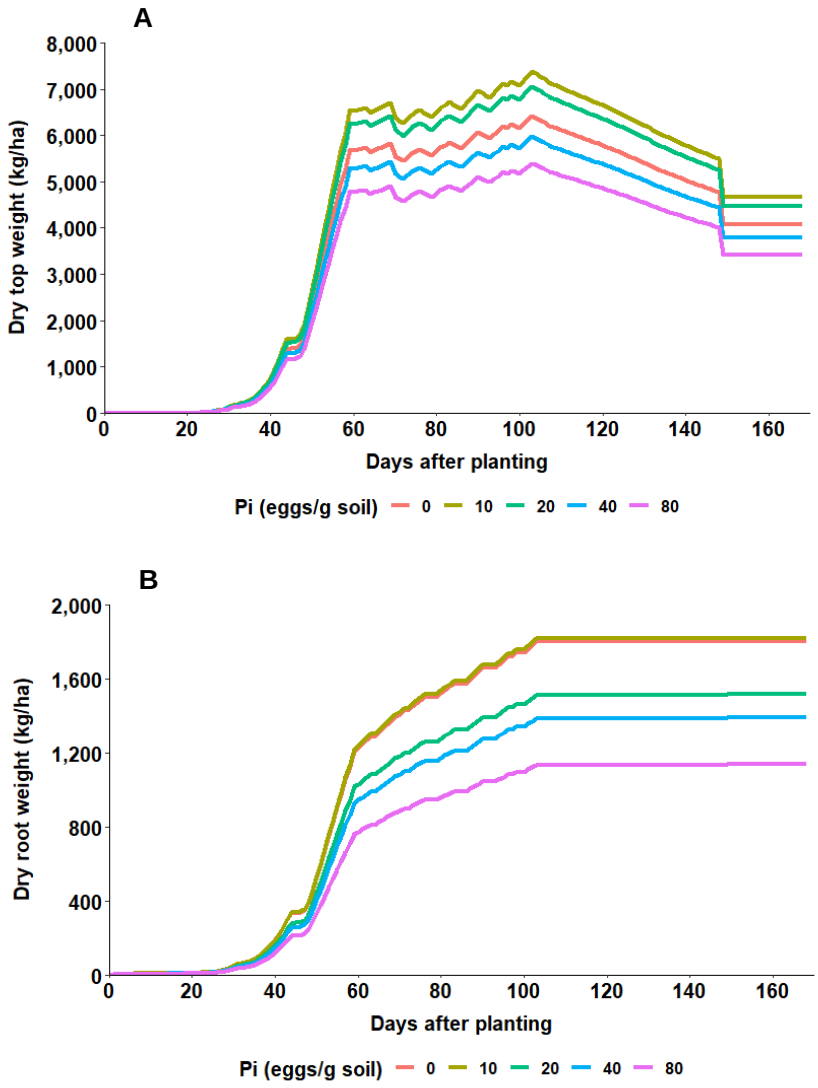

Fig. 4.7. SUBSTOR-DSSAT potato growth simulation coupled with the impact of *Globodera pallida* initial nematode densities in soil for trial 2. **A.** After 103 days after planting (DAP), dry top reached a maximum yield of 6,427 kg/ha in non-infested soil and reached a minimum yield of 5,399 kg/ha at initial nematode density of 80 eggs/g soil. **B.** From 149 to 168 DAP, dry root reached a maximum yield of 1,804 kg/ha in non-infested soil and reached a minimum yield of 1,137 kg/ha at initial nematode density of 80 eggs/g soil.

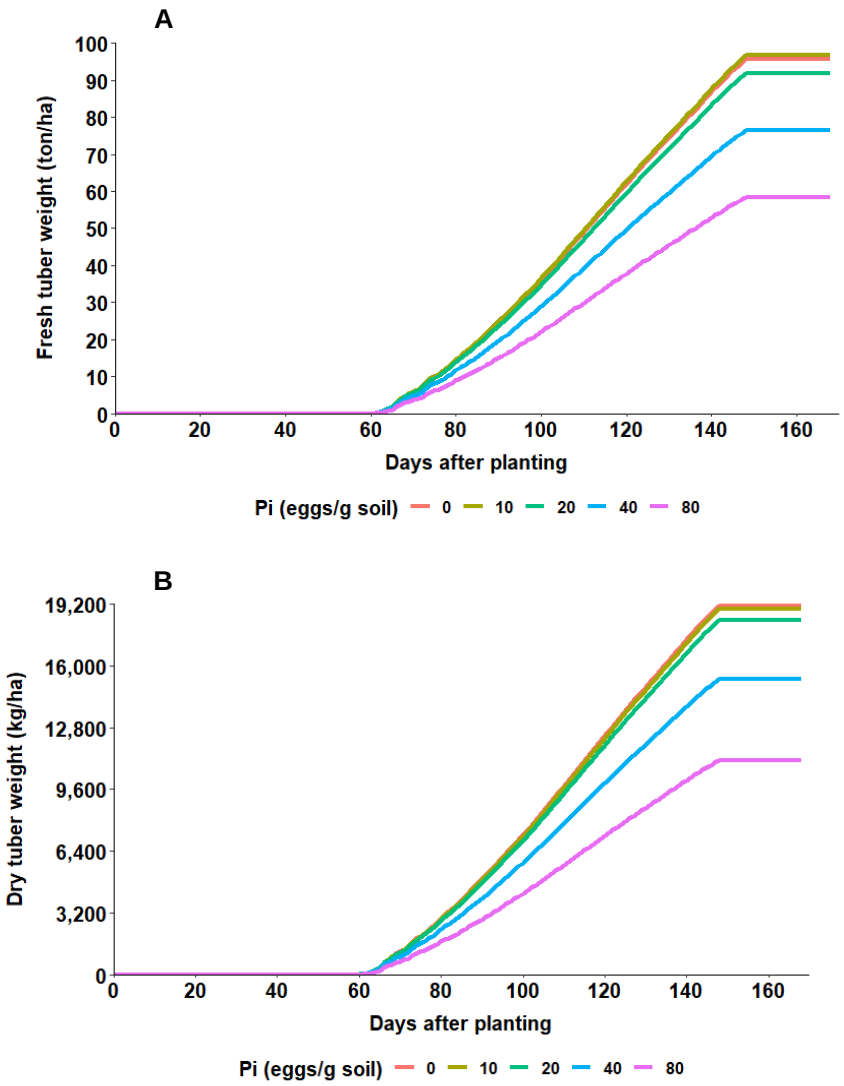

Fig. 4.8A.B. SUBSTOR-DSSAT potato growth simulation coupled with the impact of *Globodera pallida* initial nematode densities in soil for trial 2. At 149 days after planting, potato fresh and dry tubers reached a maximum yield of 96 ton/ha and 19,145 kg/ha, respectively, in non-infested soil and reached a minimum yield of 58 ton/ha and 11,104 kg/ha, respectively, at initial nematode density of 80 eggs/g soil.

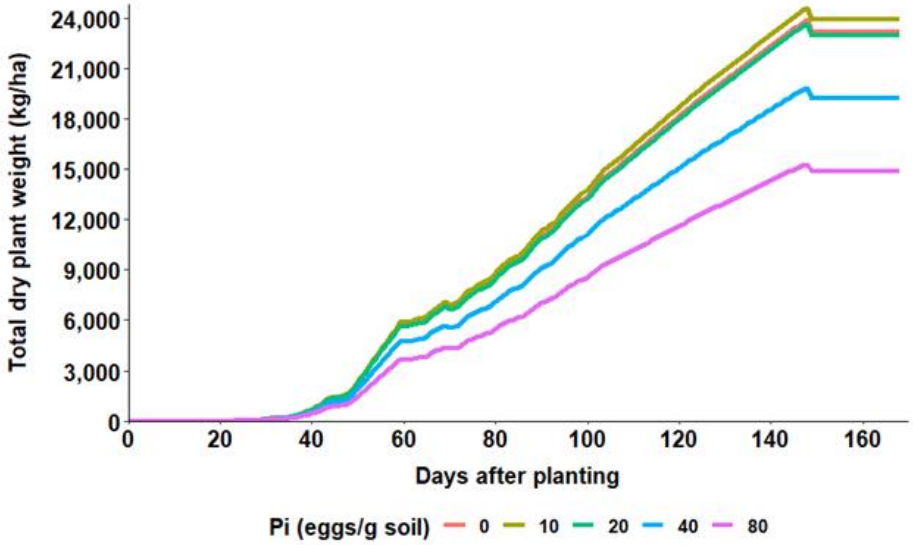

Fig. 4.9. SUBSTOR-DSSAT potato growth simulation coupled with the impact of *Globodera pallida* initial nematode densities in soil for trial 2. At 148 days after planting, total dry plant reached a maximum yield of 23,911 kg/ha in non-infested soil and reached a minimum of 15,303 kg/ha at 80 eggs/g soil.

Appendix

Letter of Permission from Phytopathology Society (APS)

Subject: Permissions request

Hello, Katherine—The American Phytopathological Society (APS) allows individuals to include in a thesis or dissertation an article published in an APS journal. The only requirement is to include as a footnote on the first page of the article the complete bibliographic citation, including DOI number.

Please let me know if you have any questions about these terms.

Good luck completing your thesis!

Regards, Sue Freese

Susan Freese
Strategic Product Development Manager
Scientific Societies
Phone: 651.994.3875
www.scisoc.org